DEVELOPMENT OF A MULTI-OBJECTIVE OPTIMIZATION CAPABILITY FOR HETEROGENEOUS LIGHT WATER REACTOR FUEL ASSEMBLIES

Alan Joseph Charles

Darwin College

Department of Engineering

University of Cambridge

This dissertation is submitted for the degree of Doctor of Philosophy

September 2019

Supervisor: Advisor:

Dr Geoff Parks Dr Eugene Shwageraus

Declaration

This dissertation is the result of my own work and includes nothing which is the outcome of work done in collaboration except as specified in the text.

It is not substantially the same as any that I have submitted, or is being concurrently submitted, for a degree or diploma or other qualification at the University of Cambridge or any other University or similar institution except as specified in the text. I further state that no substantial part of my dissertation has already been submitted, or is being concurrently submitted, for any such degree, diploma or other qualification at the University of Cambridge or any other University or similar institution except as specified in the text.

This thesis contains a total of 35,254 words and 37 figures, and therefore does not exceed the prescribed word limit of 65,000 words and 150 figures for the Engineering Degree Committee.

Alan Joseph Charles

Abstract

DEVELOPMENT OF A MULTI-OBJECTIVE OPTIMIZATION CAPABILITY FOR HETEROGENEOUS LIGHT WATER REACTOR FUEL ASSEMBLIES

Alan Joseph Charles

As pressure grows on developed nations to move away from fossil fuel-based energy sources, so does the potential for nuclear energy to make its resurgence. However, the complex nature of the design process in nuclear engineering and a regulatory culture of ever-increasing safety standards create unique challenges to the nuclear industry. As in many engineering disciplines, the question is one of trade-offs between safety, performance, cost, and time required to develop the design from paper to real life operation. The possibilities facing a designer are virtually unlimited, with fuel choice, layout and operating conditions just three of the many categories which interact with one another in a highly non-linear manner, making it difficult to quantitatively define these trade-offs. Deciding upon an 'optimal' design is therefore traditionally done through expert judgement and an iterative design process. Mathematical optimization methods offer a more formal way to optimize designs by employing algorithms to explore the myriad of possibilities in a methodical manner which can yield increased performance over expert designs. In this thesis, an extensive review of the literature revealed gaps which present opportunities for novel research. Two new algorithms are created with the ability to solve optimization problems with multiple objectives simultaneously without requiring weighting or bias from the designer. They are then applied to a series of problems drawn from both the literature and real world designs. The results demonstrate the algorithms' effectiveness and robustness as well as their ability to handle complex multi-physics problems with reasonably low computational requirements. This research offers an original and effective tool for performing optimization on nuclear fuel assembly design problems and has advanced the state of the art in both multi-objective optimization and its application to the nuclear engineering industry.

Acknowledgements

First and foremost I would like to thank my supervisor, Dr Geoff Parks, for his guidance and wisdom throughout the last four years. I am also grateful for his patience in dealing with my somewhat nonconformist style of research, and for giving me not only freedom in which direction I took my research, but also the liberty to take advantages of other academic opportunities outside of my research area, which have helped broaden my knowledge and given me a deeper understanding of the world of nuclear engineering.

I would also like to thank my advisor, Dr Eugene Shwageraus, for additional valuable advice and for helping me keep in mind that engineering is fundamentally about solving real life problems. No one will use an optimization tool if it takes longer to run than building and running a real reactor, which in today's climate is a long time indeed!

My thanks also go to the wonderful people with whom I was fortunate enough to undertake my studies, both originally at Imperial College London and later in the Nuclear Energy Group at Cambridge University. Without the ability to discuss our research or to argue bitterly over which is the best college for formal dinners, I am not sure I would have had the necessary balance of optimism and pessimism needed to finish.

A great deal of thanks must also go to the ANSWERS Software Service at Jacobs (formerly Wood Group plc), who created and maintain the WIMS reactor physics software package. In addition, the assistance and expertise of the ANSWERS team was very valuable. Special thanks in particular are owed to Ben Lindley and Brendan Tollit, who helped enormously with my abundant technical issues, and Paul Smith, who offered and arranged my internship at ANSWERS (which proved vital for my later experiments with multi-physics analysis!).

I thank my parents, Andrew and Isabel, for their tireless efforts to encourage me to explain my work in a form others might understand, and lastly, but most importantly, I thank my loving wife Azura. Her endless patience in listening to me talk about all things nuclear related has been incredible, and she has been a constant source of much-needed support throughout this journey.

This PhD was funded by the UK Engineering and Physical Sciences Research Council (EPSRC) through the Imperial College, University of Cambridge and Open University Centre for Doctoral Training in Nuclear Energy under grant EP/L015900/1ICO.

Table of contents

Table of abbreviations

ABWR	Advanced Boiling Water Reactor	MoC	Method of Characteristics
ALARP	As Low As Reasonably Practicable	MOAA	Multi-objective Alliance Algorithm
ANN	Artificial Neural Network	MOGA	Multi-objective Genetic Algorithm
BoL	Beginning of Life	MOJADE	Multi-objective JADE
BPR	Burnable Poison Rod	MOμJADE	Multi-objective μJADE
BWR	Boiling Water Reactor	MOX	Mixed Oxide
CHF	Critical Heat Flux	MTC	Moderator Temperature Coefficient
CHFR	Critical Heat Flux Ratio	NEA	Nuclear Energy Agency
CPR	Critical Power Ratio	NSGA-II	Non-dominated Sorting Genetic Algorithm II
DE	Differential Evolution	OECD	Organisation for Economic Co-operation and Development
DNBR	Departure from Nucleate Boiling Ratio	ONR	Office of Nuclear Regulation
EA	Evolutionary Algorithm	PC	Parallel Coordinates
EDF	Electricité de France	PCM	Per Cent Mille
EFPD	Effective Full Power Days	PPF	Power Peaking Factor
EPR	European Pressurized Reactor	PR + SS	Path Relinking + Scatter Search
EPRI	Electric Power Research Institute	PSO	Particle Swarm Optimization
GA	Genetic Algorithm	PWR	Pressurized Water Reactor
GDA	Generic Design Assessment	SA	Simulated Annealing
GWd/t	Gigawatt days per tonne	SCWR	Supercritical Water Reactor
HS	Harmony Search	SO	Single-objective
IWF	Inertia Weight Factor	SOGA	Single-objective Genetic Algorithm
LEU	Low Enriched Uranium	SMR	Small Modular Reactor
LMR	Liquid Metal Reactor	UOX	Uranium Oxide
LWR	Light Water Reactor	VC	Void Coefficient
MO	Multi-objective	WIMS	Winfrith Improved Multigroup Scheme

1. Introduction

1.1. Background and motivation

As of 2019, there are currently around 450 nuclear reactors operating in over 30 countries. Around 50 more reactors are currently under construction, and in 2017 nuclear energy provided around 10% of the world's energy supply (World Nuclear Association, 2019). It is acknowledged by international agencies such as the International Energy Agency (International Energy Agency, 2018) and by governments (UK Government, 2013) that nuclear power will continue to be needed as a source of stable base-load energy. This is especially true of developed nations, as GDP positively correlates with concern for climate change (although it negatively correlates with the perception of impact from it) (Lo & Chow, 2015), and who therefore may wish to reduce the reliance on energy produced from fossil fuels. To that end, nuclear power is uniquely positioned as a readily available technology which can fully meet the requirements of high density, large scale and reliable energy production. However, while the need for nuclear is recognised, Western countries have struggled to deploy the next generation of nuclear power plants. The US, France, Finland, Sweden and the UK have all grappled with construction issues, cost overruns (World Nuclear News, 2018), delays (Reuters, 2017), and, in some cases, indefinite suspensions (BBC, 2019) or cancellations (World Nuclear News, 2017) of programmes. China remains the most prolific and most active player in nuclear new build, with construction of some 15 reactors underway, and is now readying her own designs for the export market (World Nuclear, 2019). The nuclear market stands at a crossroads between multiple competing nuclear reactor technologies and the choice between full scale reactors and smaller so-called Small Modular Reactors (SMRs). One thing that does remain constant, however, is the continued use of light water (*i.e.* water without deuterium enrichment) as the prevalent coolant / moderator in reactor systems.

Although Uranium Oxide (UOX) is known universally as the ubiquitous fuel for nuclear reactors, it is by no means the only fuel source. Plutonium has been used in nuclear reactors since the dawn of the nuclear era and has featured prominently in civilian power programmes the world over in the form of Mixed Oxide (MOX) uranium/plutonium fuel. Continued use of plutonium may reflect attempts to close the fuel cycle or to use up material originally made for nuclear weapons. Reactor systems that utilize MOX fuel pins also feature UOX pins, leading to heterogeneity in the core. Heterogeneity can potentially offer benefits, such as improved neutron economy, through varying properties of the fuel radially on a pin-by-pin basis and axially along the assembly. Doing so, however, could cause a trade-off with other performance measures, such as radial power peaking or thermal-hydraulic criteria. Many new designs of nuclear reactor, such as the European Pressurized Reactor (EPR) (EDF, 2012) and the Advanced Boiling Water Reactor (ABWR) (Hitachi-GE, 2017) claim the ability to handle MOX fuels.

As analytical and manufacturing methods improve, the design of these fuels will likely become too complex to optimize these trade-offs through conventional engineering judgement alone. This is mainly due to the high number of possible variables and their non-linear interaction. Because of these factors, formal optimization methods offer a way to explore these trade-offs and are a promising area of research. Optimized designs could feature lower fabrication costs as an objective, along with improved performance. Optimization refers to the process of attempting to determine which combinations of variables within a system produce solutions which achieve the best performance or are closest to pre-defined performance objectives through minimizing the trade-offs present between objectives. Using modern computers and advances in multi-objective optimization methods it is possible to systematically and rigorously explore these trade-offs, and such a capability would be a helpful aid to decision-making. The research described in this thesis applies, in an innovative manner, the latest optimization methods to the field of nuclear heterogeneous fuel assembly design and demonstrates their effectiveness through application to a number of realistic problems. The potential applications of this project reach beyond land-based civilian power reactors and can be applied to any nuclear reactor design, such as research reactors or those used in marine propulsion. In addition, this project seeks to improve the understanding of how nuclear reactor properties interact, as well as to provide new tools and methods for the training of future reactor operators and nuclear engineers. The ability to exploit mathematical optimization as a reliable method to generate new assembly designs, to assess the performance of existing assembly designs, and to allow the engineer to more easily explore the relationships between various design parameters and performance criteria are what make this project innovative and ideally suited to an engineering PhD.

1.2. Summary of reactor physics and thermal hydraulics methods utilized in this thesis

This section is intended to give a brief overview of how the physical phenomena present inside an operating nuclear reactor are modelled in the analysis work within this thesis, in order for the reader to be familiar with common terms used extensively in the rest of this thesis.

As shown below in Figure 1, the inside of a Light Water Reactor (LWR) consists of:

1. Inlet and outlet connections to the rest of the primary circuit, transporting the coolant to and from the steam generators to transfer the heat produced in the core to the secondary system for electrical power generation
2. A reflector, typically water and steel, which serves to ‘reflect’ neutrons which leave the core back into the fuel

3. Upper and lower plenums to mix and distribute the coolant before and after it passes through the core
4. The core, which contains the fissile fuel responsible for fission and heat generation. In LWRs, neutrons are initially generated with energies of the order of 2 MeV and must be 'slowed down' or 'thermalized' before the majority of fissions can take place. To do this, a neutron must collide with something of similar size (e.g. a hydrogen atom) in order to transfer energy efficiently. This is one of the roles of the water within the core

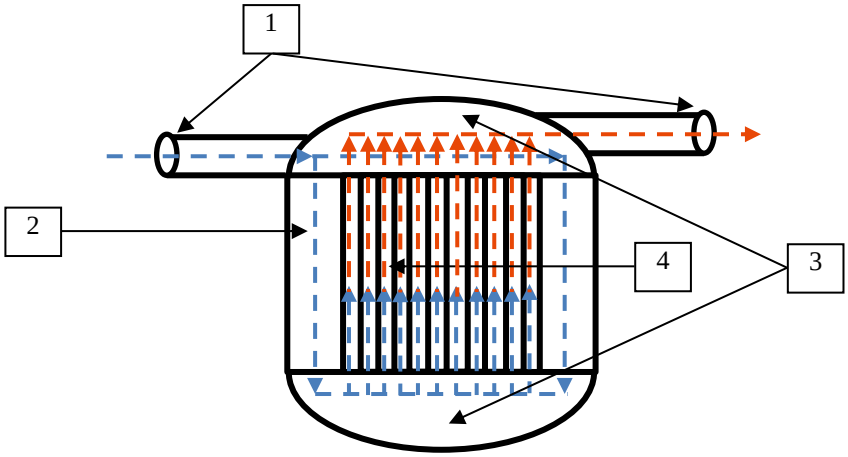

Figure 1: Layout of a typical LWR

In a LWR, the core is most commonly a structured array of square fuel assemblies[1]. Each assembly contains a structured array of fuel pins and guide tubes, which may contain control rods or instrumentation equipment (Pressurised Water Reactors – PWRs) or may contain only water for cooling and moderation (PWRs and Boiling Water Reactors – BWRs). Figure 2 and Figure 3 show the layout of PWR and BWR fuel assemblies.

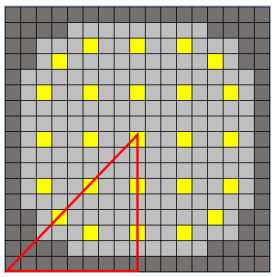

Figure 2: 17×17 PWR fuel assembly (yellow squares are guide tubes, light grey squares are Low-Enriched Uranium (LEU) pins, dark grey squares are MOX pins); red segment is the octant subunit to indicate symmetry; taken from (Charles, 2015)

[1] In Russian style PWRs these are hexagonal, rather than square.

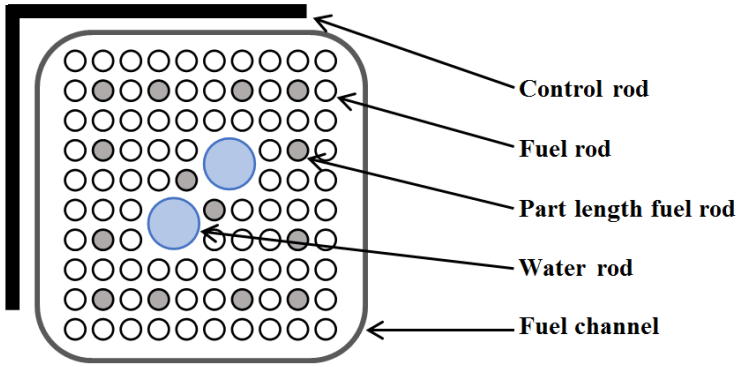

Figure 3: ¼ (lower right) of an ABWR cell, featuring one fuel bundle and the central control rod cross, adapted from (Hitachi-GE, 2017a)

Considering the fuel pins themselves in more detail, they consist of concentric circular tubes containing fuel surrounded by cladding to prevent fission product release into the coolant. This is shown below in Figure 4.

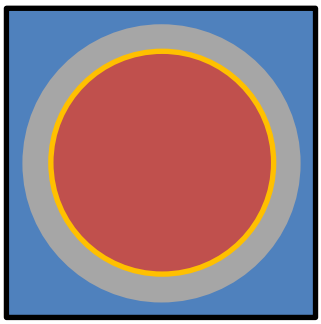

Figure 4: Fuel pin anatomy. From inner to outer segments: fuel, fuel-cladding gap, cladding, moderator/coolant (not to scale)

Of primary interest to a nuclear engineer is the amount of heat generated by these fuel pins as a result of nuclear fission. To analyze this one needs to determine the behaviour of neutrons within the system and the heat transfer that occurs as a result of the fission process.

1.2.1. *Neutron transport equation*

The solution to the neutron transport (Boltzmann, 1872) equation [1] describes the balance of neutrons within a system, their interaction with materials that results in absorption, fission, or scattering, and their change over time, energy, space and angle.

$$\frac{1}{\mathrm{v}}\frac{\partial\psi(r,E,\hat{\Omega},t)}{\partial t} = -\hat{\Omega}\cdot\nabla\psi(r,E,\hat{\Omega},t) - \Sigma_t(r,E,t)\psi(r,E,\hat{\Omega},t) + \mathrm{Q}(r,E,\hat{\Omega},t) \quad [1]$$

where $\psi(r, E, \hat{\Omega}, t)$ is the angular flux of neutrons at point r with energy E at time t travelling in direction $\hat{\Omega}$ within a unit volume, v is the average neutron speed, $\left[-\hat{\Omega} \cdot \nabla\psi(r, E, \hat{\Omega}, t)\right]$ is the number of neutrons flowing out of the space of interest, $\left[-\Sigma_t(r, E, t)\psi(r, E, \hat{\Omega}, t)\right]$ is the total absorption of neutrons and scattering to energies or points out of the space of interest, $\mathrm{Q}(r, E, \Omega, t)$ is the total production of neutrons within the space of interest (fission, scatter, or source). $\left[\frac{1}{\mathrm{v}}\frac{\partial\psi(r,E,\hat{\Omega},t)}{\partial t}\right]$ is therefore the rate of change in the neutron distribution over time. There are many methods used to solve the neutron transport equation and an exhaustive discussion is outside the scope of this thesis. For this work, the primary method used to solve this equation involves reducing the partial differential equation [1] to a series of ordinary differential equations by the Method of Characteristics – MoC (Bell & Glasstone, 1970).

A number of assumptions can be made to simplify the neutron transport equation. Firstly, the current work is solely concerned with steady-state problems where the delayed neutron effect is in equilibrium with the neutron flux and the fission production term describes both prompt and delayed neutron production, so $\frac{\partial\psi}{\partial t}$ can be assumed to be zero. Secondly, treatment of the energy distribution in the Boltzmann equation is usually performed in one of two ways. Either the neutron energy distribution is represented as a continuous spectrum (as often seen in Monte Carlo codes), or as a series of discrete groups with variable widths designed to sufficiently model the fidelity needed in the important energy regions (known as multigroup codes). The discrete group representation is used in this research. For LWRs in this work which predominantly feature UOX and MOX fuel, these regions are as follows (also highlighted in Figure 5):

- The thermal spectrum for U235 and Pu239 (where the majority of fissions will take place)
- The resonance regions for fissile fuels (e.g. uranium and plutonium) which feature strong variation in cross-sections due to the quantum nature of nuclear force
- The fast region. Fission that occurs here in both U235 and U238 (the latter due to high presence of U238 in the reactor) forms the fast fission factor contribution to k-effective, the effective neutron multiplication factor

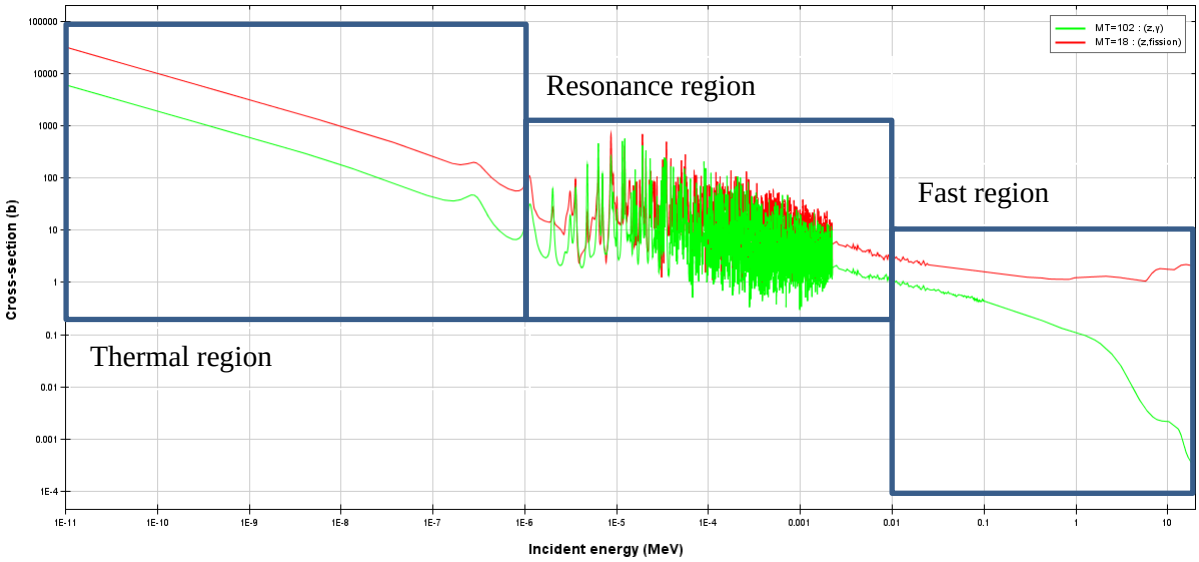

Figure 5: Fission (red) and radiative capture (green) cross-sections (barns) for U235 for different energies of incident neutrons, adapted from (OECD, 2019)

The methods for describing exactly how these regions are defined in modern reactor physics multi-group codes will not be covered here, nor how sub-groups within the resonance regions are treated to capture effects such as nuclide-specific resonance self-shielding as this section is meant only to give an overview of the theory. However, it should be noted that resonance effects are highly important (for example in U238 self-shielding).

Finally, we can also assume neutron transport medium is isotropic. This yields the steady state equation [2] below.

$$\hat{\Omega} \cdot \nabla \psi_g(r, \hat{\Omega}) + \Sigma_g^t(r) \psi_g(r, \hat{\Omega}) = \mathrm{Q}_g(r, \hat{\Omega}) \qquad [2]$$

where $\psi_g(r, \hat{\Omega})$ is the angular flux of neutrons per unit volume at point r within energy group g travelling in direction $\hat{\Omega}$, $[\hat{\Omega} \cdot \nabla \psi_g(r, \hat{\Omega})]$ is the net number of neutrons flowing out of the space of interest with the angular neutron flux ψ_g (for a given group g) over the space and angle $(r, \hat{\Omega})$, Σ_g^t is the total macroscopic cross section of absorption and scattering in the g-th group at point r and $\mathrm{Q}_g(r, \hat{\Omega})$ is the g-th group total neutron production over $(r, \hat{\Omega})$.

Q_g can then be given by equation [3], which shows the eigenvalue group form of the steady-state neutron transport equation with no external source.

$$\mathrm{Q}_g(r, \hat{\Omega}) = \sum_{g'=1}^{G} \int_{4\pi} \left(\frac{\chi_g \nu \Sigma_{fg'}(r)}{k} + \Sigma_{sg' \to g}(r, \hat{\Omega}' \cdot \hat{\Omega}) \right) \psi_g(r, \hat{\Omega}') d\hat{\Omega}' \qquad [3]$$

where $\sum_{g'=1}^{g}\int_{4\pi}$ represents the integration over all groups and angles, χ_g is the g-th group fission spectrum, v is the average number of neutrons produced from fission, $\Sigma_{fg'}$ is the g-th group fission macroscopic cross section, k is the fundamental mode eigenvalue, and $\Sigma_{sg'\to g}(r, \widehat{\Omega}' \cdot \widehat{\Omega})$ represents neutron scattering into the region of interest.

Using the MoC (Bell & Glasstone, 1970), the integral neutron transport equation can be converted into a set of ordinary differential equations to describe the variation of the angular flux along a characteristic defined by a series of straight lines $r = r_0 + s\widehat{\Omega}$, giving equation [4].

$$Q_g(r_0 + s\widehat{\Omega}, \widehat{\Omega}) = \frac{d}{ds}\Psi_g(r_0 + s\widehat{\Omega}, \widehat{\Omega}) + \Sigma_g^t(r_0 + s\widehat{\Omega})\psi_g(r_0 + s\widehat{\Omega}, \widehat{\Omega}) \quad [4]$$

where s is a distance to r measure from a starting point r_0 on the characteristic line or 'track'. Equation [4] can then be used to represent the model using a number of these characteristic tracks. In the Winfrith Improve Multigroup Scheme (WIMS), the reactor kinetics software used in this research, tracking parameters are set by the user to divide up the model into a number of azimuthal (x-y plane) and polar (z plane) angles, as well as the track separation. These numbers should be high enough (or low enough for track separation) in order to accurately represent the model without requiring an unacceptable increase in computational time. In this research, the Method of Characteristics is used by the CACTUS module with 9 azimuthal angles, 5 polar angles and a track separation of 0.1 cm (consistent with (ANSWERS, 2018)) to solve the neutron transport equation and produce a value for the eigenvalue k-effective (the average number of neutrons produced from one fission that cause another fission). The fission power can then be calculated by multiplying the fission rate with the average energy produced from fission (~200 MeV). Performing this calculation on a per pin basis gives the relative pin power distribution and allows one to work out the pin with the highest relative power. The ratio of the power of this pin to the average power produced within all the pins is known as the Power Peaking Factor (PPF). Fuel assemblies with high PPFs result in uneven depletion and are at greater risk from fuel exceeding temperature limits.

1.2.2. *Heat and fluid transport equations*

Modelling heat conduction through the fuel pellet, gap and cladding is performed using the steady-state heat conduction equation (Poisson equation for steady-state conditions) and requires knowing the thermal conductivity of the fuel, gap and cladding. Heat transfer *via* convection within the fuel-cladding gap through the inert and fission product gases will also occur (although this is not typically modelled except in very high-fidelity codes). Heat transfer from the cladding to the boundary layer of the coolant is by conduction, and transfer into the bulk *via* convection is described by Newton's law of cooling.

For LWRs, the heat transfer coefficient can be calculated using the Dittus-Boelter equation [5] to determine the Nusselt number, which is the ratio of the convective heat transfer in the coolant to the conductive heat transfer on the surface of the fuel pin (Hewitt, et al., 1994).

$$Nu_{Dh} = 0.023\, Re_{Dh}^{0.8} Pr^{0.4} \quad [5]$$

where Re is the Reynolds number and Pr is the Prandtl number, for a given hydraulic diameter[2] Dh. This describes the heat transfer within the channel assuming a single-phase coolant. In reality, LWRs feature two-phase flow. In BWRs there is bulk boiling in each channel, and in PWRs there will be some local nucleate boiling, followed by condensation further up the channel. In both cases various experimentally derived correlations exist for describing the boiling mechanism. The Navier-Stokes equations for conservation of mass, momentum and energy describe the flow up the channel, and there are various methods for solving these equations, through assumptions and simplifications. These equations must also take into account the multiphase nature of the problem, either through solving the equations for both phases (two-fluid) or assuming a mixture model (Homogeneous Equilibrium Model) with appropriate corrections for voidage, sub-cooled quality and slip. Finally, further correlations are used to determine performance parameters such as the Critical Heat Flux (CHF), which describes a point in the boiling regime beyond which a layer of vapour forms at the cladding surface and drastically decreases heat transfer performance. This is also known as Departure from Nucleate Boiling (DNB). This can result in excessive fuel temperatures and potential fuel failures. Two such correlations are the Westinghouse-3 (W3) correlation and the Electric Power Research Institute (EPRI) correlation. The W3 correlation is given by (Tong & Weisman, 1996):

$$q_{CHF}^{"} = K_1(p, x_e) \times K_2(x_e, G) \times K_3(x_e, D_h) \times K_4\left(h_f, h_{in}\right) \quad [6]$$

where p is the pressure, x_e is the local quality, G is the mass flux, D_h is the equivalent heated diameter, h_f is the saturated liquid enthalpy and h_{in} is the inlet enthalpy. $K_1 - K_4$ are empirically-derived functions. Here the calculated CHF is then corrected for axially non-uniform heat flux to find the local CHF at the point of DNB.

The EPRI correlation developed for PWRs and BWRs is given by (Reddy & Fighetti, 1983):

$$q_{CHF}^{"} = \frac{A - x_{eq,in}}{C + \frac{x_{eq} - x_{eq,in}}{q_w^{"}}} \quad [7]$$

[2] The hydraulic diameter is equal to $\frac{4A}{P}$ where A is the area of flow and P is the wetted perimeter.

Where $x_{eq,in}$ and x_{eq} are the inlet and local equilibrium qualities respectively, q''_w is the local heat flux and A and C are functions of the local mass flux and reduced pressure $\left(\frac{local\ pressure}{critical\ pressure}\right)$. Further empirical correction factors can be included for the effects of space grids and cold bundle walls.

As part of my industrial internship at Jacobs (then Amec Foster Wheeler), I was responsible for programming the capability for the thermal-hydraulics module ARTHUR to calculate CHF values using these correlations, as well as implementing the Tong 68 (Tong & Weisman, 1996) CHF correlation and the Groeneveld CHF lookup table (Groeneveld, et al., 2017). I was also responsible for implementing an axial channel pressure drop model consisting of gravity, acceleration and friction (Blasius, 1913), and incorporating Armand (Armand, 1959) and EPRI (Reddy, et al., 1982) two-phase friction correlations. In addition to implementing these correlations, I took part in validation of the model against the OECD/NRC 2012 PWR Benchmark (OECD/NEA, 2012). This features experimental measurements for a series of single channel tests to determine void fraction up the channel. The results of the ANSWERS code (then referred to as SUBCHANNEL) can be seen in Figure 6, which also features the results of the other benchmark participants, as well as the measured value.

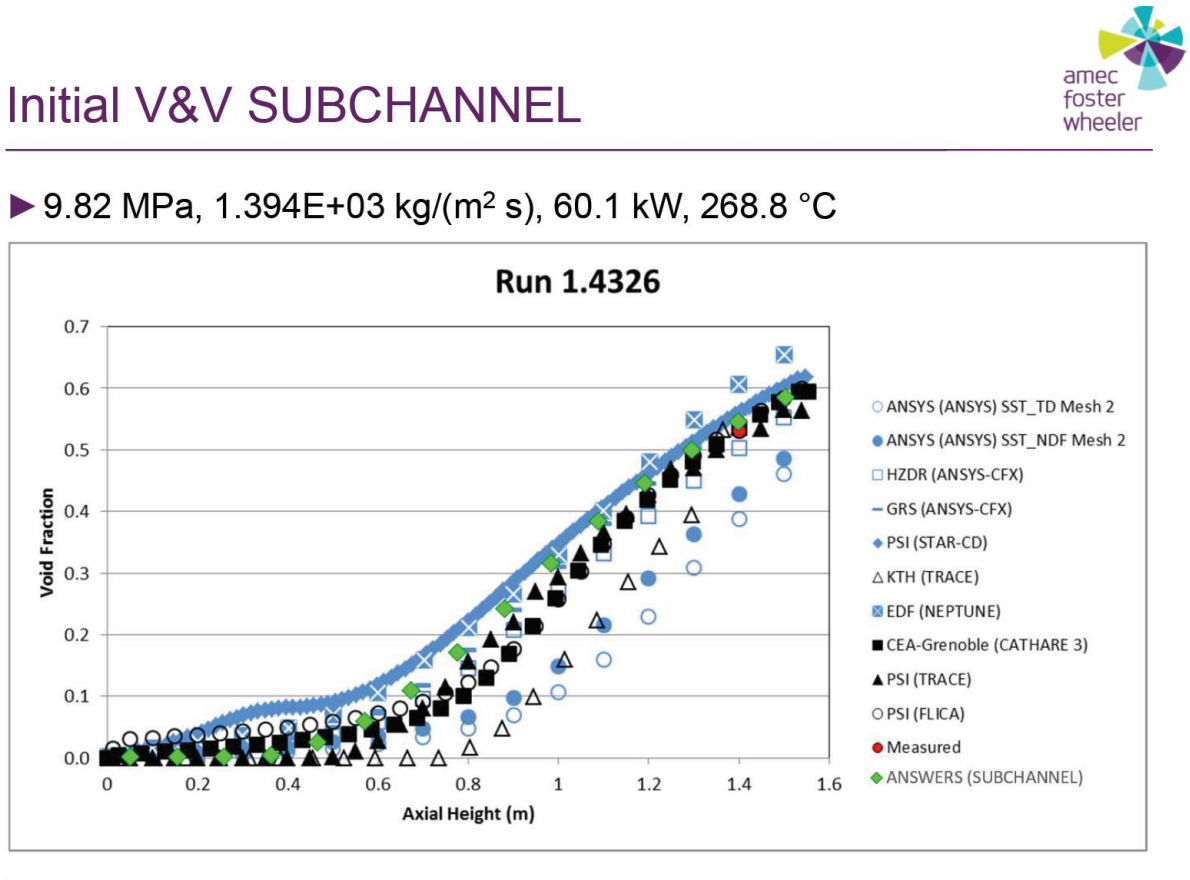

Figure 6: Results of SUBCHANNEL validation against the OECD/NRC 2012 PWR Benchmark (ANSWERS, 2017)

The results showed that SUBCHANNEL performed comparably with the other benchmark participants and accurately predicted the void fraction in multiple tests. These developments and validation results were featured at the ANSWERS Seminar in 2017 (ANSWERS, 2017).

1.3. Optimization in nuclear engineering

Two of the main challenges currently facing the nuclear industry are how to deliver continual improvements in safety and at the same time pursue innovative designs, which can reduce the overall cost of manufacturing and operating new nuclear plants. Satisfying both demands is not easy, since the adherence to the former tends to increase capital cost, and the latter often cannot be implemented if it adversely affects the former. However, even when one sets aside the effects of regulation and governmental policy, nuclear reactor design remains a highly complex and non-linear problem, where parameters are interrelated and are subject to a large number of constraints. As will be shown later in this section, one of the most common forms of optimization involves maximizing k-effective whilst minimizing local PPFs. As optimization techniques have developed, the range of parameters which can be considered simultaneously has expanded, and, as this section will show, metaheuristic algorithms (algorithms designed to converge to an optimal solution given limited data) in particular show great promise in finding the best combination of design parameters which satisfy the constraints and optimize the objective function of the design. The landscape is also changing: conventional PWR designs typically use a single fuel type with variations limited to a small number of zones. This is partly to ease the manufacturing process, but also because each fuel type must undergo a qualification process and, without demonstrable benefits in performance, it is cheaper to have fewer fuel types. However, there is growing interest in the use of heterogeneous fuel assembly designs, where both radial and/or axial changes in fuel type and composition have been shown to provide advantages over conventional designs. It is clear that formal optimization methods are needed here, where highly non-linear functions, fixed constraints, and multiple desired objectives give rise to a high-dimensionality problem. For example, the increase in local power peaking of a fuel pin as its radius increases is expected to be non-linear as its volume and hence mass of fissile material increases with r^2, and constrained by factors such as the distance between pins, CHF in the channel, or structural limits within the fuel gap and cladding. Neighbouring and nearby pins, their composition, and the fluid dynamics of the system will all have an impact. There is a large variety of optimization methods on offer (see below), and some have been previously applied to problems in nuclear engineering in real life, such as core reloading optimization problems, which constitute the majority of the research literature. The current state-of-the-art in optimization methodologies with respect to representative fuel assembly design problems is detailed in the following section, as well as optimization methods applied to burnable absorber designs and control

rod programming. By demonstrating the current gaps in this area, this review seeks to justify claims for the originality and innovation of this thesis.

Metaheuristic algorithms covered in this review generally fall into one of four distinct approaches. These are Simulated Annealing (SA), Particle Swarm Optimization (PSO), Genetic Algorithms (GAs), and Differential Evolution (DE). This overview will begin with an explanation of single-objective *vs*. multi-objective optimization and the concept of Pareto-dominance, followed by a brief introduction to each method. The state of the literature will then be discussed, concentrating on optimization of nuclear fuel assemblies. Key references including methods and strategies that directly pertain to this project will be highlighted, before final concluding remarks are given.

Techniques that will not be discussed in detail in this thesis include more classical approaches such as linear (Suzuki & Kiyose, 1971), quadratic (Tabak, 1968) and dynamic programming (Stout & Robinson, 1973). All have been used in the past to optimize activities such as nuclear fuel reloading. However, all such approaches require some simplifying assumptions or the use of single-objective functions in order to tackle the problem. (Pereira, et al., 1999) showed that not only did the GA outperform classical methods, but also that the linear programming method is especially susceptible to becoming trapped in local optima.

One general observation within the area of mathematical optimization is that many papers reporting 'new' algorithms enthuse about their analogies with the natural world, and perhaps overextend such analogies on occasions. Indeed, a particularly interesting paper (Sorensen, 2015) exposes the overuse of claimed parallels with the biological world when describing algorithms, and shows that in practice these 'new' algorithms actually differ very little from traditional algorithms. This opinion is supported by two papers (Weyland, 2010) and (Weyland, 2015) which critique specifically a method called 'harmony search'[3] showing that it fails to differ substantially from existing methods and also showing that the performance is bounded by existing methods. Instead, it is important to focus on exactly how a new algorithm differs from predecessors and how the algorithm demonstrates clear improvements on previous work. Including some standardised comparison(s) (such as the one used in (Pereira, et al., 1999)) would be a good way to demonstrate improvements. Furthermore, lengthy algorithm run times described in older studies become less of a concern given the advantages of modern computing technologies such as parallelization.

[3] The Harmony Search (HS) algorithm was developed by (Geem, *et al.*, 2001) and is based on the improvisation of music players. In (Geem, 2009), the application of HS to a wide variety of problems, both in engineering and other disciplines, is explored.

However, computational efficiency is not to be disregarded completely, especially when looking at more complex problems, such as those featuring radial and axial fuel assembly optimization simultaneously. Since the evaluation step is the most computationally intensive, simplifying the problem by means of decreasing the resolution or using simpler methods (*e.g.* collision probability *vs.* MoC) or performing optimization in stages (*e.g.* neutronics followed by thermal hydraulics) are all common methods of reducing the time taken to evaluate solutions. However, these will all impact the ability to model objective trade-offs accurately. Furthermore, determining the algorithm efficiency itself on a given problem requires knowledge of the Pareto-front, which is not usually available in real-world problems and requires accurate results with which to compare. Therefore, comparisons between algorithms on real-world problems are usually done based on relative performance, not on computational efficiency. Since the goal of this research is to produce a reliable tool that can aid nuclear engineering design problems in the real world, the requirement is for an algorithm that can produce accurate results in a reasonable (*i.e.* days to weeks, depending on the complexity of the problem) length of time rather than an algorithm that requires only a few evaluations but produces inaccurate (and therefore unreliable) results.

1.3.1. *Single-objective versus multi-objective optimization*

When an optimization problem consists of evaluating solutions against their performance on one objective, it is considered single-objective (SO). When solutions are evaluated against their performance on more than one objective simultaneously, it is considered multi-objective (MO). Many different objectives in engineering problems often compete with one another (such as maximizing k-effective *vs.* minimizing PPF, margin to DNB *vs.* maximum heat flux, size of the core *vs.* coolant channel gap), and so MO solutions represent the trade-off between objectives. It is, however, possible to use SO algorithms in a MO environment, and the following two techniques are commonly employed in order to do so (Sawaragi, et al., 1985) and (Parks & Miller, 1998). These are:

1. Weighting the individual objectives to create a single composite objective function
2. Constrain all objectives but one to focus optimization upon the remaining objective

Since the order of sequencing the constraints and the constraint limits or the degree to which the objectives are weighted are most likely based on the judgement of the designer (Parks, 1996), the results of such an approach would be impacted by the subjectivity of the individual. This is especially true of problems which have high-dimensionality and adversely affects the confidence in the results and the ability of the algorithm to find the global optimum, *i.e.* the solution which outperforms all other possible solutions with respect to the desired objective.

For MO problems without weighting or constraining to a SO problem, the concept of 'Pareto-dominance' (which avoids reliance on designer judgement) can be used to find the area of the global optimum (Yilmaz & Tufekci, 2017). The term 'area' is used, because there is unlikely to be one global 'best' solution in a MO problem. Pareto-dominance is used to describe a solution that 'dominates' another which it does if it is equal or better in all objectives and strictly better in at least one. This is shown below in Figure 7, where Obj1 and Obj2 are two objectives to be minimized. The theoretical optimal solution in this case lies at the origin, although in reality this theoretical optimum may not be possible.

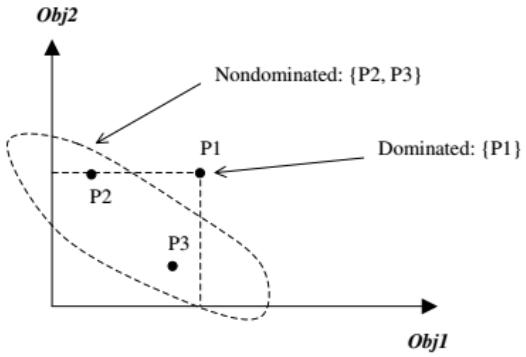

Figure 7: Diagram showing non-dominated and dominated solutions for two objectives (Pereira, 2004)

P2 and P3 can be said to 'dominate' P1, with P2 being equally as good as P3 (better in one objective and worse in the other, also known as 'Pareto-equivalence'). By finding and evaluating all possible solutions, the set of optimal non-dominated solutions (the Pareto-front) can be found for the problem, shown in Figure 8 below.

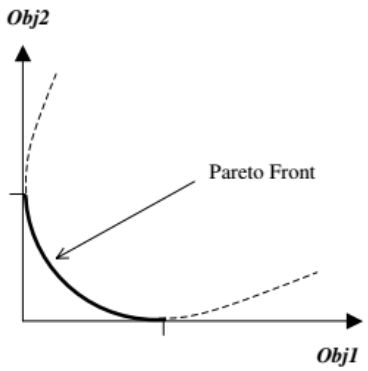

Figure 8: An example of a Pareto-front in a two-objective optimization problem (Pereira, 2004)

In summary, for MO problems the global optimum can be seen as a set of solutions which perform equally well against the given objectives, such that no solution exists which performs better than any of

the set for all objectives. This set of solutions is therefore described as "non-dominated" and forms the Pareto-front of possible optimal solutions. Exhaustive enumeration of all possible solutions is usually not practicable for real-world problems, and thus the found Pareto-front is an approximation of the true one. A MO algorithm that performs well should always find the Pareto-front covering the global optimum regardless of the initial starting point.

Evolutionary algorithms (EAs) attempt to navigate the solution space by improving on the discovered Pareto-front through successive iterations, until a maximum (*i.e.* non-dominated or best) is found, which can represent the area of the global optimum. Whether or not a MO or SO algorithm is required will generally depend on the problem being optimized. If a great deal is known about the search space of the problem, then the objectives can safely be constrained or modelled as a single function. However, for nuclear engineering problems such as those covered in this work, the search space is generally unknown and it is here where MO algorithms utilizing the concept of Pareto dominance can really 'dominate'. For example, (Pereira, 2004) compared a Single-objective Genetic Algorithm (SOGA) to a Multi-objective Genetic Algorithm (MOGA) for a typical nuclear fuel pin optimization problem of maximizing the average neutron flux whilst minimizing the PPF. For the SOGA, these were combined into a single linear function. For the problem, the MOGA was found to produce better solutions than the SOGA by treating both objectives simultaneously. Another example is (Jayalal, et al., 2015b), who compared a penalty function based SOGA to a MOGA and found the MOGA to outperform the SOGA in both convergence speed and diversity in solutions.

Elitism and diversity (*i.e.* the chance for solutions not considered 'best' to be preserved in the population) are other key differences between SO and MO problems. In SO problems, the solution which performs best with respect to the objective is often all that is required. In MO problems, the population needs to maintain a diverse set of solutions (unless there is a single solution dominating all others), otherwise the algorithm loses knowledge of the solution space and risks getting stuck in local optima, behaviour which is known as "premature convergence". Local optima (also known as local minima when the objective(s) are to be minimized) are clusters of possible solutions in the search space which are superior to neighbouring solutions but remain dominated by the Pareto-front. Algorithms which display premature convergence lack the ability to accept an inferior solution with the hope that in the future it may lead to a globally superior solution. In real-world problems, the response of a single objective function with respect to its variables may likely exhibit non-linear and complex behaviour (*e.g.* maximizing the heat flux to the coolant from a fuel pin), which may itself influence the convergence of an algorithm. In algorithms featuring a population, this is characterised by the speed of members of the population as they move through the search space. If some members encounter an area of the search space where convergence is quick, this can bias the population as a whole, as those individuals are more likely to create improved offspring. For GAs with a fixed population, this means other individuals which

occupy part of the search space where optimization is difficult are less likely to produce offspring that can successfully compete to stay in the population. For MO problems, this effect is compounded as some trade-offs involved produce n-dimensional hypervolumes within the existing n-dimensional search space that are more difficult to search than others, which therefore can bias the convergence of the algorithm to only a subset of the true Pareto-front (Ando & Suzuki, 2006). As is discussed below, algorithms are vulnerable to becoming trapped in 'local' optima, and often a key feature of modern algorithms is the inclusion of mechanisms for avoiding this problem.

1.3.2. *Simulated annealing*

SA was originally developed by (Metropolis, et al., 1953) and is designed to simulate the change in atomic structure, grain sizes and distribution in a solid in a heat bath as it cools to thermal equilibrium, using the Monte Carlo technique. It was further developed into a local search heuristic by (Kirkpatrick, et al., 1983) and (Cerny, 1985), and mimics the physical annealing process of solids, where changing the rate of cooling affects the final state of the solid. SA considers solutions similar to existing ones as potential solutions. Selection of a new solution is based on both the performance of the solutions against the pre-defined objective (fitness value) and the probability that poorly performing solutions will be accepted. This probability is governed by the amount of time the algorithm has been running for and decreases over time. How quickly it decreases (known as the 'cooling rate') is set by the algorithm control parameters. Like the mutation and crossover processes seen in Genetic Algorithms (GAs) and in Differential Evolution (DE) (see sections 1.3.4 and 1.3.5 respectively), the retention of solutions which lead to poorer values of fitness helps prevent the SA algorithm from becoming trapped in 'local optima' (Parks, 1990). This feature is very important for problems which feature a high degree of non-linearity in solution performance and thus contain many local minima. An example SA flowpath is given below in Figure 9.

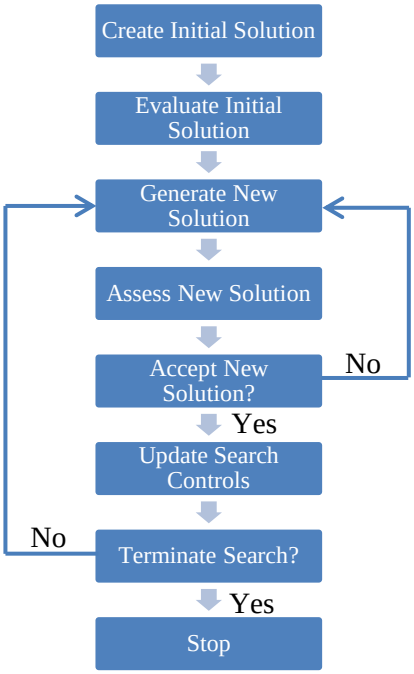

Figure 9: Example of a SA flowpath, adapted from (Parks, 1990)

SA has been actively used in optimization for nuclear reactors. Examples include a study by (Parks, 1990), who used SA to minimize the running cost of the fuel by varying fuel enrichment, burnable poison worth, poison burnout irradiation, fuel discharge irradiation, average reactor flux level, and coolant flow rates, subject to a number of constraints. As mentioned by the author, choosing the right cooling rate is vital to avoid becoming trapped in local minima. The cooling rate should be set sufficiently low so as to avoid premature convergence ('quenching'), and a study by (van Laarhoven & Aarts, 1987) indicated that under the right conditions SA will always converge to the global minimum, given enough time. However, this guarantee is not of much comfort to the average nuclear engineer, who usually has a set budget and delivery time to work to! It is also noted by (Smith, et al., 2008) that SA requires significant alteration in order to deal with a multi-objective problem, without resorting to weighted sums of objectives.

1.3.3. *Particle swarm optimization*

PSO was first proposed by (Eberhart & Kennedy, 1995), and is based on the flocking behaviour of animals. PSO represents solutions as 'particles', and the population is a 'swarm'. Each particle has a position in the search space and a velocity, which moves that particle to a new position. Once all particles have been moved, the best positions of each particle and the swarm are updated, and each velocity is adjusted in order to move the swarm towards the most optimal area of the search space. The history of the swarm's position and its performance is recorded, and a control measure, known as the Inertia Weight Factor (IWF) (Khoshahval, et al., 2011), is set by the user and determines the impact of the previous history of velocities on the current velocity. Larger IWF values encourage broadening of the

swarm and a greater global exploration, whilst smaller values allow for narrower, refined local searches. The velocity is updated based on three components: the previous velocity, the history of the individual particle, and the history of the whole swarm. Each component has its own weighting factor set by the user. A flowpath of PSO can be seen below in Figure 10.

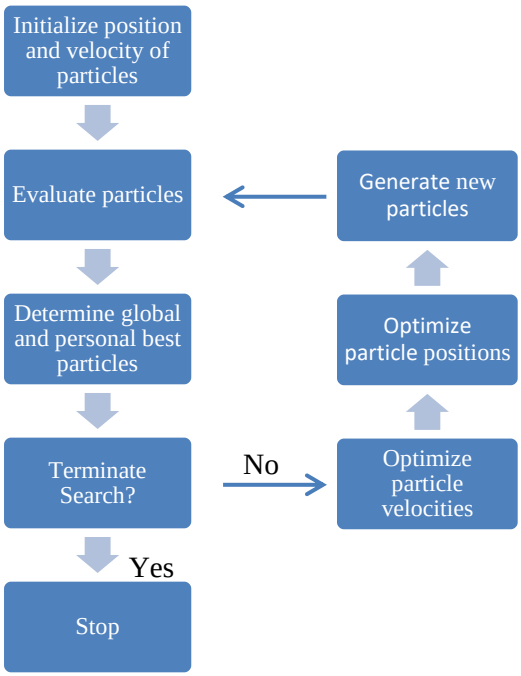

Figure 10: Example of a PSO flowpath, adapted from (Babazadeh, et al., 2009)

Using IWF to direct the swarm using a guided, rather than a random, factor was shown to cause PSO to become stuck in local optima by (Yadav & Gupta, 2011). Various attempts to avoid premature convergence have been made, including combining PSO with an adaptive local search method in a hybrid algorithm (Tang & Zhao, 2010), using an alternative control measure to IWF called the Constricted Factor Approach (Clerc & Kennedy, 2002) and (Yoshida, et al., 2000), and regrouping the swarm once premature convergence is detected (first proposed by (Bergh, 2002) and later employed by (Evers & Ben Ghalia, 2009)). As a result, multi-objective PSO algorithms typically employ some sort of mutation operator (known as a 'turbulence' operator), thus making them behave more similarly to GAs (Reyes-Sierra & Coello, 2006). Several different methods have been proposed to adjust the selection of the leader particles (which dictate velocities of other swarm particles) to apply them to multi-objective problems. These include nearest neighbour density estimation (Deb, et al., 2002), and a 'Kernel' density estimator, also known as 'niching' (Goldberg & Richardson, 1987). Niching involves forcibly maintaining a heterogeneous population and has also been used for GAs, known as 'Fitness Sharing' (Goldberg, 1989). Developing PSO algorithms for MO problems generally involves expanding the ability to hold particle / swarm history, as noted by (Trivedi, et al., 2020), in order to increase

diversity and prevent local convergence. Despite the IWF feature, PSO is inherently weaker in its use of histories for ensuring diversity when compared to EAs.

1.3.4. *Genetic algorithms*

GAs are part of the class of EAs. All EAs attempt to find an optimal solution by mimicking the biological concepts of selection, reproduction and mutation by modifying a 'population' of solutions. GAs, the most well-known implementation of EA, were pioneered by (Bremermann, 1962) as a way to search for the optimum of a function in a population of individuals (possible solutions) by recombining their components, and the methodology was further developed by (Holland, 1992).

As (Pereira, et al., 1999) explain, in a conventional GA implementation the variables are codified into 'genes' comprised of binary bits. This means that GAs are fundamentally more suited to problems featuring discrete variables (*i.e.* variables with stepped values). Once all the variables for a particular solution have been acquired, this forms a 'genotype', which is then evaluated to determine its performance against the objectives. Genotypes are ranked, and superior genotypes are given a higher chance to survive the selection process and pass their genes on to the next generation. Reproduction is carried out through the twin processes of *crossover* and *mutation*. Crossover involves swapping of pairs of genes between parents during the creation of 'offspring' solutions, and mutation is the spontaneous conversion of individual genes to their binary complement. Mutation ensures diversity in the population and provides chances for weaker or unknown genes to survive. This reduces the risk of the algorithm converging prematurely, specifically known as "genetic drift" for GAs (Goldberg, 1989).

The offspring, or next 'generation' of solutions, represent the evolution of the population, and it was shown by (Goldberg, 1989) that, with suitable choices for the selection scheme and the crossover and mutation operators, this process statistically results in an overall trend of stronger individuals in each generation, gradually concentrating to near-optimum regions. An example flowpath for a GA is shown below in Figure 11. The evaluation step in nuclear engineering problems usually requires running some sort of physics software which models the phenomena under consideration so as to determine the performance of the solution against the pre-determined objective.

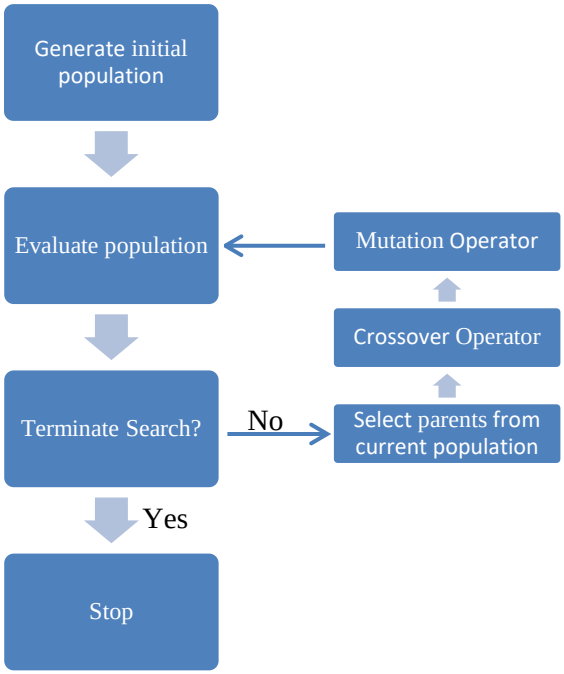

Figure 11: Example of a GA flowpath, adapted from (Khoshahval, et al., 2011)

A downside of GAs is the many control parameters which govern the behaviour of the algorithm, making certain operations (such as crossover or mutation) more or less likely depending on the values of these parameters. When applied to a new problem for which little is known about the search space, where optimal solutions might lie, or how the design variables interact (as is most often the case with engineering problems), these algorithms may exhibit poor performance if a period of parameter 'tuning' is not performed first on the chosen problem. This results in increased computational requirements and can potentially mislead the engineer about the nature of the search space. Tuning can be simplified significantly if the algorithm contains some form of adaptive parameter control, whereby the parameters are dynamically adjusted using feedback from the search process, enabling the algorithm to adjust itself as it searches, leading to faster and more reliable convergence. For MO problems, these issues are compounded further. However GAs are still considered the "go-to" algorithm for many approaches, including MO, as their population closely mimics the idea of a Pareto-set (Marler & Arora, 2004).

1.3.5. *Differential evolution*

DE algorithms are another EA, developed by (Storn & Price, 1997) and based on GAs but with some significant differences between the two. New solutions are created by first determining the difference in parameter values of two selected solutions from the current population. This pseudo-solution of differences is scaled with a mutation factor, and then crossover occurs with a third member of the current population to create the new solution. New solutions are evaluated and their performance is compared to a current member of the population, only replacing that member if the new solution is superior. This

makes DE inherently more greedy (*i.e.* prioritising superior over inferior solutions) than GAs (in which solutions which perform worse than the current ones have a chance of surviving to the next generation) and thus DE algorithms typically have higher convergence rates as a result, as (Zio & Viadana, 2011) explain, with the downside of increased risk of premature convergence. As mutation happens before the crossover step, it has a greater influence over the searching methodology. The weighted difference method of mutation creates a self-organizing perturbation on the evolutionary process, because, as solutions converge, the range of possible mutations decreases and thus helps the algorithm to converge. Therefore, for DE, crossover is more important for maintaining diversity in the population, and also differs from GAs in that the crossover happens between a current member of the population and the new mutated pseudo-solution. The exact process of creating the weighted difference is referred to as the mutation strategy.

Two commonly used examples are (Storn & Price, 1997):

"DE/rand/1"

$$v_{i,g} = x_{r1,g} + \mathrm{F}_i \times \left(x_{r2,g} - x_{r3,g}\right) \quad [8]$$

where $v_{i,g}$ is the new mutated pseudo-solution (population member i in generation g), and $x_{r1,g}$, $x_{r2,g}$, and $x_{r3,g}$ are three randomly chosen parent solutions from the current generation (g). F_i is a weighting factor, which is either common for all i (classic DE, $\mathrm{F}_i = \mathrm{F}$) or is unique for each member of the population (adaptive DE).

"DE/current-to-best/1"

$$v_{i,g} = x_{i,g} + \mathrm{F}_i \times \left(x_{best,g} - x_{i,g}\right) + \mathrm{F}_i \times \left(x_{r1,g} - x_{r2,g}\right) \quad [9]$$

where $x_{i,g}$ is the solution of current member of the population, and $x_{best,g}$ is the best solution in the population.

In (Storn & Price, 1997), DE was noted for its computational speed compared to traditional EAs. This difference in performance also features in MO problems (see Section 1.3.1), as was noted in a study by (Tusar & Filipic, 2007) that compared well-known GAs against a DE algorithm. The results showed that DE outperformed GAs against the quality indicator for ~83% of the measured benchmark problems. The authors concluded that DE explores the solution space more efficiently than GAs. One drawback to the use of DE algorithms is the uncertainty over whether convergence has been achieved, as noted in (Hu, et al., 2013). Here, a number of conditions necessary to achieve global convergence are presented and the authors demonstrate how these allow the DE algorithm to escape local minima. However, it is noted that the addition of these auxiliary operators did impact on the computational cost, which is to be

expected as convergence algorithms tend to be more robust at the expense of computational competitiveness. A review of the DE state of the art by (Das & Suganthan, 2010) revealed a difficulty for DE in traversing the search space in problems that feature high degrees of clustering. Since areas of local optimality could feature in nuclear optimization problems, it is clear that any DE algorithm used in this research should therefore feature some mechanism to avoid clustering. This review also showed that DE was effective in MO problems and has been employed in a wide variety of real-world applications. DE algorithms have been applied to nuclear reactor core optimization, most notably by (Sacco, et al., 2009), who compared DE to both GA and PSO and found DE outperformed both and was less sensitive to parameter specification, which supports a finding by (Lampinen & Zelinka, 1999). In this research, DE algorithms were the chosen optimization methodology as they offer a competitive alternative to traditional optimization methods which have not yet been applied to fuel assembly optimization and offer the end user a "black box" method for optimization with minimal tuning.

1.3.6. *Core loading and control rod optimization*

Optimizing PWR and BWR loading patterns is the most common application of optimization algorithms to nuclear engineering problems. As assemblies burn at different rates depending on their material composition and position within the core, balancing the flux profile within the core becomes a challenge, particularly when fresh fuel is introduced. During a LWR core reload, around 1/3 of the fuel assemblies are replaced with fresh fuel and existing assemblies change position within the core. As a combinatorial problem, GAs have been highly utilized in this area, in both SO (DeChaine & Feltus, 1996) and (Yilmaz, et al., 2006), and in MO (Parks, 1996) and (Khoshahval & Fadaei, 2012) form for PWRs, in MO on Russian PWRs (Karahroudi, et al., 2013), and in SO on BWRs (Francois, et al., 2013). SA has also been used (Engrand, 1997), (Kropaczek & Turinsky, 1991), (Jessee & Kropaczek, 2007), as has PSO (Babazadeh, et al., 2009), and (Ahmad & Ahmad, 2018). Non-metaheuristic methods including non-linear programming (Hirano, et al., 1997) also feature in this field**.**

Loading pattern optimization is a very active and growing area of interest, as Figure 12 shows:

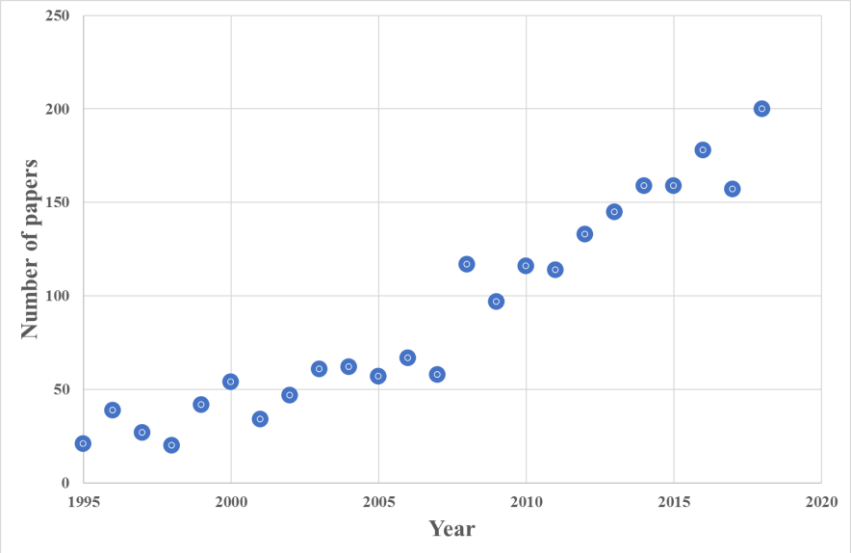

Figure 12: Number of papers published in Elsevier journals on loading pattern optimization of nuclear reactor cores, 1995–2019

However, since the focus of this research is fuel assembly optimization which relates to the physical design of the assemblies themselves, rather than the positioning of assemblies within the reactor core, a full discussion on the area of core loading optimization is outside the scope of this work. For further information on this subject the reader should refer to a recent comprehensive review article (Nissan, 2019).

Another area in nuclear engineering outside the focus of this research but still worth mentioning due to the successful implementation of optimization algorithms, is control rod programming for movement of grey control rods (used to flatten the distribution of power, or power-shape, as the core is depleted). Initially, the main methods used from the early 1970s until the early 1990s were simplified neutronics models combined with knowledge-based algorithms. A number of papers (Fadilah & Lewins, 1975), (Sekimizu, 1975), (Tsouri, et al., 1975), (Kawai, et al., 1976), (Hayase & Motoda, 1980), (Zhong & Weisman, 1984), (Tokumasu, et al., 1985), (Lin, 1990), (Lin & Lin, 1991) and (Taner, et al., 1992) show how expert knowledge was the main source of optimization, consistently applied to more and more complex neutronics models as computational power increased. More recently, however, metaheuristic algorithms have again shown application, exemplified by studies using GAs (Na & Hwang, 2006), (Liu, et al., 2009), and (Pan, et al., 2011), and PSO (Wang & Lin, 2013). The problems of control rod programming and fuel loading were combined in a study by (Ortiz, et al., 2007) and tackled using a

combination of PSO, GA and Artificial Neural Networks (ANNs)[4] to produce a successful iterative optimization system. Control rod programming for load following operation has also been demonstrated in the literature with GAs by (Lee, et al., 2011) and (Kim, et al., 2014), where the algorithm was able to track the various step-changes in demand.

Finally, before a discussion of optimization on LWR fuel assemblies, it is worth pointing out that optimization has also been investigated for other nuclear fuel applications, such as optimization of Liquid Metal Reactor (LMR) fuel (Raza & Kim, 2008) using a MOEA and (Qvist, 2015) using expert knowledge, or for non-nuclear related parts of a nuclear power plant, such as the use of MOGA to optimize a steam generator (Chen, et al., 2013).

1.3.7. *Optimization of LWR fuel and core design problems*

The application of formal optimization methods to the design of nuclear fuel assemblies and cores has received less interest than for loading pattern design problems. There are many possible reasons for this. For example, reusing burnt fuel in a loading pattern reduces the need to produce fresh fuel, lowering cost. It also allows one to flatten the radial power distribution to achieve a more even burnup, as well as increase performance margins. Conversely, a suboptimal loading pattern can cause the opposite. Historically, therefore, there has been a more pressing need to optimize loading patterns given that the fuel already exists and has been depleted. It is also easier to justify a loading pattern design that uses existing fuel than a design for a new assembly that uses a new fuel composition. Furthermore, the desire to optimize individual fuel assemblies has had to accommodate the presence of different fuel types within the same design (*i.e.* MOX fuel, which has only seen commercial use since the late 1980's (Fukuda, et al., 2000)) and is also driven by the desire to use up existing stockpiles of plutonium, a more recent objective in the nuclear industry. Nevertheless, three of the four most prominent metaheuristic methods detailed above have been applied in the area of fuel assembly design. These are discussed below, followed by consideration of some non-metaheuristic examples. Finally, literature on the more complex problems involving heterogeneous fuel types is reviewed. SO studies that do not use formal optimization methods or fail to include details of the optimization method used, such as the one by (Li, et al., 2018) which optimized a breeder blanket for a molten salt reactor with Th-U fuel, or (Liu & Cai, 2014) who optimized fuel pin geometries in a Th-U Supercritical Water Reactor (SCWR), are not discussed in detail here but do serve as examples of the wide variety of problems to which optimization can be applied to.

[4] ANNs are machine-learning algorithms that can be used to generate initial fuel lattice designs and loading patterns. Examples include (Montes, *et al.*, 2007) and (Ortiz, *et al.*, 2009). The main drawback is their learning phase, which must be repeated whenever new variables are introduced, similar to the 'tuning' period for EAs. However, unlike EAs new designs are not generated by ANNs until after the training period is over.

One of the most common fuel assembly optimization studies concerns radial optimization of a BWR fuel assembly for radial fuel enrichment including burnable poisons. Here, a combined and weighted objective function of k-effective, PPF, gadolinium oxide content and enrichment was used to form a SO problem. Algorithms were given a set range of fuel pin types to arrange in a 10×10 assembly with ½ symmetry and fixed water zones to try to minimize the objective function. Some examples of approaches to this problem include knowledge-based methods by (Tung, et al., 2015) and (Montes-Tadeo, et al., 2015). Whilst effective, knowledge-based methods as applied in the studies above necessarily require the use of heuristics: tailor made processes for solving a problem. They are unique to a single problem and do not work at all on other problems. A key focus of this research is a capability for optimizing many different problems, which requires the use of metaheuristics (a higher-level procedure which produces its own heuristic for a given problem, e.g. one of the methods discussed above). The BWR fuel assembly problem has also been investigated using PSO in (Montes, et al., 2011), (Castillo, et al., 2011), and also by (Lin & Lin, 2012) where it was combined with a local search method. These studies were able to produce solutions using PSO that improved with respect to a reference lattice design in under 24 hours of runtime, which is a testament to the convergence speed of PSO. In the case of (Lin & Lin, 2012) these were simple numerical weights, but in (Montes, et al., 2011) these were complex functions, making comparisons between the two studies even more difficult. GAs have also been used to optimize the BWR problem. The study by (del Campo, et al., 2007) focuses on gadolinium oxide distribution whilst (del Campo, et al., 2001) looks at axial distribution of fuel. Finally Tabu Search[5] has been applied by (del Campo, et al., 2002) (again focusing on the axial fuel distribution), (Francois, et al., 2003) and again in (del Campo, et al., 2007), this time combining Tabu Search with fuzzy logic. In all cases the use of a weighted objective function restricts the search space for the algorithm by prioritising certain areas.

Although there have been very few comparative studies performed, the paper by (Castillo, et al., 2014), is a particularly useful example which considered a number of methods applied to this problem. The algorithms investigated include the Ant Colony System (a type of PSO algorithm, originally developed by (Dorigo, 1992) and (Dorigo, et al., 1996)), ANNs, GAs, Greedy Search and Path Relinking with Scatter Search (PR+SS)[6]. Results were ranked according to performance against the objective function at zero burnup, at 70 MWd/kg, and against a custom "global cost" objective which considered computational requirement. For fresh fuel, the authors found that direct search methods and PSO found

[5] Tabu Search is a hill-climbing algorithm with a memory capacity to overcome local optima yet avoid revisiting previous solutions, formally proposed by (Glover, 1986). This has proven to be effective in both the design of BWR (Jagawa, *et al.*, 2001) and PWR (Hill & Parks, 2015) reload cores for a given initial loading pattern.

[6] PR+SS was developed by (Glover, 1998) and was used previously by (Castillo, *et al.*, 2011) to optimize a BWR fuel lattice for enrichment and gadolinia content. It is another population-based metaheuristic with a technique (Path Relinking) to force diversity within the population.

the best lattices.[7] For high burnup, the Greedy Search and GAs performed the best. For the global cost objective, GAs and the hybrid PR+SS algorithm had the best results. The authors noted that direct search methods (*i.e.* methods which search neighbours for superior solutions and do not use information such as the gradient of the objective function) were the most unpredictable.

(Washington & King, 2017) used a MOGA to optimize a fuel assembly for plutonium and actinide transmutation in LWRs, with three objective functions of achieving 1400 Effective Full Power Days (EFPD), reducing the quantity of fissile plutonium and reducing the quantity of minor actinides. The study was performed in three stages, focusing first on the geometry of a single pin, then to test the quantity and placement of these pins within a ¼ assembly, and then to reassess the fuel pin geometry. The resulting Pareto-front showed the trade-off between plutonium transmuted and curium produced as an unwanted by-product and suggested that the best compromise was for reductions of > 80 wt% Pu and > 50 wt% minor actinides. This study is a good example of the additional information about the system (*i.e.* quantifying the trade-off) that can be obtained through employing formal MO optimization methods, as the results are not tainted by the designer's choice of weighting factors.

GAs also frequently feature in hybrid methods for core optimization problems. For example, a study by (Janin, et al., 2016) used a surrogate model trained on 1000 pre-generated fuel assembly designs (then assessed on 1000 other pre-generated designs) and then combined that with a genetic algorithm to optimize a high-conversion SMR concept design with assemblies loaded with MOX fuel. The concept of Pareto-dominance was used with the objectives of maximizing k-effective, whilst minimizing relative peak power and void coefficient by varying three enrichment zones. By using the surrogate model, the genetic algorithm was run with a population of up to 30,000 in the tests (since the computational time required for evaluation was practically negligible), and a well-populated picture of the resulting Pareto-front was formed. This is a good goal for any optimization study as it gives confidence in the algorithm's ability to cover the search space. However, the high population of the GA would have been infeasible without using a surrogate model to eliminate the evaluation computational time. This surrogate model must be set up beforehand and trained on a set of results (in this case obtained using the APOLLO2 code), and can limit the scope of a problem to a lower dimensionality (as noted by the authors). As the present research focuses on a system that can easily adapt to many different problems with potential high dimensionality, combining metaheuristics with a surrogate model is not expected to a viable solution.

[7] The main focus of PSO appears to be on fuel reload, although this is not due to an inherent inferiority to GA. In fact, a study by (Lima Jr., *et al.*, 2011) found PSO to have both superior convergence rates and to produce better solutions than a comparative GA.

The reasoning behind hybrid methods is to utilize the GA's ability to quickly find the approximate optimal area, and then to use other methods to search locally. A study by (Turinsky, et al., 2005) showed that a GA followed by local SA optimization is an effective tool in nuclear fuel management; in core optimization, (Sacco, et al., 2004) used a GA and fuzzy logic to optimize three enrichment zones within a PWR. This used an extreme simplification of a reactor, shown in Figure 13.

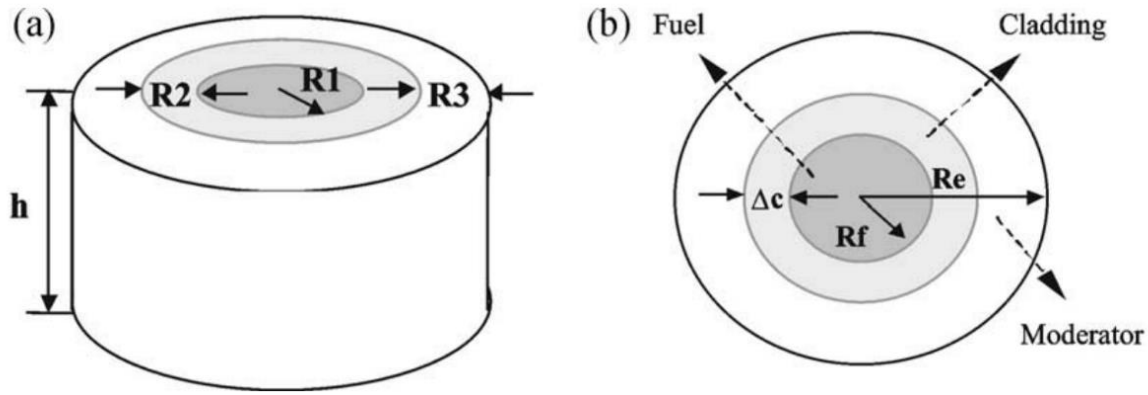

Figure 13: Radial enrichment optimization problem as featured in (Sacco, et al., 2004)

Parameters included the fuel radius (Rf), cladding thickness (Δc), moderator thickness (Re – Rf – Δc), as well as three different enrichments. The objective of the problem is to minimize the average PPF whilst constraining the k-effective to unity. This problem was also featured in a study by (Pereira & Lapa, 2003) using a GA and again in a follow-up study by (Pereira & Sacco, 2008) where the algorithm was hybridised with an "Island GA" (Cantu-Paz, 2000). Whilst the theory behind the methodology of each algorithm is explained in good depth in the papers, the actual testing of performance was underwhelming in comparison. As is common in optimization studies, comparison was done against competing algorithms rather than real-world data since the global optimum is rarely known. In (Pereira & Sacco, 2008) in particular, there was no statistical analysis of the results to determine whether the differences were due to differences in the methodology of the algorithms or just random chance, and the research featured just six individual experiments, a far cry from the usual 20–30 independent runs. For any system that can claim to be applicable to real-world nuclear engineering problems (such as the present research), some demonstration on real-world data must be performed and problems cannot be as heavily simplified as the one here. However, one notable conclusion of (Pereira & Sacco, 2008) was to point out the usefulness of parallelized architecture for reducing run time in GAs. This is necessary, as according to a review by (Jayalal, et al., 2015a) the main shortcoming of the GA process is the computational time and the requirement to tune control parameters to particular problems. A large number of evaluations are required in order to converge on a global optimum, and this performance varies substantially depending on how likely the population is to mutate, how often the crossover operation occurs between parents, and how elite or greedy the algorithm is. This makes intuitive sense

given the basis of evolution, a process which occurs over thousands and thousands of generations. For real-world problems, where evaluating a generated solution could potentially require hundreds of hours of run time on a supercomputer, algorithms like GAs, which take many generations to converge, are at a severe disadvantage compared to other methods. Selecting the correct parameters for mutation, crossover and the greediness of the algorithm takes additional training time, so a balance must be found.

Another hybrid method, (Odeh & Yang, 2016), used a SA algorithm to optimize the enrichment of fuel assemblies where individual pin cell optimization had first taken place, albeit based on expert knowledge and trial-and-error rather than any formal optimization method. Nevertheless, this study is notable as it combined neutronics (PARCS) with thermal-hydraulics (RELAP) *via* a general-interface.

(Shirvan & Kazimi, 2017) also combined SA with expert knowledge in their optimization of a BWR for high power density. Here optimization was performed over many aspects of the full reactor design, including neutronics, thermal hydraulics, fuel performance and economics. SA here was used to find the optimal power density given the constraints and to optimize pin location within assemblies to reduce pin and reactivity peaking. Given the design space consisted of 77 trillion possible combinations of designs predicted to take over 730 million years to evaluate, SA was clearly highly effective at finding an optimum design, however no details of the parameters used for the algorithm were included in the paper.

(Rogers, et al., 2009) used an adaptive SA algorithm to optimize radial pin enrichment and burnable poison location in a 15×15 fuel assembly, with an objective function consisting of PPF, enrichment and difference from a target k-effective. In this case, weights set by the designer were used to formulate a SO problem. The authors reported that the optimization took around 12 hours to run on a fairly standard PC set-up of a dual core 3.2 GHz processor, which is also a useful insight into how long one might expect more complicated and detailed optimization studies to last.

Other non-metaheuristic examples include the Simplex method, which was applied by (Vivas, et al., 2002) to optimize rod enrichment levels in a MOX LWR fuel assembly to achieve a target PPF, and (Dall'Osso, 2016) which used inverse perturbation theory (Ronen, 1979) to optimize densities of Gd, U235 and water to maximize k-effective in a PWR fuel assembly. Whilst being examples of LWR fuel and core design optimization, these are not MO, and indeed there do not seem to be any MO examples of non-metaheuristic algorithms applied to nuclear engineering design optimization problems.

For more complex fuel types, an example particularly relevant to this research is a study on PWR heterogeneous fuel assembly optimization conducted by (Yang, 2013), who looked at using a MOGA to optimize a PWR assembly using MOX fuel for minimum PPF and maximum plutonium loading in the form of MOX. The CORAIL MOX was chosen as the reference design and constraints were set on

a minimum number of Low Enriched Uranium (LEU) pins and a maximum allowable PPF (two common safety constraints). Using the WIMS lattice physics code (see Section 2.4), the algorithm was shown to converge on an optimum that produced a 1.03% higher PPF for a 7.02% increase in MOX loading, demonstrating the applicability of MO optimization for achieving higher burnups of plutonium, which is advantageous particularly for the UK, which has a large civilian plutonium stockpile (ONR, 2016).

Another good example is the Multi Objective Alliance Algorithm (MOAA) developed by (Lattarulo & Parks, 2012) that was used to optimize MOX CORAIL assemblies. MOAA is an EA, functionally similar to a GA (Lattarulo, et al., 2014). The MOAA was compared to Non-dominated Sorting Genetic Algorithm II (NSGA-II), a common MOGA used in other benchmark studies (Deb, et al., 2002). The objective functions consisted of maximizing the plutonium loading and minimizing the PPF. Similar to (Yang, 2013), a constraint was also set on the number of LEU pins, and WIMS was used to calculate the PPF. The results of MOAA and NSGA-II were graphically demonstrated to show a more optimal Pareto-front as the number of evaluations increased, and, by using the Kruskal-Wallis statistical test, (Lattarulo, et al., 2014) showed that MOAA outperformed NSGA-II through achieving better convergence, a better spread and a more optimally-distributed set of solutions, whilst NSGA-II found fewer solutions and these had a tendency to cluster, producing gaps in its Pareto-front. It is important to note that the MOAA used in (Lattarulo, et al., 2014) was not adapted for use and was employed as a generic problem solver. The authors state that further work could lead to improvements on the optimal solution, such as tuning of the control parameters.

1.3.8. *Notable optimization studies from research literature*

To summarize, Table 1 highlights a number of important studies of relevance to this project. These are studies which show effective optimization methodologies, perform extensive comparison testing between algorithms, or demonstrate the wide applicability of optimization methods in nuclear engineering design problems. These studies represent the current state of the art in fuel assembly optimization. From them a number of conclusions can be drawn which will help guide this project going forward, organised by reactor type and date of the study.

Table 1: Key references on optimization of fuel assembly designs

Authors & Year	Type	Objective Function	Design Method	Design Variables	Constraints	Notes
(Rogers, et al., 2009)	**PWR** assembly	Minimize weighted function of PPF, enrichment and k-effective	Adaptive SA	Gd pin concentration & locations Pin enrichment & locations	Enrichment limit Gd pin limit	It can be expected that MO problems similar to this without using a weighted objective would take significantly longer than 12 hours
(Lattarulo, et al., 2014)	MOX CORAIL **PWR** assembly	Maximize Pu content Minimize PPF	MOAA	Pin enrichment & locations	LEU pin limit	Good example of MOX LWR optimization using Pareto-Dominance
(Janin, et al., 2016)	**PWR** assembly	Maximize k-effective Minimize PPF Minimize Void coefficient	ANN + GA	Pin enrichment & locations	Not mentioned	Surrogate model with GA produced a well-populated Pareto-front but highlighted the limitations of such an approach
(Washington & King, 2017)	**PWR** assembly	Target EFPD Reduce Pu Reduce minor actinides	MOGA	Pin geometry & locations	Not mentioned	Additional information outside the objective function was learned
(del Campo, et al., 2001)	**BWR** assembly axial	Maximize function of weighted physics/thermal properties	GA	Pin enrichment (axial)	Physics/thermal property limits	GA applied to axial, rather than the normal radial fuel distribution

Authors & Year	Type	Objective Function	Design Method	Design Variables	Constraints	Notes
(Jessee & Kropaczek, 2007)	**BWR** assembly with simplified neutronics	Maximize function of weighted physics / thermal properties	Perturbation + SA	Pin enrichment & locations	Rod type limit Gd pin locations	Example of hybrid methods as applied to a coupled bundled-to-core optimization
(Montes, et al., 2011)	**BWR** assembly	Maximize function of weighted physics/thermal properties	Ant Colony	Pin enrichment & locations Gd pin concentration & locations	Not mentioned	Good example of PSO on the BWR problem using a more complex form of the weighted objective function
(Castillo, et al., 2014)	Comparison of methods for **BWR** assembly	Maximize function of weighted physics/thermal properties	Ant Colony ANN GA Greedy Search PR+SS	Pin enrichment Gd concentration	PPF limit	Rare example of a comparative study performed between different algorithms
(Odeh & Yang, 2016)	**BWR** assembly	Maximize k-effective	SA	Pin locations	Void Coefficient Shutdown Margin Minimum Critical Power Ratio Fast Fluence	Example of a combined neutronics and thermal-hydraulics study using SA
(Liu & Cai, 2014)	ThU breeder **SCWR** through trial and error	Target burnup Maximize breeding ratio Minimize PPF	Not mentioned	Pin geometry Pin enrichment & locations	Not mentioned	Example of optimization done on pin geometry for less conventional reactor design

1.4. Addressing the research gap

Several conclusions can be drawn from the current state of the research literature:

1. The majority of optimizations using formal methods, including metaheuristics, are done on a single-objective basis. Whilst most studies recognise the compound and multi-objective nature of the area, the problem is usually confined to a single objective using subjective weighting values, constrained parameters, and performing optimization in several stages.
2. Studies which utilise multi-physics confine the use of optimization algorithms to a single stage using a single analysis code, due to concern over the potentially exponentially higher computational cost.
3. There are few comparisons between new algorithms and existing algorithms to determine their relative performance. This makes it hard to determine which algorithms are more suited to these kinds of problems. In comparisons that have been done, metaheuristic methods are superior to non-metaheuristics in reliability, although a well-tuned direct search algorithm is likely to find a local optimum sooner.
4. Existing fuel assembly design studies generally have the algorithm choose types of fuel pins from a pool that has been pre-selected. Only (Lattarulo, et al., 2014) features material composition of plutonium and uranium as a continuous variable.
5. GAs, whilst featured the most in the literature, have the highest number of control parameters which require setting by the designer. The most common design variables are the location and types of pin in the assembly. Studies involving changing pin geometries are less common. There are a variety of constraints (*e.g.* limits on the number of different enrichments or limitations on the placement of gadolinium-containing pins), but the objectives are generally attempting to improve / achieve a target k-effective and PPF, and most studies focus on radial or axial enrichment. An aim of this project is to be able to consider both axial and radial optimization simultaneously.

Despite the current limitations of research in this area, this review has shown it to be a continually evolving area with active research. The use of optimization algorithms, particularly multi-objective metaheuristics, can be used not only to provide more information about the search space, but also to discover new ‘dormant margins’ in the world of trade-offs (Maldonado, 2005). The onus remains on the engineer to decide how best to utilize this new information, but tools which can offer a more comprehensive optimization package, neglecting as few real-world effects as possible, will prove very useful in nuclear applications. Such a system could help the design engineer make choices about proposed new designs, to further improve existing designs, or to help the nuclear regulator assess the

As Low As Reasonably Practicable (ALARP) principle in designs undergoing assessment, such as the UK Generic Design Assessment (GDA) process.

1.4.1. *Requirements capturing*

The work done in this thesis intends to help fill this gap by developing a new optimization system fulfilling the following requirements:

1. The system should be capable of tackling MO problems without requiring objective weighting or severe parameter constraints imposed on the problem, which introduce subjectivity and the potential of bias into the results. This requires the algorithms to feature the concept of Pareto-dominance, as discussed in Section 1.3.1.
2. The system should not require extensive tuning of control parameters by the operator in order to perform effectively, and should work reliably in finding the best solutions.
3. The optimization algorithm should be able to utilize multi-physics analysis and evaluate solutions to objectives from different physics packages, such as k-effective in neutronics, and departure from nucleate boiling in thermal hydraulics.
4. The system should consider both radial and axial variables, and be capable of optimizing a fuel assembly in three dimensions.
5. The system should be able to converge to a set of best solutions within a reasonable time limit on a high-performance computing machine of reasonable computational power.

The remainder of this thesis details the work done to achieve these requirements and is laid out as follows:

Chapter 2 details the creation of new multi-objective algorithms designed for the high-dimensionality and non-linearity of nuclear engineering problems, founded on existing algorithms from the literature that have previously demonstrated high reliability and performance in complex problems. This forms the basis of the optimization package and, whilst other algorithms may be added in the future to the design package, these algorithms will be used to demonstrate the proof-of-concept of the system.

Chapter 3 considers the first stage of testing of these algorithms in MO problems. In this phase, comparison with existing algorithms from the literature is performed on a suitable fuel assembly optimization design problem. Statistical analysis is then used to draw quantifiable conclusions as to the efficacy of the new algorithms. Further testing is done on another problem from the literature to demonstrate reliability and performance on a more complex problem, and a sensitivity study on the control parameters is performed to determine how robust the algorithm is in adapting to different problems. This is a reproduction of the paper (Charles & Parks, 2019) as published in the peer-reviewed

journal Annals of Nuclear Energy, with some additional information included based on feedback following the PhD examination.

Chapter 4 considers the multi-physics and multi-dimensional analysis requirements by evaluating two further fuel assembly optimization problems, using real-world data as references for comparison and to draw conclusions. There is no previous work in the literature that has tackled these sorts of problems, so comparison must be done with a real-world design. This is a reproduction of the paper (Charles & Parks, 2020) also published in Annals of Nuclear Energy.

Chapter 5 concludes the thesis by assessing the developed system against the aforementioned requirements and proposes what supplementary work is necessary to expand the scope and capability of the system to increase its value to engineers.

2. Development of multi-objective DE algorithms

2.1. Introduction

EAs are by far the most ubiquitous metaheuristic algorithm applied to optimization problems, having been around since the early 1960s and used in computational tasks since the 1990s (Coello-Coello, et al., 2007). Many researchers have employed the basic concepts involved in these EAs. Crossover, mutation and selection are used with various modifications to try to create an algorithm which sufficiently mimics the process of evolution as quickly and as reliably as possible. Of these, GAs are the most common, and in the few comparisons that have been done, a GA is inevitably one of the standard algorithms to be used as a benchmark (e.g. NSGA-II (Deb, et al., 2002)). However, this by no means indicates they are the best kind of EA. Crucially for this work in multi-objective problems, it was shown by (Tusar & Filipic, 2007) that DE algorithms perform better than GAs and can explore the search space more efficiently. Furthermore, the weighted difference methodology allows both discrete and continuous variables to be modelled simultaneously with ease, whereas traditional GAs struggle with the representation of continuous variables (due to their representations as 'bits' within a 'gene') and require greater memory allocation and processing time.

Following an extensive review of the relevant literature, DE was chosen as a suitable flagship algorithm that showed promising capability to deal with problems with high numbers of variables and constraints without requiring special consideration for different data types.

The next stage was to determine what form of DE algorithm to use, namely, the type of *mutation strategy* that would be employed. As mentioned previously, the original strategy consists of taking two randomly selected solutions in the population and creating a weighted difference, known as "DE/rand/1" (the notation indicates the basic methodology, the choice of solutions to create a difference (i.e. random choice), and the number of differences (i.e. 1) to use in creating a new solution). This difference is then applied to a third solution to create a new candidate solution to evaluate. If the new solution is superior to the current one, it replaces the current solution in the population. An extensive discussion as to how different strategies have been developed in the area of DE is outside the scope of this work, but in principle, strategies are designed to use a subset of 'best' solutions to help guide and to accelerate convergence towards the Pareto-front. This increased greediness is then offset by including archives of past successful solutions that can help maintain the diversity within the population and prevent premature convergence (Bezerra, et al., 2015).

Another important consideration is the number of control parameters which rely on user input and can potentially have a significant effect on the performance of the algorithm. The population size, chance of

mutation, crossover and convergence criteria all require setting by the user, and in the case of complex problems might well require extensive tuning in order to give good performance. However, some algorithms, including many DE-type algorithms, do not require user-specified control parameters and instead handle parameter value setting within the algorithm itself. This approach is known as featuring self-adaptive parameter control, and is a proven technique in increasing the robustness and reliability of an algorithm (Zhang & Sanderson, 2009).

2.2. JADE and µJADE: implementation and verification

Given these considerations and after a search of the literature, the DE algorithms JADE (Zhang & Sanderson, 2009) and µJADE (Brown, et al., 2015) were chosen for investigation as suitable algorithms. JADE features self-adapting control parameters, an archive of previous members of the population preserving diversity in the population, and a mutation strategy that has proven its effectiveness, as explained below.

JADE – "DE/current-to-*p*best/1"

$$v_{i,g} = x_{i,g} + F_i \times \left(x^p_{best,g} - x_{i,g}\right) + F_i \times \left(x_{r1,g} - \overline{x}_{r2,g}\right) \quad [10]$$

where $x_{i,g}$ is the current member of the population, i, in the current generation, g. $x_{r1,g}$ is a random member of the population in the current generation, and $\overline{x}_{r2,g}$ is a randomly chosen solution from the archive of previous members of the population. F_i is the mutation scaling factor, and $v_{i,g}$ therefore represents the created pseudo-solution that will be combined with $x_{i,g}$ during crossover to create the new solution. This is a variation on "DE/current-to-best/1", which will always take the difference between the best solution and the current solution. Here, $x^p_{best,g}$ is used in place of the 'best' solution, and is a randomly chosen solution from a list of the 100p% best individuals in the current population (where p is the greediness selection strategy, a number between 0 and 1 that indicates the length of the list of best individuals, and therefore how greedy (elite) the algorithm is). The self-adapting control parameters are the mutation and crossover rates. In JADE, these are no longer fixed values set by the user, but are instead sampled from a distribution which depends on the values of previously successful mutation and crossover rates. Each time a solution is successful it has its mutation and crossover values added to a list. At the end of each generation, the distributions from which mutation and crossover are sampled are reinitialized using a mean derived by taking the mean of the list of successful values. If no superior solutions have been found, the distributions decay towards zero, which serves to indicate that convergence has occurred. This allows the algorithm to use feedback from the search process to adjust its own control parameters, and significantly reduces the amount of training time needed to 'tune' the

algorithm on new problems. Obviously, the population must be sufficiently large to avoid premature convergence, so this process is handled differently in µJADE. Further explanation of the JADE methodology is available in the original paper by (Zhang & Sanderson, 2009). In (Zhang & Sanderson, 2009), JADE showed better or competitive optimization performance on a set of benchmark functions compared to other classic and adaptive DE algorithms. The original JADE paper has had over 1100 citations since publication, and the algorithm is specifically mentioned as a potential candidate for MO optimization.

µJADE was designed as a small-population variant of JADE that still offers high performance. It was chosen to address a potential future problem in using the JADE algorithm with nuclear engineering problems which would require a substantial computational effort (e.g. whole-core calculations in high-fidelity). This could make an algorithm featuring a large population (such as JADE) unsuitable for these sorts of problems, as the time required to evaluate an entire population could become unreasonably high. µJADE's smaller population could mitigate this issue. Like JADE, µJADE features self-adapting parameter control, archiving, and uses a modified form of JADE's "DE/current-to-*p*best/1", which (Brown, et al., 2015) state was designed to improve the exploratory power of using smaller populations whilst maintaining convergence performance. This modified form and other methodology changes are explained below:

µJADE – "DE/current-by-rand-to-*p*best/1"

$$v_{i,g} = x_{i,g} + F_i \times \left(x^p_{best,g} - x_{r1,g}\right) + F_i \times \left(x_{r2,g} - \overline{x}_{r3,g}\right) \quad [11]$$

In µJADE, a randomly chosen solution, $x_{r1,g}$, from the current population (which unlike JADE must be different to $x_{i,g}$) is used for calculating the difference from $x^p_{best,g}$. It should be noted that this differs from the traditional DE/current-to-best/1 approach of $\left(x_{best,g} - x_{i,g}\right)$ with the intent of increasing the diversity of created solutions and avoid clustering. In addition, µJADE also uses a slightly modified self-adaptive crossover rate (for details see (Gong, et al., 2014)), and perturbation of the final new candidate solution to increase diversity (again an issue with smaller population algorithms) and reduce the risk of premature convergence. For full details of µJADE the reader should refer to the original paper by (Brown, et al., 2015).

In (Brown, et al., 2015), µJADE was shown to be more reliable than standard sized DE algorithms whilst performing comparably to other standard sized DE algorithms, including JADE, making it a suitable test algorithm for this work alongside JADE. When a newly created solution contains variables outside their acceptable bounds, this is known as a constraint violation. Both JADE and µJADE deal with constraint violations by reflecting the offending variable back from the boundary by the amount of violation. Both (Zhang & Sanderson, 2009) and (Brown, et al., 2015) state that this is a simple but not

necessarily optimal solution for constraint violation; however, it was judged to be sufficient for implementation in this work.

An initial investigation to confirm the suitability of JADE and µJADE was performed. Implementations of JADE and µJADE were created using C++ and were based on the pseudo-code found in (Zhang & Sanderson, 2009) and (Brown, et al., 2015). Validation was performed to show that the algorithms had been implemented successfully by minimizing the Ackley function shown in equation [12] (Ackley, 1987). This is a common test for optimization algorithms featuring many areas of local minima, and was one of the test problems covered in both the JADE and µJADE papers. For this test, the implementation of JADE used a population of 30, and the implementation of µJADE used a population of 8. The algorithms were run for 500 generations:

$$f(x) = -a\exp\left(-b\sqrt{\frac{1}{d}\sum_{i=1}^{d}x_i^2}\right) - \exp\left(\frac{1}{d}\sum_{i=1}^{d}\cos(cx_i)\right) + a + \exp(1) \qquad [12]$$

where $a = 20$, $b = 0.2$, $c = 2\pi$ and $d = 30$. The global minimum is $f(x^*) = 0$, at $x^* = (0, \ldots, 0)$.

Results are shown in the table below. Performance is measured as the success rate in locating the global minimum within an accuracy of 1.0E-08, and the mean number of function evaluations taken. Table 2 shows that the C++ implementations created for this project performed consistently with the performance of both JADE and µJADE reported in the original papers.

Table 2: Comparison of implemented DE algorithms to reference papers

	JADE (Zhang & Sanderson, 2009)	Implementation of JADE	µJADE (Brown, et al., 2015)	Implementation of µJADE
Success rate	100%	100%	100%	100%
Average number of functions required	4.7E+04	4.6E+04	3.8E+04	3.9E+04

2.3. Creating MOJADE and MOµJADE, and initial testing

JADE and µJADE were converted to work in a multi-objective environment with the following modifications:

- Since selection and ranking are no longer done based on one objective, the 'best' solutions are now a list of non-dominated solutions, which represent the current Pareto-front. These are determined from the current population.
- The archive was changed to accept solutions from that population that have been dominated by new solutions, and a second archive was added to accept new solutions that are Pareto-

equivalent to the existing population. MOJADE and MOμJADE were first presented in (Charles & Parks, 2017).

The pseudo-codes for Multi-objective JADE (MOJADE) and Multi-objective μJADE (MOμJADE) are shown on the following pages.

Nomenclature

μCR = adaptive Crossover Rate probability
μF = adaptive mutation probability
A1 = archive used for dominated solutions
A2 = archive used for Pareto-equivalent solutions
BIR = restart variable used if no improvement is made
c = rate of parameter adaptation
D = number of dimensions (variables)
G = number of generations
meanA = arithmetic mean
meanL = Lehmer mean[8]
NP = last member of the population
p = greediness of the mutation strategy, i.e. the number of solutions considered 'best'.
P = population
randn = normal distribution
randc = Cauchy distribution
SCR = set of successful crossover factors
SF = set of successful mutation factors
up_lim / low_lim = limits set by the variable bounds
b_i = crossover rate repair modifier following perturbation
v_i = i-th test vector following mutation
u_i = i-th test vector following crossover and perturbation
x_i = i-th member of the population

[8] The Lehmer mean with a parameter value of 2 is used here. In conjunction with the Cauchy distribution, this means that mutation rates are chosen from a distribution with a slightly higher weighting towards larger values (*i.e.* more chance of mutation) compared to a normal distribution. This is done to increase diversity within the population (Zhang & Sanderson, 2009).

MOJADE

```
Begin
Set μCR = 0.5; μF = 0.5; A1, A2 = 0
Create a random initial population {xi,0|i = 1, 2, . . . , NP}
Evaluate and rank initial population to determine 100p% best vectors
For g = 1 to G
        SF = 0; SCR = 0;
        For i = 1 to NP
                Generate CRi = randni (μCR, 0.1), Fi = randci (μF, 0.1)
                Randomly choose xp_best as one of the 100p% best vectors
                Randomly choose xr1 =/= xi from current population P
                Randomly choose xr2 =/= xr1 =/= xi from P ∪ A1 + A2
                vi = xi + Fi · (xp_best − xi ) + Fi · (xr1 − xr2), check constraints
                Generate jrand = randint(1, D)
                For j = 1 to D
                        If j = jrand or rand(0, 1) < CRi
                                ui,j = vi,j
                        Else
                                ui,j = xi,j
                        End If
                End For
                If f (ui) dominates f (xi)
                        xi → A1 (replacing random member of A1 if A1 is full)
                        xi = ui
                        CRi → SCR, Fi → SF
                Else
                        If f(ui) is Pareto-equivalent to f (xi) && f(ui) is NOT dominated by f (A2)
                                ui → A2 (remove members of A2 that are dominated by ui)
                        End If
                End If
                Rerank 100p% best vectors
        End For
        μCR = (1 − c) · μCR + c · meanA(SCR)
        μF = (1 − c) · μF + c · meanL (SF)
End For
End
```

MOμJADE

```
Begin
Set μCR = 0.5; μF = 0.5; A1, A2 = 0
Create a random initial population {xi,0|i = 1, 2, . . . , NP}
Evaluate and rank initial population to determine 100p% best vectors
For g = 1 to G
SF = 0; SCR = 0;
        For i = 1 to NP
                Generate CRi = randni (μCR, 0.1), Fi = randci (μF, 0.1)
                Randomly choose xa =/= xi from current population P
                Randomly choose xb =/= xa =/= xi from current population P
                Randomly choose xp_best =/= xa as one of the 100p% best vectors
                Randomly choose xc from P ∪ A1 + A2
                Generate jrand = randint(1, D)
                vi = xi + Fi · (xp_best − xa ) + Fi · (xb − xc), check constraints
                For j = 1 to D
                        If j = jrand or rand(0, 1) < CRi
                                ui,j = vi,j
                                bi,j = 1
                        Else
                                ui,j = xi,j
                                bi,j = 0
                        End If
                End For
                For j = 1 to D
                        If rand(0, 1) <= 0.005
                                ui,j = lower_lim + rand(0,1)*(upper_lim - lower_lim)
                                bi,j = 0
                        Else
                                ui,j = ui,j
                                bi,j = bi,j
                        End If
                End For
                CRi = Σ b  / D;
                If f(ui) dominates f(xi)
                        xi → A1 (replacing random member of A1 if A1 is full)
                        xi = ui
                        CRi → SCR, Fi → SF
                Else
                        If f (ui) is Pareto-equivalent to f(xi) && f(ui) is NOT dominated by f(A2)
                                ui → A2 (remove members of A2 that are dominated by ui)
                        End If
                End If
                Rerank 100p% best vectors
                If ui ∈ 100p% best vectors
                        BIR = BIR + 1
                End If
        End For
        If mod(g,max(100,10D) = 0
                μCR = (1 − c) · μCR + c · meanA(SCR), μF = (1 − c) · μF + c · meanL (SF)
        End If
        If mod(g,max(1000,100D) = 0
                If BIR==0
                        Reinitialize population apart from best member
                End If
        End If
End For
End
```

Before testing out these algorithms on a nuclear engineering design problem, both MOJADE and MOμJADE were tested on the Zitzler-Dep-Thiele function 1 (ZDT-1) problem (Zitzler, et al., 2000), a constrained continuous n-dimensional (n>1) MO problem, along with the NSGA-II algorithm (Deb, et al., 2002), a multi-objective GA used widely as a benchmark for optimization performance studies in the literature. This involves fulfilling the following two objectives:

$$f_1 = x_1 \quad [13]$$

$$f_2 = g \cdot \left(1.0 - \sqrt{\frac{f_1}{g}}\right) \quad [14]$$

where $g(x_2, \dots, x_n) = 1.0 + \frac{9}{n-1}\sum_{i=2}^{n} x_i$, $0 \leq x_i \leq 1$, and, for this problem, a value of 41 was used for n (a similar number of dimensions as used in the problem in (Lattarulo, et al., 2014), which will be covered in Section 3). NSGA-II and MOJADE were run with a population of 30, whilst MOμJADE uses its smaller population of 8. All three algorithms were run with a generation limit of 5000, chosen as it should allow all the algorithms to converge to the best of their ability. The number of function evaluations taken was recorded in Table 3 below, which highlights the difference in function evaluations between MOJADE and the smaller population MOμJADE.

Table 3: Function evaluations for different algorithms on ZDT-1

Algorithm	NSGA-II	MOJADE	MOμJADE
Function evaluations	142367	150000	40000

The Pareto-front solution to this problem is $f_2 = 1 - \sqrt{f_1}$. As shown in Figure 14 below, both MOJADE and MOμJADE clearly perform comparably to the more established NSGA-II. The smaller number of MOμJADE solutions on the Pareto-front is due to the smaller population. This test shows that these algorithms are able to optimize competing objectives through changing multiple variables.

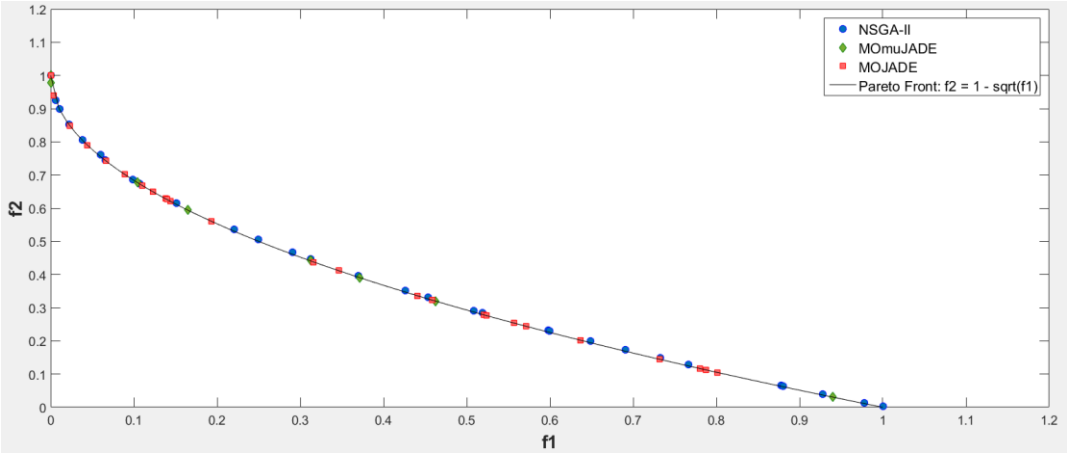

Figure 14: Performance of MOJADE, MOμJADE and NSGA-II on the ZDT-1 problem

2.4. Coupling MOJADE and MOμJADE with the reactor physics software WIMS

Now that the algorithms are ready to deal with multi-objective problems, they must link to a suitable reactor physics solver to evaluate the assembly designs they generate and determine their performance against the objectives. In this research, WIMS, a general-purpose reactor physics code developed by the ANSWERS Software Service, is used for core physics calculations. WIMS is a versatile software package used for neutronics calculations and has been used for numerous optimization studies in the literature (such as (Khoshahval, et al., 2014b), (Khoshahval, et al., 2014a), (Yang, 2013) and (Lattarulo, et al., 2014)). WIMS is an industry rated code for performing lattice and whole core calculations and will provide a standardised user input for the algorithms to interact with. For a given problem, every generated assembly design will be evaluated in the same manner, so both the input and output files will be very similar, with the differences only coming from the variables related to the current problem (*e.g.* U235 enrichment in the assembly). Therefore, a template file will be used for each problem that the algorithm will copy and create an input file from for each generated design, overwriting the input variables with those related to the specific solution it is testing.

WIMS uses a modular structure that breaks down calculations into groups of well-defined operations. The initial step is to generate the cross-sections and calculate resonance shielding effects for the specified geometries and materials in the problem. To do this, WIMS reads from a nuclear library data

set which contains neutron reaction data for 313 nuclides, thermal scattering data, radioactive decay data for 2345 radionuclides, and photo-atomic interaction data. This data set is part of an ongoing project administered by the Nuclear Energy Agency and has a number of project releases. In this work the JEFF 2.2 data set is used (OECD/NEA, 1992). Following the initialisation, WIMS offers a number of flux solvers, including both stochastic and deterministic methods, to evaluate the neutron transport equation. For most of the problems covered in this work, flux solutions are calculated using the MoC, which explicitly integrates the differential form of the neutron transport equation along predetermined characteristic neutron paths, for a given geometrical layout and material composition. Using an explicit method such as MoC to generate flux solutions ensures that WIMS performs in a deterministic (and thus reproducible) manner (as opposed to a stochastic method such as Monte Carlo), which is important for this project as some of the optimization algorithms use pseudo-random parameter generation. Therefore, variation in results from repeated experiments reflects the variability in the results generated by the optimization algorithm only, and hence can be used as a performance measure. Once a WIMS run has finished, the algorithm will read the output file and record the results in order to perform selection on the solutions. In Chapter 3 solutions are evaluated using WIMS10a (Lindley, et al., 2015). The problems covered in Chapter 4 use a development version of WIMS11 obtained directly from the ANSWERS Software Service in order to utilize the newly developed thermal hydraulics solver.

3. Application of differential evolution algorithms to multi-objective optimization problems in mixed-oxide fuel assembly design

3.1. Introduction

This chapter presents the first complete study to investigate the performance of the two multi-objective DE algorithms MOJADE and MOμJADE, whose creation was described in Chapter 2, on a number of nuclear engineering fuel assembly design problems. This is the first step in demonstrating a MO optimization capability in this area and covers Requirements 1 and 2 from Section 1.4.1.

The first problem investigated concerns optimization of a so-called 'CORAIL' assembly (Youinou, et al., 2001) containing both LEU and plutonium MOX pins. The performance test consists of comparing the DE algorithms' ability against an EA from the literature in optimizing the CORAIL assembly with the objectives of minimizing the PPF and maximizing the plutonium content. Minimizing the PPF increases margins to safety, whilst maximizing the plutonium content increases the attractiveness for operators that seek to reduce the UK's plutonium stockpile. In 2014 this stood at 126 tonnes, which makes it the largest civil separated stockpile in the world (UK Government, 2016). The second problem involves optimization of a MOX assembly which includes gadolinium burnable absorber pins, thereby investigating the performance of the DE algorithms on a more complex problem. Finally, the sensitivity of the better performing DE algorithm is investigated. Low sensitivity indicates that the algorithm performs robustly and does not require excessive parameter tuning before it can be run on a new problem. All three algorithms execute the reactor physics analysis code package WIMS10a to determine the performance of created solutions. Section 3.1.1 details the control parameter settings used by MOJADE and MOμJADE, while Section 3.1.2 introduces the comparator algorithm MOAA. Section 3.2 defines each of the three problems covered in this chapter. Section 3.3 contains the results obtained for each problem and discusses the trends and statistical significance of the findings. The chapter concludes with a summary of the main findings in Section 3.4.

3.1.1. *MOJADE and MOμJADE*

The implementations of MOJADE and MOμJADE used in this study are as described in Section 2.3, with the following control parameters as given in Table 4. For both MOJADE and MOμJADE, the parameters were kept the same as those in the original JADE and μJADE papers. Population size and generation were set to keep an equivalent number of function evaluations (see 3.2.1), with MOμJADE set to the minimum population size as recommended by the original μJADE paper.

Table 4: MOJADE and MOμJADE control parameters

Parameter	MOJADE	MOμJADE
Rate of parameter adaptation *c*	0.1	0.05
Greediness of selection strategy *p*	0.05	3 / population
Population size	32	8
Generations	50	200

3.1.2. *Multi-Objective Alliance Algorithm*

In order to assess the performance of MOJADE and MOμJADE, they are compared to an algorithm from the literature that has previously demonstrated effectiveness in optimizing nuclear fuel assembly design problems – the MOAA (Lattarulo & Parks, 2012).

The MOAA is a metaheuristic optimization algorithm which is built around the concept of tribes struggling to conquer a resource-rich environment. Functionally, the algorithm is a form of EA which combines parameters from successful solutions to further improve later generations of solutions. Solutions are initially created randomly, but, once a Pareto-front has been established, they become either copies of Pareto-front solutions or are modified from the Pareto-front using a normal distribution. This distribution has an adaptive standard deviation to increase diversity initially and then speed up convergence towards the end of the optimization. The algorithm also analyzes the distance between solutions on the Pareto-front to determine which solutions to remember. This feature also functions adaptively: as the algorithm converges and the average gap between solutions becomes smaller, dominated solutions near areas of the Pareto-front that have larger gaps are preserved in an archive to encourage the finding of a non-dominated solution in that area in the future. These features are all governed by control parameters and for this work these parameters are the same as those used in (Lattarulo, et al., 2014). Further details concerning the application of the MOAA to nuclear fuel assembly design can be found in (Lattarulo, et al., 2014). In that case study, the MOAA found solutions superior to previous 'expert designs' and out-performed another EA (NSGA-II).

3.2. Test problems

3.2.1. *Problem 1*

The first problem investigated was originally presented in (Lattarulo, et al., 2014) and DE results were first presented in (Charles & Parks, 2017). The task is to optimize a two-dimensional nuclear fuel 'CORAIL' type assembly containing two types of fuel pin, LEU and uranium-plutonium MOX (see Figure 15) with reflective boundary conditions.

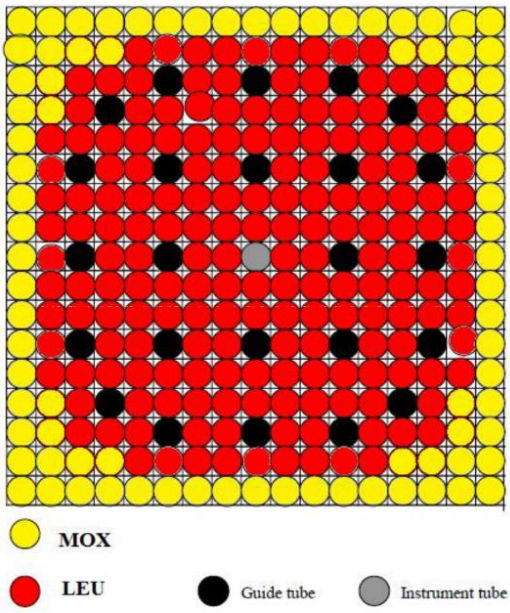

Figure 15: CORAIL assembly with LEU pins surrounded by MOX pins at the periphery (Lattarulo *et al.*, 2014)

The presence of both Pu and LEU pins inside an assembly can create uneven reaction rates between the pins. Plutonium fission favours a harder neutron energy spectrum due to resonance capture, whilst fission with uranium prefers a softer energy spectrum. This can result in variations in the radial neutron flux and power distribution, which could pose a challenge for both thermal-hydraulic performance and fuel performance limits. By optimizing the distribution of pins inside the assembly this imbalance can be minimized. Optimization can be carried out by changing both MOX pin positions and the concentration of plutonium within the MOX pins, as (Lattarulo, et al., 2014) demonstrated, increasing the overall Pu content above that of the standard CORAIL expert design. For reasons of safety, at least half the total number of pins should always be LEU only and the %Pu within the MOX pins can be no more than 20% (Lattarulo, et al., 2014). The plutonium composition was assumed to be reactor grade, and is detailed in Table 5.

Table 5: Plutonium isotopic composition (wt%) used for Problem 1 (Youinou, et al., 2001)

Pu238	Pu239	Pu240	Pu241	Pu242	Am241
3.90	40.57	30.08	12.32	11.89	1.24

LEU enrichment is kept fixed at 5% U235. The geometry was fixed to be that of a standard CORAIL assembly containing 264 fuel pins. Using octant symmetry this can be simplified to give 39 unique fuel pin positions. Pin types 1, 2 and 3 refer to MOX type 1, MOX type 2 and LEU, respectively. N_1, N_2 and N_3 are therefore the quantities of each pin type, with the sum total being equal to the number of

pins in the assembly octant ($N_1 + N_2 + N_3 = 39$). Two MOX pin types are allowed with different wt% Pu amounts (W_1, W_2). The total plutonium content (MOXT) in the assembly is therefore given by $\mathrm{MOXT} = W_1 \cdot N_1 + W_2 \cdot N_2$. Pins along the lines of octant symmetry within the assembly are weighted by 0.5, to avoid double counting. The constraints are $N_3 \geq 16.5$, which represents a maximum MOX loading of 50% of the pins in the assembly, and $0 \leq W_1, W_2 \leq 20$, which represent the range of possible wt% Pu values. The objectives to be minimized are PPF at Beginning of Life (BoL) and –MOXT (minimizing –MOXT maximizes the Pu content, –MOXT is used hereon to make visualization of the results easier). PPF values are obtained using the reactor physics code WIMS10a (Lindley, et al., 2015) to solve the neutron transport equation, using the MoC, to calculate pin power and hence the PPF. To calculate the PPF, WIMS fixes the mean pin power to a nominal value.

MOJADE, MOμJADE and MOAA were each run 30 times, with a unique random seed each time. Each individual run had a limit of 1600 solution evaluations, which allowed for 50 generations of MOJADE using a population of 32, and 200 generations of MOμJADE using a population of 8. Algorithms were run on the 'Ray' computer cluster used by the University of Cambridge's Department of Engineering Nuclear Group, with specifications shown in Table 6.

Table 6: Ray computer cluster specifications

Processor	Intel Xeon Processor E5-2650 (2.6 GHz, 20 MB cache)
Threads	16 (WIMS operating in single-threaded mode)
RAM	64 GB DDR3

3.2.2. *Problem 2*

The second problem was chosen to investigate the effectiveness of DE in analyzing a more complex situation without performing any control parameter tuning. This concerns the optimization of MOX fuel assemblies containing gadolinium oxide (Gd_2O_3) pins, e.g. Japanese MOX assemblies (Yamate, et al., 1997). The use of gadolinium oxide pins in these assemblies potentially reduces the need to use Burnable Poison Rods (BPRs) in the guide tubes, normally employed to compensate for higher PPF values caused by higher levels of Pu content compared to other designs. By optimizing the design using gadolinium oxide pins, the PPF can be reduced without using BPRs and can even allow for increased Pu content in the assembly.

In (Yamate, et al., 1997), expert judgement was used to reduce the PPF over the life of one assembly, using a fixed wt% Gd content, fixed pin types and changing wt% Pu contents for two types of U-Pu MOX pin. To reproduce the conditions of the original paper, a slightly different plutonium composition was used to mimic Japanese-style MOX pins (see Table 7).

Table 7: Plutonium isotopic composition (wt%) used for Problem 2

Pu238	Pu239	Pu240	Pu241	Pu242	Am241
1.90	57.50	23.30	10.00	5.40	1.90

Using MO optimization algorithms, it is possible to extensively explore the search space for this problem, with the objectives once again of maximizing plutonium content and minimizing the PPF at the assembly BoL. The design variables were changed to include all five originally proposed assembly layouts, allowing wt% Gd and wt% Pu to change, and allowing all non-Gd pins to be of either type of Pu MOX pin. The different assembly layouts used are shown in Figure 16.

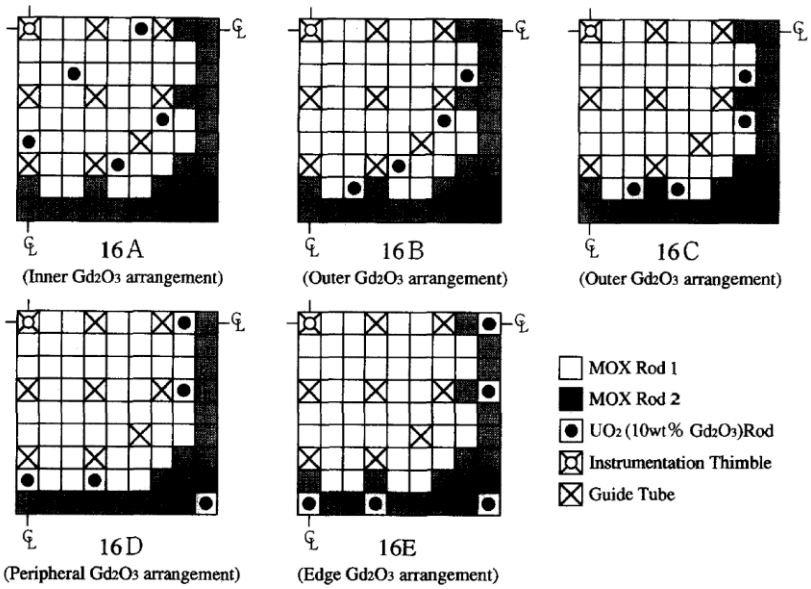

Figure 16: Japanese U-Pu MOX ¼ assembly layouts used in Problem 2 (Yamate, et al., 1997)

Similar to the previous problem, the assembly contains 264 fuel pins and has 39 unique fuel pin positions, for octant symmetry. Pins are labelled as fuel types 1, 2 and 3 (MOX type 1, MOX type 2, and gadolinium oxide, respectively). Total numbers of each pin type are given by N_1, N_2 and N_3, with $N_1 + N_2 + N_3 = 39$. The quantity and positions of the gadolinium oxide pins are dependent on which assembly layout is chosen, from the five possibilities (shown in Figure 16), with some pins weighted by 0.5 due to octant symmetry in the assembly. The two MOX pin types can be placed anywhere in the assembly except at guide tube or gadolinium oxide pin locations. The two wt% Pu weights are W_1 and W_2, and one concentration of gadolinium oxide is allowed (W_G). Constraints of $0 \le W_1, W_2 \le 20$, and $0 \le W_G \le 10$ were used. As in Problem 1, the total Pu content is $\mathrm{MOXT} = W_1 \cdot N_1 + W_2 \cdot N_2$.

Both MOJADE and MOμJADE were run on Problem 2 and their performance compared. Following this, depletion of a solution on the elbow of the found Pareto-front solution was performed to see how

the PPF changed over the life, with results compared to those in (Yamate, et al., 1997). Both algorithms were used with the same control parameter values as used for Problem 1 to see how well the algorithms performed without custom tuning of parameters. Again, the reactor physics code WIMS10a (Lindley, et al., 2015) was used to calculate PPF values and to perform depletion calculations. WIMS was run with a standard set of modules, performing resonance-shielding calculations in 172 energy groups before condensing down to 22 and running a MoC solver to find the flux solution. Burnup was performed in steps of 200 MWd/t. MOJADE was run with a population of 32 for 50 generations. MOμJADE was run with a population of 8 for 200 generations, giving both algorithms a total of 1600 function evaluations in each run. Both algorithms were run 20 separate times. Algorithms were run on the 'Lux' computer cluster used by the University of Cambridge's Department of Engineering Nuclear Group, with specifications shown in Table 8.

Table 8: Lux computer cluster specifications

Processor	Intel Xeon Processor E5-2690 (3.5 GHz, 35 MB cache)
Threads	28 (WIMS operating in single-threaded mode)
RAM	128 GB DDR3

3.2.3. *Sensitivity analysis*

The sensitivity of DE to the values of its control parameters was measured using Problem 2 (Section 3.2.2). Only MOJADE was investigated in this case, since it was shown to perform better than MOμJADE on Problems 1 and 2 (see below), and is arguably more suited to nuclear engineering problems where parallelization of the evaluation step offers a significant execution time advantage.

Constraints were kept the same, and the optimization objectives were again to maximize the Pu content of the assembly and minimize the BoL PPF. It was decided to confine the study to looking at assembly performance at BoL to reduce the computational cost of the investigation, as including burnup calculations in the evaluation step increases the computational load significantly. It was judged that the BoL design problem was sufficiently complex due to presence of multiple fuel types to provide a good test of the performance sensitivity to the rate of adaptation (c) and the greediness of the algorithm (p).

MOJADE was run with a population of 32 for 40 generations. The focus of this study was on the impact on performance of the algorithm's degree of elitism and self-adaptive nature, as the trade-off between increased population size providing more diversity and greater search space coverage *vs.* computational load is already well established (Bezerra, et al., 2015). Table 9 shows the control parameter ranges tested along with their default values. Work by the original authors of JADE suggests that the rate of parameter adaptation (c) works well with values in the range 0.05–0.2, and the greediness (p) works well between 5 and 20% (*i.e.* the 'best' results are chosen from between 5 and 20% of the current population) (Zhang

& Sanderson, 2009). Both very high and very low values of *p* and *c* were investigated to determine the effect these control parameters have on the algorithm's performance (Table 9). Each test was run 10 times (varying only the random number generator seed used in each run) to obtain a suitable statistically significant set of results. Runs were executed on the 'Lux' computer cluster.

Table 9: MOJADE control parameter values used in sensitivity analysis tests

Test number	Greediness of selection strategy, *p*	Rate of parameter adaptation, *c*
Default Values	0.05	0.1
1	0.05	0.0
2	0.05	0.025
3	0.05	0.25
4	0.05	0.75
5	0.05	1.0
6	0.01	0.1
7	0.25	0.1
8	0.75	0.1
9	1.0	0.1

3.3. Results and discussion

3.3.1. *Problem 1*

The output of each run was the final Pareto-front found by the algorithm. The results were analyzed by comparing these Pareto-fronts. Analysis presented in (Charles & Parks, 2017) involved using two separate indicators to determine the relative performance of each algorithm. Firstly, the epsilon indicator (Zitzler, et al., 2000) represents the minimum translational distance necessary to move all points on a given Pareto-front to weakly dominate a reference set (a combined Pareto-front formed from all solutions from all algorithms representing the most optimal set of solutions). Secondly, the hypervolume indicator (Knowles, et al., 2006) calculates the difference between the hypervolume of the dominated objective space formed from the Pareto-front of one particular algorithm and the hypervolume of the objective space dominated by the reference set, using the least-optimal solution found as a reference point for the calculation of the hypervolume. In both cases smaller values indicate better performance. These same indicators will also be used later to analyze the results of the sensitivity study. To determine the statistical significance of the performance indicator values, the Kruskal-Wallis test was used (Kruskal & Wallis, 1952) as results produced by the algorithm may not be normally distributed. For this work, the Kruskal-Wallis test results represent the probability that the given indicator values are not a true representation of the algorithm's relative performance against another and are instead the result of random chance.

Results are plotted in PPF against (–MOXT) space. More negative values of –MOXT indicate a higher amount of plutonium in the assembly. Both objectives are to be minimized; therefore the bottom-left

corner represents an ideal solution. Figure 17 shows the results of every generated Pareto-front for each algorithm. Figure 18 shows these results filtered to show the overall best Pareto-front for each algorithm. A line depicting the overall Pareto-front formed from all the algorithms together is added for reference.

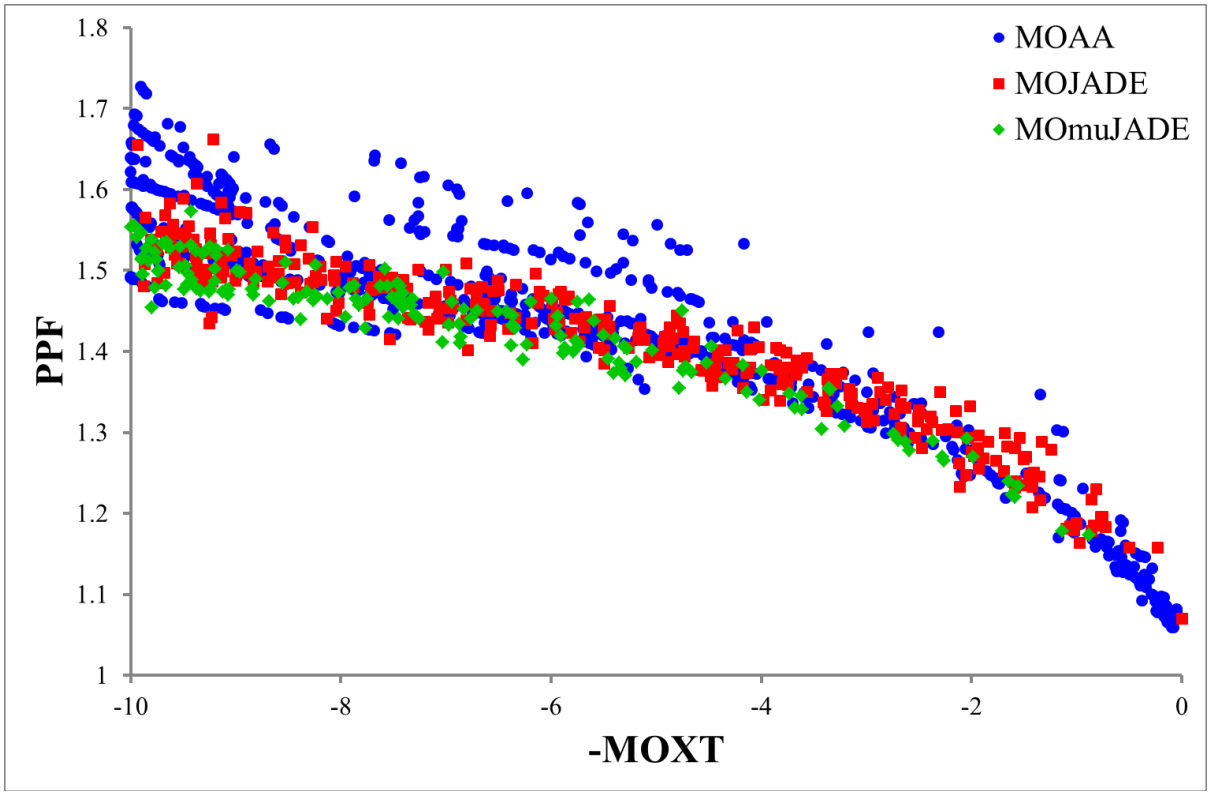

Figure 17: Results of MOAA, MOJADE and MOμJADE optimization of MOX fuel assemblies in Problem 1, adapted from (Charles & Parks, 2017)

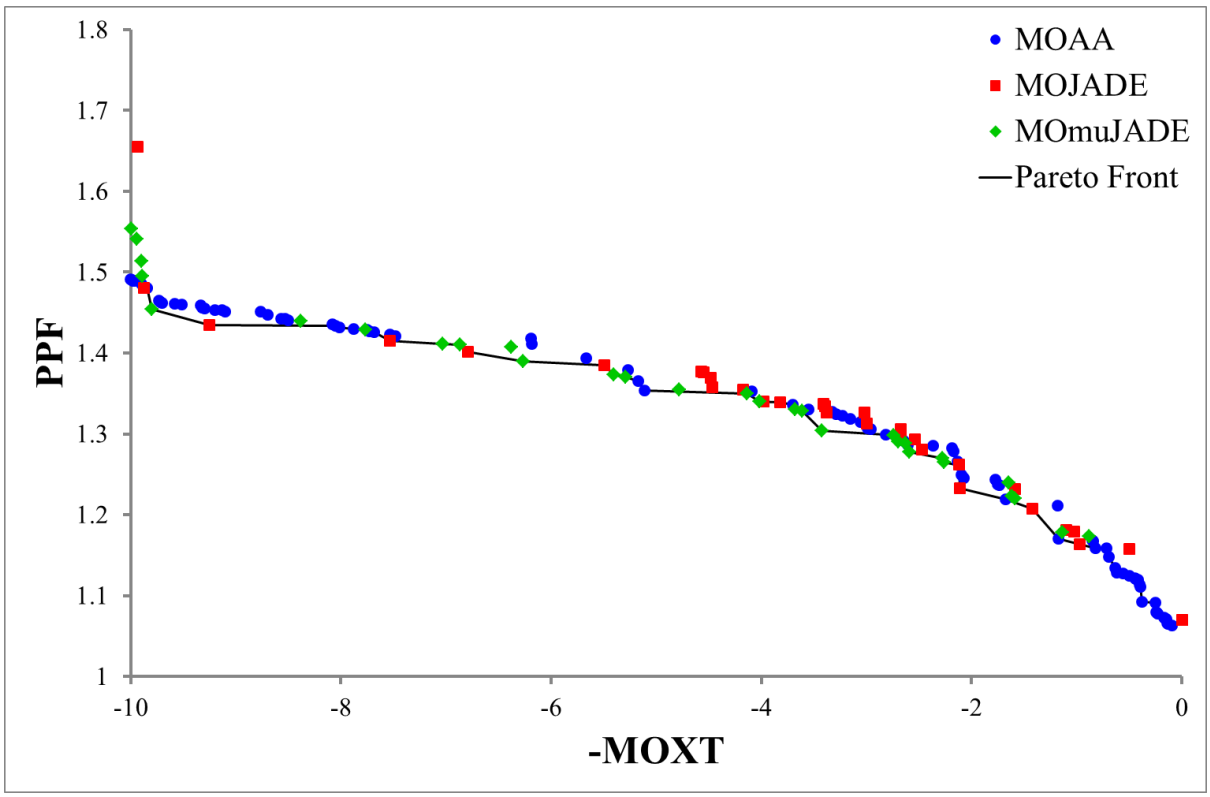

Figure 18: Comparison of non-dominated solutions found using the MOAA, MOJADE and MOμJADE algorithms to optimize MOX fuel assemblies in Problem 1, adapted from (Charles & Parks, 2017)

Figure 17 and Figure 18 demonstrate that MOJADE and MOμJADE perform comparably to MOAA, significantly contributing to the overall Pareto-front, as highlighted in Figure 18. The solutions found by MOAA appear to exhibit some degree of clustering in the Pareto-front, with the gaps populated by MOJADE and MOμJADE solutions. MOAA tends to converge on a single MOX-LEU pin pattern during the course of a run, and thus the output from that run will typically be non-dominated solutions which show the effect of increasing or decreasing the values of W_1 and/or W_2 within the same pin pattern. This produces a number of solutions that have very similar values for –MOXT and PPF. In contrast, both MOJADE and MOμJADE do not necessarily converge on a single pin pattern in any given run, and thus arguably better explore the search space of different pin arrangements.

The means and standard deviations of the hypervolume and epsilon indicators, along with their corresponding significance level values from the Kruskal-Wallis test, are given in Table 10 and Table 11, respectively.

Table 10: Hypervolume and epsilon indicator values in Problem 1, adapted from (Charles & Parks, 2017)

Algorithm	Hypervolume Indicator		Epsilon Indicator	
	Mean	Standard Deviation	Mean	Standard Deviation
MOAA	1.6664	0.5169	0.3897	0.1478
MOJADE	0.7672	0.1047	0.3941	0.1204
MOμJADE	1.1267	0.7723	0.3320	0.1081

Table 11: Kruskal-Wallis test results in Problem 1, adapted from (Charles & Parks, 2017)

Algorithms	Hypervolume Indicator	Epsilon Indicator
MOJADE *vs.* MOAA	3.879E-11	9.528E-01
MOμJADE *vs.* MOAA	8.513E-07	7.363E-02
MOμJADE *vs.* MOJADE	9.497E-05	5.650E-02

The hypervolume indicator results in Table 10 show that MOJADE, with the lowest mean and standard deviation, is the most consistent at producing results which dominate the entirety of the known search space, followed by MOμJADE. Results for the epsilon indicator, however, suggest that MOμJADE solutions are more likely to be closer to the 'true' Pareto-front, but do not give as much information as to the exact nature of the Pareto-front (MOμJADE search being limited by a smaller population size which leads to worse hypervolume indicator values).

Table 11 gives the significance level results of the Kruskal-Wallis test for the hypervolume and epsilon indicators for both DE algorithms *vs.* MOAA, as well as against each other. Values lower than 0.05 are indicative of a statistically significant difference. The results of Table 10 and Table 11 indicate that MOJADE and MOμJADE yield superior hypervolume performance compared to MOAA due to the methodological differences in the algorithms. However, differences in epsilon indicator performance are not shown to be statistically significant. Finally, MOJADE shows superior hypervolume performance to MOμJADE, again due to methodological differences. In a given run for a fixed number of solution evaluations, the larger population of MOJADE is able to better cover the search space (and thus the Pareto-front) compared to the small population of MOμJADE. There is some evidence that MOμJADE may be able to converge quicker than MOJADE and thus require fewer evaluations, which may offset the lack of inherent parallelization currently present in MOμJADE due to it evaluating each solution as it is created, unlike MOJADE which evaluates all created solutions at the end of a generation.

3.3.2. *Problem 2*

Figure 19 shows the results given by MOJADE and MOμJADE, the Pareto-front, and the solution chosen for depletion to 15 GWd/t.

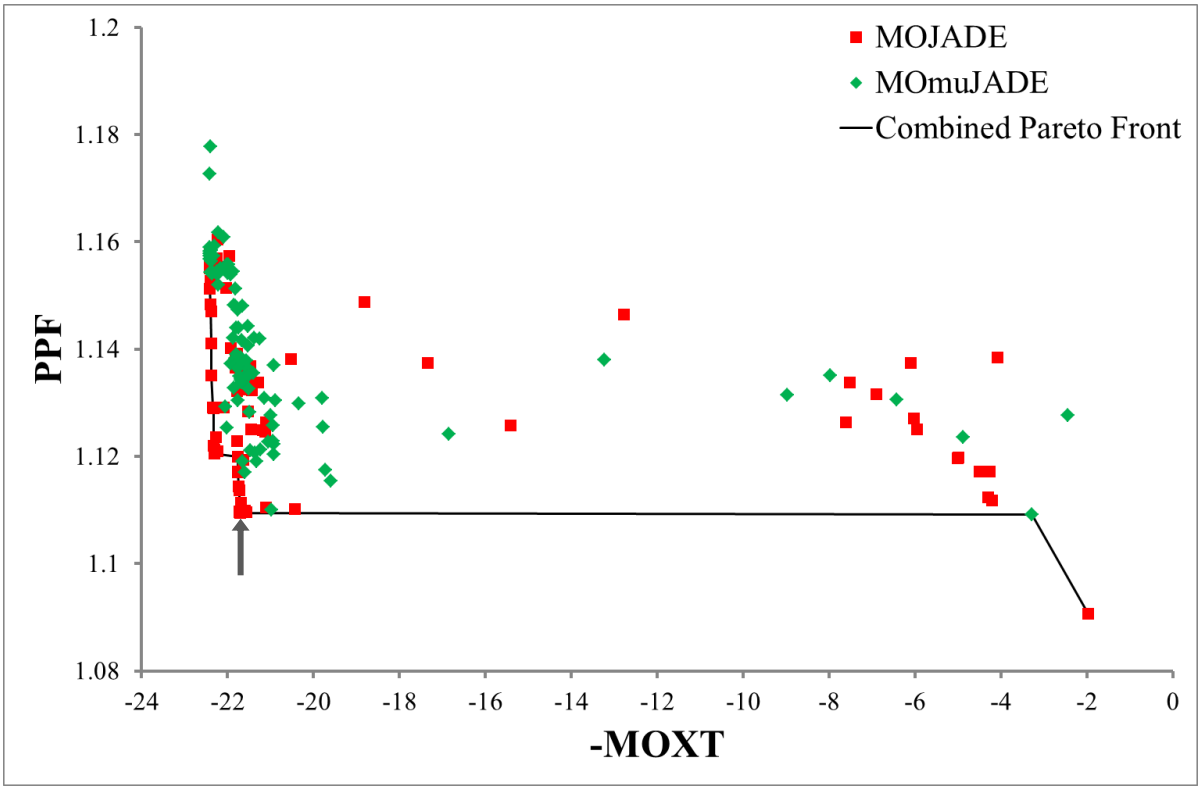

Figure 19: Results of DE optimization of MOX fuel assemblies with gadolinium oxide pins (Problem 2). The arrow indicates the solution chosen for the burnup study.

Figure 19 indicates that both MOJADE and MOμJADE tend to converge on solutions containing high amounts of Pu, and the Pareto-front for solutions with less negative values of –MOXT is poorly populated. It was originally thought that this may be due to some form of premature convergence causing a loss of diversity in the population around a local optimum of solutions containing high amounts of Pu. The crossover and mutation rates are self-adapting control parameters, which are, in turn, affected by the greediness (p) and the rate of parameter adaption (c), as specified in Table 9. To test this hypothesis, a modified form of the problem was run with MOJADE, with the amount of Pu constrained such that solutions would only be permitted if the value of –MOXT was between –11 and –5. Figure 20 shows that constraining the problem in this way results in a Pareto-front that is dominated by the original results, and thus that the solution clustering is a feature of the problem, not the algorithm. This is due to the presence and layout of gadolinium pins having a large effect on the PPF at BoL, which can be seen in the original paper (Yamate, et al., 1997).

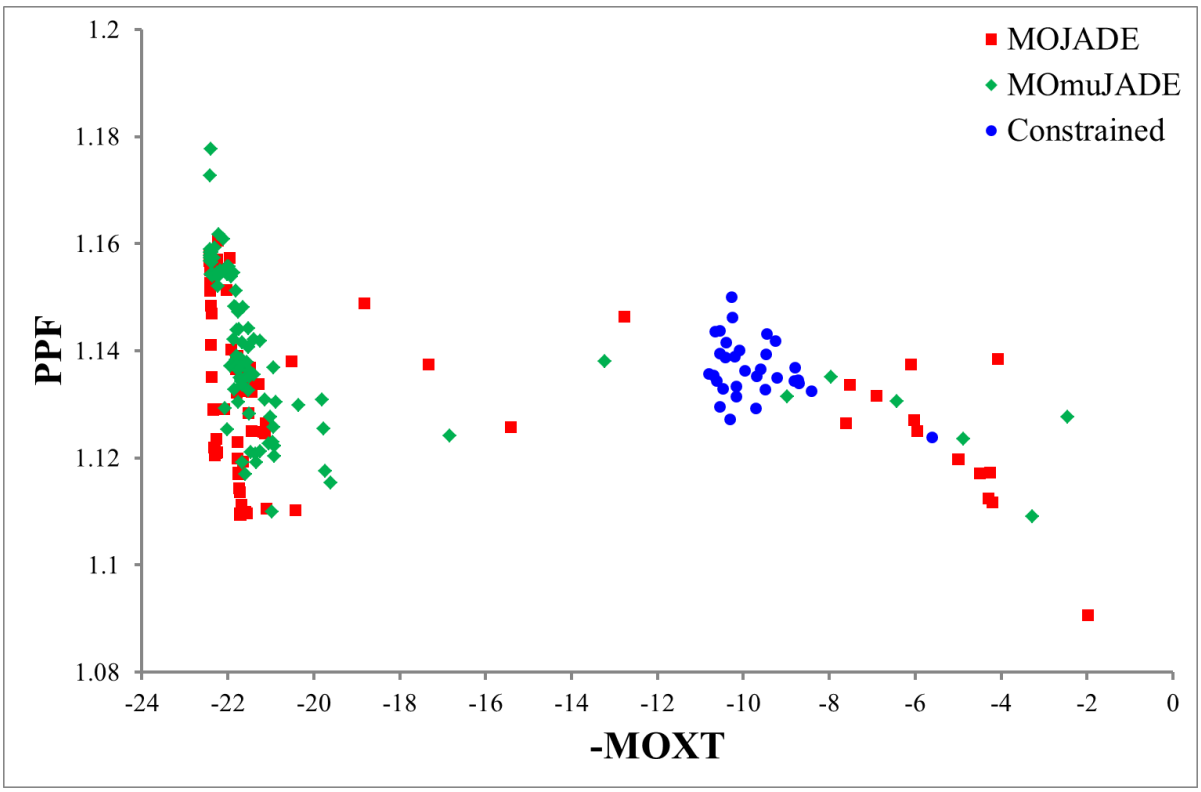

Figure 20: The effect of constraining the wt% Pu within the MOX pins (Problem 2)

Figure 19 and Figure 20 only show PPF *vs.* the total Pu content of the assembly, as these are the two objectives optimized; they do not show the amount of gadolinium contained within the gadolinium oxide pins. For a given assembly layout and Pu content, changing the concentration of gadolinium will not only change the flux in nearby pins, but it will also cause the energy spectrum of the assembly to shift, dependent on the absorption cross-section of the gadolinium oxide pins. Therefore, increasing the gadolinium concentration may shift the spectrum in such a way as to cause the gadolinium oxide to be less effective as an absorber, and thus potentially increase the PPF value. This highlights the complex and interrelated nature of the objectives when optimizing the design of a nuclear fuel assembly.

The Pareto-front in Figure 19 is almost entirely populated by MOJADE solutions. These results suggest that MOJADE performs better than MOμJADE on these types of problems, which supports the finding from Problem 1. The solution found at the elbow of the Pareto-front (shown by the arrow in Figure 19) was depleted to 15 GWd/t, which covers the same time period investigated in the original paper. However, it should be noted that PPFs will continue to change over the multiple cycles and entire lifetime of the assembly (i.e. up to the 60 GWd/t seen in typical LWRs). Results from Problem 2, therefore, do not show the full lifetime performance of PPF. The evolution of the PPF against burnup for this MOJADE-generated assembly design can be seen in Figure 21 as the blue line, overlaid on the original results of (Yamate, et al., 1997).

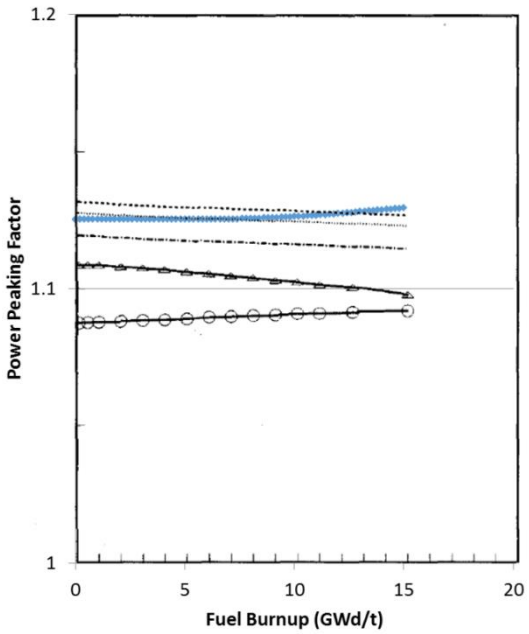

Figure 21: PPF progression with burnup for gadolinium oxide-MOX fuel assemblies with MOJADE-generated assembly design shown in blue, compared to other designs evaluated by (Yamate, et al., 1997), adapted from (Yamate, et al., 1997)

The original paper (Yamate, et al., 1997) investigated assemblies which ranged from 5.7 to 6.4 average Pu-pin wt% content. The chosen MOJADE solution had an average Pu-pin content of 19.5 wt%, which is a significantly higher, albeit unrealistic level for a 100% MOX loaded core. This test thus shows that DE algorithms are able to find designs that contain more Pu and keep internal PPF performance over one cycle comparable to that of assemblies with much lower Pu contents. Figure 22 compares the assembly layouts of the MOJADE solution chosen for depletion and an example 'expert' assembly design from the (Yamate, et al., 1997) study. The less conventional MOJADE design performs comparably with the 'expert' design, and illustrates the solution space searching capability of a stochastic optimization algorithm.

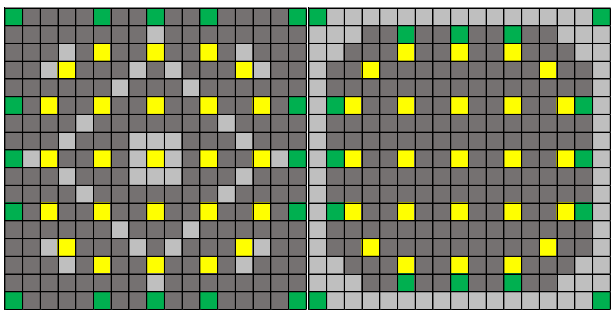

Figure 22: U-Pu MOX assembly layouts with gadolinium oxide poison rods produced using MOJADE (left) and from the literature (Yamate, et al., 1997) (right). Light grey and dark grey indicate MOX pins (dark grey have higher wt% Pu contents), green indicates a poison rod, and yellow indicates guide tubes.

3.3.3. *Sensitivity analysis*

Figure 23 and Figure 24 show the Pareto-fronts of each test using MOJADE with different control parameters in plots of PPF against –MOXT. Figure 23 compares the Pareto-fronts from each test run with the default parameter values and each test which changed the parameter adaptation rate (*c*). Figure 24 compares results with default parameter values to tests which changed the greediness of the selection strategy (*p*). As seen in Section 3.3.2, there is a high degree of result clustering, with few MOJADE solutions with –MOXT values between 0 and –15, for the reasons explained above. Figure 23 indicates that larger rates of parameter adaptation may reduce MOJADE's ability to converge, whereas Figure 24 suggests that varying the greediness parameter does not appear to have a large effect on the algorithm's performance for this problem. Further analysis of these results is performed by determining their statistical significance in Section 3.3.4.

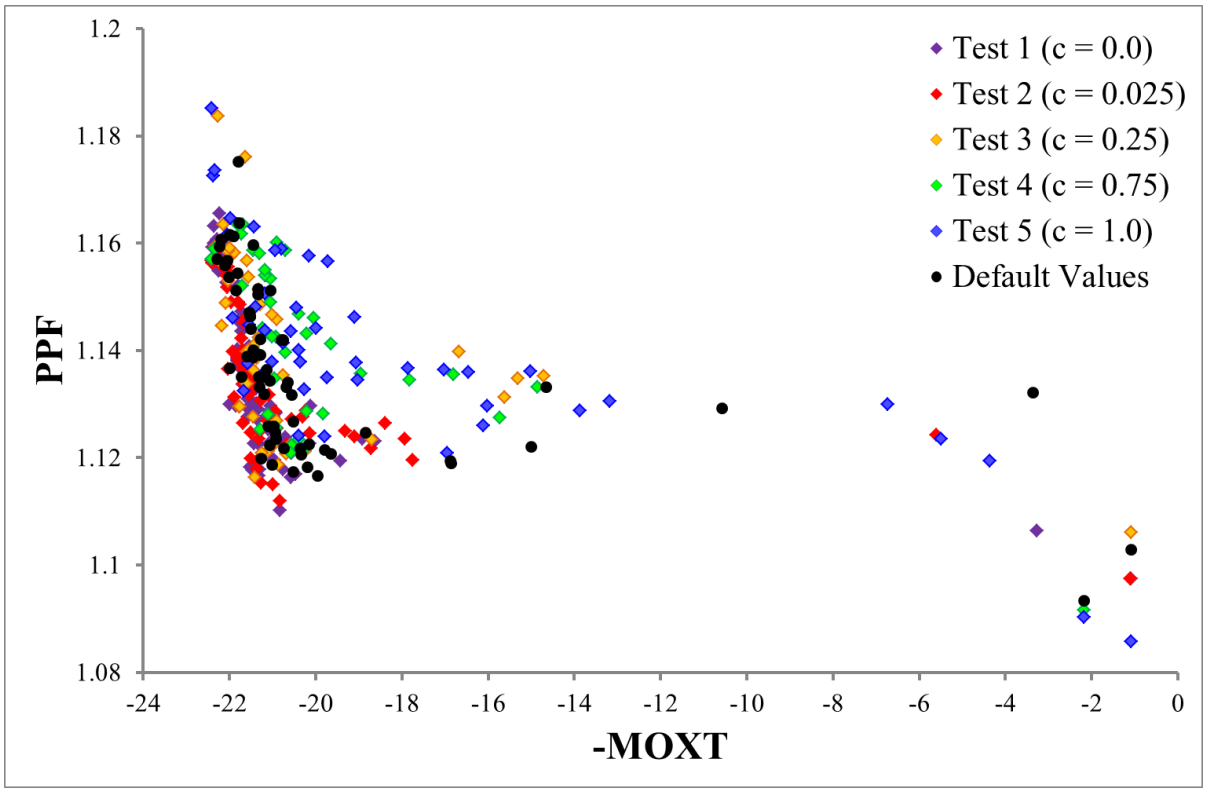

Figure 23: Pareto-front results for the parameter adaptation rate (*c*) sensitivity study

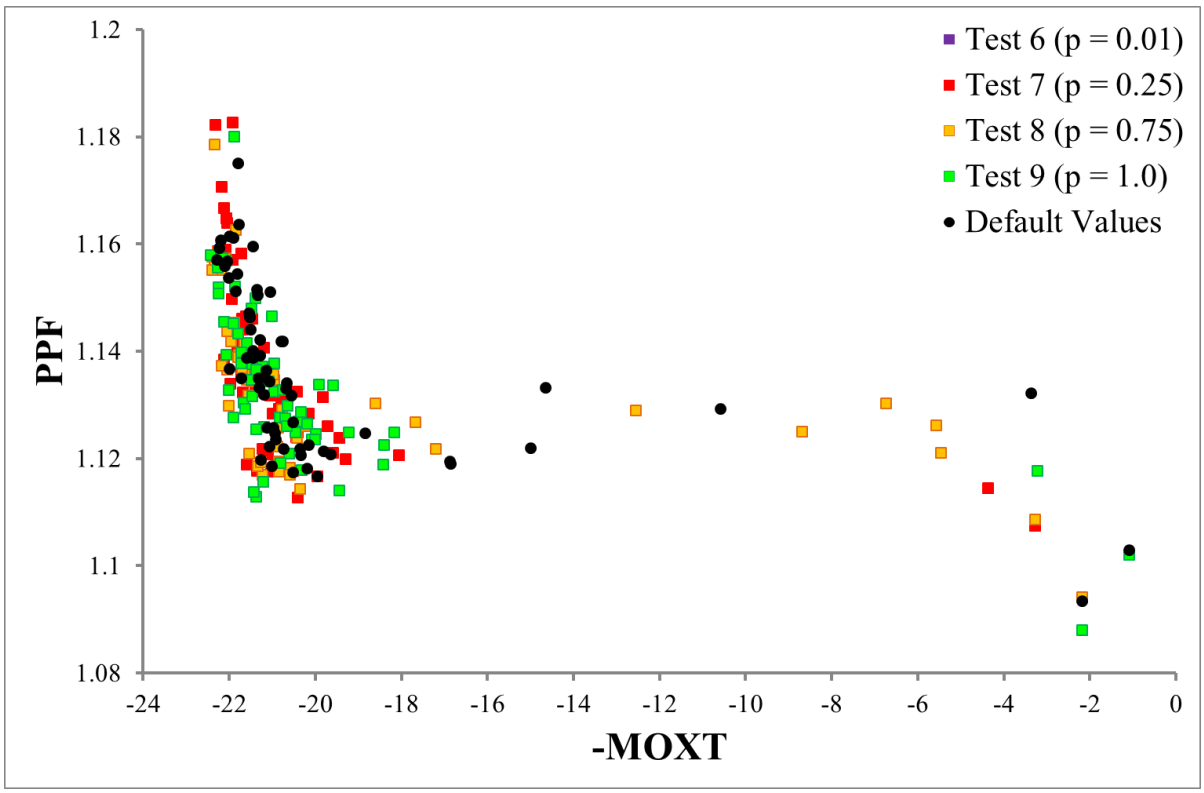

Figure 24: Pareto-front results for the greediness parameter (*p*) sensitivity study

3.3.4. *Statistical analysis of sensitivity study results*

Once again, the hypervolume and epsilon indicator values were used to quantify performance. The progression of the hypervolume indicator value was monitored to confirm that the relative performance of the algorithm with default parameters had stabilized within the 40 generations allowed and would not significantly change were it run for more generations. This provided a consistent number of evaluations by which to compare the effect of changing parameters, as allowing more generations for some parameter values would give them an unfair advantage in overall performance. This progression over the 40 generations (averaged over the 10 runs) can be seen in Figure 25.

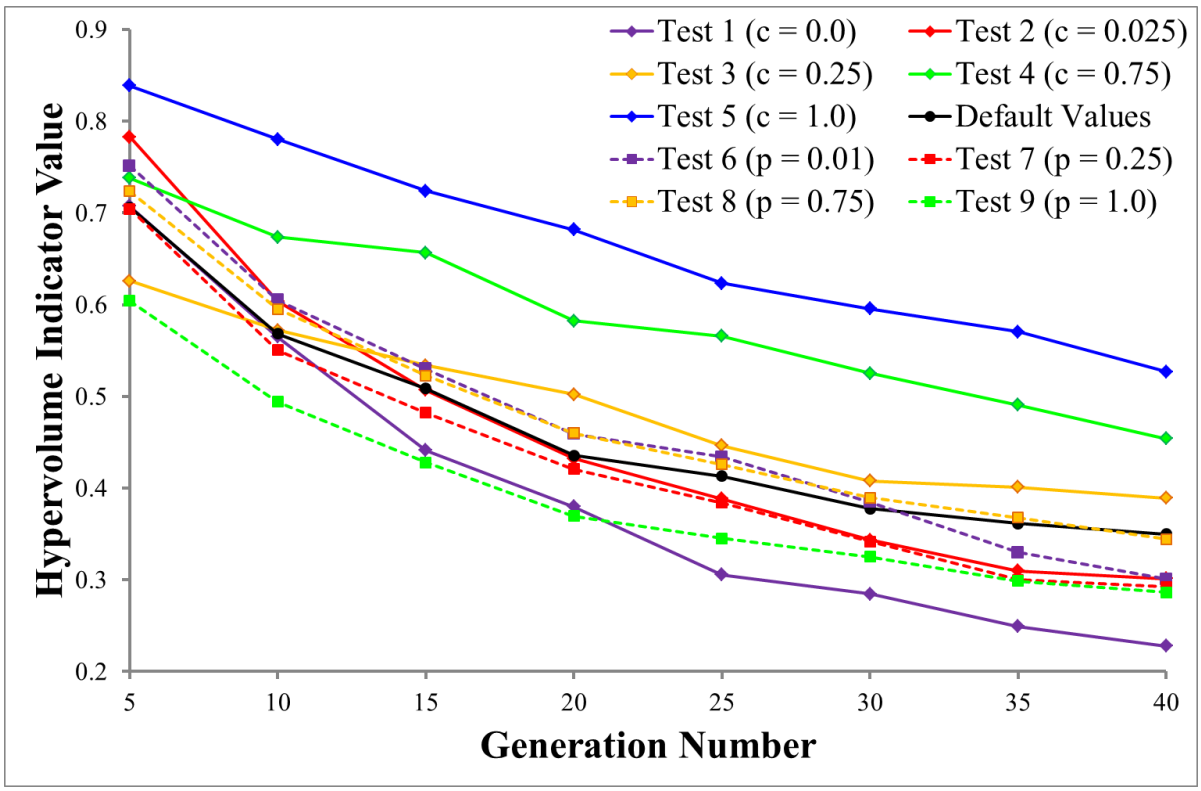

Figure 25: The average hypervolume indicator value for each sensitivity study test every 5 generations

Final hypervolume and epsilon indicator values were calculated (Table 12), as well as performing the Kruskal-Wallis test (Table 13) to determine whether observed differences are statistically significant. In this study, the Kruskal-Wallis test significance level values represent the probability that the difference between the performance indicator values for MOJADE runs with default parameter values and for each test could have occurred by chance. This is used to ascertain whether the performance of the DE algorithm MOJADE is significantly sensitive to changes to its control parameters.

Table 12: Sensitivity study hypervolume and epsilon indicator values: statistically significant results from the Kruskal-Wallis test (Table 13) are shown in bold

Test Number	Hypervolume Indicator		Epsilon Indicator	
	Mean	Standard Deviation	Mean	Standard Deviation
Default values	0.3204	0.1324	3.0770	2.6952
1	0.2249	0.0798	**0.6934**	**0.8192**
2	0.2857	0.1065	1.1678	1.1824
3	0.3692	0.1489	2.0480	2.5493
4	**0.4319**	**0.1024**	1.7474	2.1725
5	**0.5146**	**0.0836**	4.1147	2.4837
6	0.2886	0.0619	**0.9181**	**0.9652**
7	0.2805	0.1064	**0.8389**	**0.8338**
8	0.3329	0.1145	2.2707	2.5475
9	0.2713	0.0956	1.2848	0.9661

Table 13: Sensitivity study Kruskal-Wallis test results: statistically significant results (< 0.05) are shown in bold

Test	Hypervolume Indicator	Epsilon Indicator
1 *vs.* default values	6.96E-02	**1.02E-02**
2 *vs.* default values	9.40E-01	5.88E-02
3 *vs.* default values	3.26E-01	1.12E-01
4 *vs.* default values	**1.91E-02**	1.12E-01
5 *vs.* default values	**5.20E-03**	4.06E-01
6 *vs.* default values	8.80E-01	**2.84E-02**
7 *vs.* default values	7.06E-01	**4.94E-02**
8 *vs.* default values	5.45E-01	2.27E-01
9 *vs.* default values	8.80E-01	1.99E-01

Table 12 shows that none of the tests show a statistically significant change in both performance indicators compared to algorithm performance with default values for parameter adaptation and greediness. This suggests that MOJADE is reasonably robust in handling nuclear fuel assembly design optimization problems with heterogeneous fuel types. There is some evidence to suggest that hypervolume performance does deteriorate at higher rates of parameter adaptation. The parameter adaptation rate controls the distributions from which mutation and crossover rates are chosen for new solutions. Successful (i.e. non-dominated) solutions have their related crossover and mutation rates stored in normal and Cauchy distributions, respectively. Increasing the rate of parameter adaptation increases the importance of crossover and mutation rates most recently added to the archive. Lower rates make the algorithm less adaptive as it searches, which may cause it to miss areas of optimality and reduce its rate of convergence. Excessively high rates however cause the algorithm to utilize only the most recently successful crossover and mutation rates, which could result in premature convergence and becoming trapped in local minima for highly non-linear problems. There is also some evidence to suggest that epsilon indicator performance is affected by both parameter adaptation and greediness. Greediness directly impacts the diversity maintained in the population as the algorithm moves around the search space. An excessively greedy algorithm may not be able to maintain a sufficiently diverse population to properly explore the search space, whilst a lack of elitism can slow algorithm convergence. These results suggest that some tuning of the MOJADE control parameters may produce results which are more consistently closer to the true Pareto-front (i.e. improved epsilon performance), but do not suggest that the true Pareto-front itself can be improved further (i.e. changing parameters did not produce statistically significant results with improved hypervolume indicator).

3.4. Conclusions

This study has introduced and investigated the use of multi-objective Differential Evolution algorithms for optimizing nuclear fuel assembly design problems. Beginning with a performance comparison against an EA on a typical problem, the MO DE algorithms MOJADE and MOμJADE demonstrated that DE is able to find solutions comparable in quality to those found by MOAA and arguably better explore the search space of fuel pin patterns. Both DE algorithms exhibit good performance in this exploratory optimization problem, despite the algorithms originally being designed for single-objective optimization with a known global optimum. MOJADE and MOμJADE were then tested on a more complex design problem involving both plutonium management and gadolinium distribution within a MOX assembly. Again, the DE algorithms were shown to be capable of generating designs that contain more plutonium compared to those from the reference literature and featured a lower PPF at BoL, though they show a reduced performance with depletion.

From these two problems it was concluded that MOJADE exhibits superior performance to MOμJADE. For the final test, the sensitivity of the performance of the MOJADE algorithm to the settings of its control parameters was investigated on the second problem. The two control parameters, the rate of parameter adaptation and the greediness of the algorithm, were varied and the relative performance of the algorithm was analyzed for statistical significance. The results indicate that MOJADE is robust to changes in its control parameters and does not require tuning to individual problems, which supports an earlier finding by (Zhang & Sanderson, 2009) on the underlying JADE algorithm. This work demonstrates that DE algorithms are capable of optimizing MO nuclear engineering design problems in an effective and reliable manner. These algorithms can now be tested on more complex problems with a wider range of objectives, including introducing thermal-hydraulic feedback mechanisms and using three-dimensional models for additional axial optimization of fuel.

4. Multi-objective, multi-physics optimization of 3D mixed-oxide LWR fuel assembly designs using the MOJADE algorithm

4.1. Introduction

Optimization problems as seen in the research literature are typically simplified and/or heavily constrained real-world problems which reduce the highly complex process of design to one or two objectives. These are then optimized through combining a search algorithm with some analysis package to simulate a single set of physical processes, such as neutronics or thermal hydraulics, in order to evaluate and converge on an optimal solution. However, real-world nuclear engineering problems feature complex multi-physics phenomena and require equally complex analysis software. For optimization to demonstrate its usefulness in this area it must demonstrate an ability to handle numerous competing objectives whilst simulating environments more realistic to those inside a nuclear reactor. To address this, this chapter applies the previously demonstrated metaheuristic optimization algorithm MOJADE to two design problems, a 3D PWR Supercell and a 3D BWR fuel assembly. Common performance objectives related to both neutronics and thermal hydraulics are evaluated simultaneously, in 3D design space, using the concept of Pareto dominance. This study is intended to fulfil Requirements 3 and 4 of Section 1.4.1, whilst maintaining the timescale in Requirement 5.

Both problems tackled in this chapter are multi-objective, and no weighting was given to any of the objectives; nor was the problem treated as a series of sequential single-objective problems by introducing constraints on some of the objectives. This is in order to avoid contaminating the results with factors that are mostly subjective and based on the designer's judgement (Parks, 1996). Furthermore, the problems are based on real-world multi-physics fuel assembly design challenges concerning two of the latest reactor designs on the market: the EPR by Areva and the ABWR by Hitachi GE. Optimization was performed using the multi-objective DE algorithm MOJADE, which has already demonstrated both its effectiveness and its insensitivity (discussed in Chapter 3 above) to different nuclear engineering fuel assembly optimization problems (Charles & Parks, 2019). MOJADE was combined with a development version of the reactor physics analysis package WIMS (Lindley, et al., 2015) to evaluate both the reactor physics and thermal-hydraulic performance of the algorithm-generated solutions.

The rest of the chapter is laid out as follows. Sections 4.2 and 4.3 detail the two complex and realistic problems in the nuclear engineering design of LWR fuel assemblies on which the algorithm was tested. The first seeks to optimize a 2×2 supercell of UOX – MOX assemblies relating to the EPR design; the second a 3D BWR fuel assembly relating to the ABWR design. The results of these two computational experiments are detailed in Sections 4.4.1 and 4.4.2 respectively. The chapter concludes with a summary of the main findings and their implications for future work in Section 4.5.

4.2. EPR test problem

4.2.1. *The EPR*

The UK European Pressurized Reactor or EPR is a Pressurized Water Reactor (PWR), designed by Framatome and Electricité de France (EDF) for construction and operation in the UK (Orano & EDF, 2007). It has a rated thermal power of 4500 MW and an electrical power of around 1630 MW. It was designed to improve over existing technology in a number of ways, including core damage frequency, plant availability, load following capability, and an ability to load up to 50% of the core with MOX fuel assemblies. As part of the UK's Generic Design Assessment regulatory process with the Office of Nuclear Regulation, documents were made publicly available and contain significant details pertaining to the design and operation of the UK EPR (Orano & EDF, 2007). From these it is possible to construct a representative model of the EPR reactor core fuel assemblies.

4.2.2. *WIMS and the ARTHUR subchannel module*

The lattice reactor physics code WIMS is used to solve the neutron transport equation, to produce the flux map for the supercell and to calculate individual pin powers. A development version of WIMS was used for this work to include the recently developed 'ARTHUR' subchannel module, which is due to be released in the quality assured release of WIMS 11 (Tollit, et al., 2018). Based on established approaches such as the COBRA code series (Pacific Northwest Laboratory, 1983), ARTHUR provides an integrated thermal hydraulics solver capable of modelling at the fuel assembly average resolution and also at a pin-by-pin / channel-by-channel resolution. ARTHUR solves the energy conservation equation for pins, coupled to coolant channel mass, momentum and energy conservation equations. Using an integrated solver avoids the difficulties involved in attempting to couple two separate codes together, and has potential benefits in avoiding the increased computational loads associated with coupled codes. Coupled codes requires each code to either pause during runtime to await the output of the other (requiring continued memory usage), or to exit completely and restart once the other code has finished (increasing the read / write demand). Integrated codes on the other hand continue without interruption. This feature requires modelling the assembly in 3D to provide an axial length over which to calculate the rise in coolant temperature and density as it flows up the channel and is not possible in a purely 2D model. This is performed in the problems below by solving the multigroup eigenvalue neutron transport equation for each spatial element to give a 3D power distribution, which can then be applied to ARTHUR's "pin and channel" model to determine thermal-hydraulic feedback for each corresponding region, developed during my internship with ANSWERS as detailed in section 1.2.2.

Some features of the ARTHUR module as implemented in this work include:

- The Finite Volume Method to solve for enthalpy, axial mass flow rate and pressure drop
- The pin conduction model which includes user-specified material properties and fuel-cladding-gap heat transfer, featuring the Dittus (Dittus & Boelter, 1985) and Thom (Thom, et al., 1965) heat transfer correlations
- EPRI (Lellouche & Zolotar, 1982) correlations which are used for sub-cooled boiling and vapour slip
- The Blasius friction model and two-phase factors (Blasius, 1913)
- The EPRI correlation (Reddy & Fighetti, 1983) which is used for Critical Heat Flux prediction

New material densities and temperatures are then used to update the appropriate cross-sections for the model, and the process repeats until a convergence criterion has been achieved (*e.g.* on temperature, k-effective, or a hard iteration limit).

4.2.3. *Test problem*

This investigation uses a 2×2 supercell of UK EPR-type fuel assemblies with translational (top-bottom, left-right) boundary conditions around all four radial edges, and vacuum boundaries at the top and bottom. The supercell consists of two UOX fuel assemblies and two MOX fuel assemblies arranged in a checkerboard pattern, as shown in Figure 26, without axial reflector. All assemblies are fresh fuel, with the exact MOX compositions and uranium enrichments depending on the supercell created. This model therefore represents a UK EPR core of 50% MOX assembly loading.

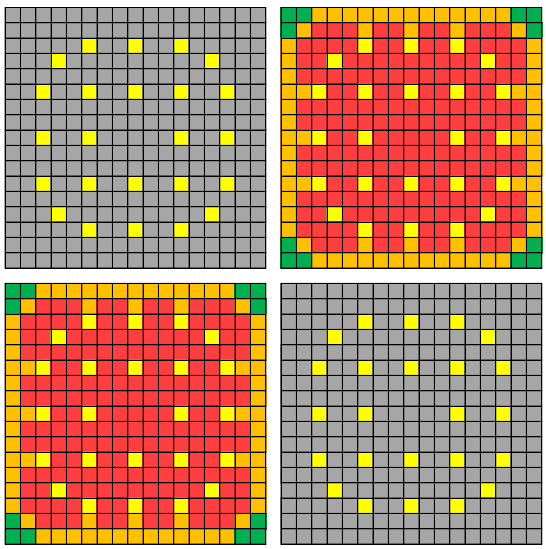

Figure 26: EPR supercell of 2 MOX fuel assemblies and 2 UOX fuel assemblies arranged in a 2×2 grid. Yellow pins are Guide Tubes, grey pins are UOX, green pins are MOX type 1, orange pins are MOX type 2, red pins are MOX type 3.

The design problem concerns optimizing the distribution of plutonium and gadolinium within the MOX and UOX fuel assemblies to optimize the following objectives:

1. Maximize the amount of plutonium in the assembly (MOXT) at BoL
2. Minimize the PPF over the life of the assembly
3. Maximize the minimum Departure from Nucleate Boiling Ratio (DNBR) encountered over the life of the assembly[9]

These objectives were chosen as they represent desirable performance and safety criteria for nuclear fuel assemblies. To achieve these objectives, the algorithm generates different sets of 2×2 assemblies with three types of MOX pin with varying MOX pin amounts. These supercells are then evaluated using the WIMS reactor physics code in order to determine their performance against the objectives. The algorithm then selects which supercell designs are allowed to proceed to the next generation, and the process repeats until a generation limit has been reached. Through a process of trial and error, a generation limit of 50 was chosen for this problem, as by then the Pareto-front had been most clearly established and was no longer undergoing significant change from generation to generation.

To offset the additional reactivity and potential for power asymmetry within the reactor produced by including plutonium, the algorithm has the ability to substitute MOX pins and UOX pins with gadolinium oxide pins of up to 10 wt% gadolinium. There is no upper limit to the number of gadolinium oxide pins that can be placed, but the presence of gadolinium oxide in the MOX assembly necessarily reduces the amount of Pu contained within the assembly. Therefore, it provides another means of balancing the trade-offs between the objectives.

The level of burnup of the supercell was set at 15 GWd/t as a simplified representation of the length of a single PWR cycle. In real-world operation, assemblies do not have a fixed uniform burnup as the radial and axial powershapes are not completely flat. In addition, the shuffling of fuel during reloading will place fresh fuel next to once or twice burned fuel. However, for the purposes of the study a fixed burnup is used as a proof-of-concept for the applicability of the methodology to real-world engineering problems. A rating of 38 MW/t was assumed for all evaluated assemblies when calculating depletion. Burnup was performed in 4 steps: an initial depletion of 1×10^{-12} MWd/t during which saturated

[9] Operating closer to the departure from nucleate boiling point increases the amount of heat transfer and is therefore more beneficial from a performance standpoint. However, in this study the DNBR is used purely as a safety parameter and hence is maximized, in order to determine the minimum safety margin that exists for this design, which would inform the design engineer on how much potential safety margin they have to work with when considering other factors.

quantities of Xe135 are calculated and added to fuel materials (achieved by using the 'XENON' keyword in the BURNUP module in WIMS), to represent xenon equilibrium with fresh fuel. Following this depletion was carried out to 1 GWd/t, then to 8 GWd/t and finally 15 GWd/t. These steps were chosen after a period of trial-and-error to determine the sufficient resolution to accurately model total burnup to 15 GWd/t whilst minimizing the number of steps (and hence the computational cost). Each depletion step consisted of a neutronics / thermal hydraulics solver loop to include the thermal-hydraulic effects and recalculate the PPF and DNBR objective values for every depletion step, in order to evaluate these objectives over the life of the assembly.

To include thermal-hydraulic feedback affecting criticality, WIMS was executed iteratively a number of times to allow convergence between neutronics and thermal hydraulics. Through testing, it was found that an iteration of 2 cycles was sufficient to reliably give agreement between cycles of around 500 pcm. This is also justified by the nature of the problem, which is to explore a very large possible search space for potentially good solutions, and not to claim that a detailed design evaluation has been performed on every solution. Furthermore, for generated solutions that have extremely heterogeneous layouts (such as large gradients of plutonium concentration within the MOX assembly), the resulting PPF- and DNBR-evaluated objectives are likely to be too poor for the solution to be selected for the next generation, much less for the solution to be on the Pareto-front. It is therefore not worth the additional computational effort required to fully converge the multi-physics simulations.

The model was set up using material and design data sourced from the Pre-Construction Safety report, specifically Chapter 4 – Reactor and Core Design (EDF, 2012), which sets out the physical dimensions for the supercell (Table 14), as well as material data such as the plutonium vector (Table 15) and coolant properties (Table 16). Material property data were sourced from (IAEA, 2006). Some properties will be changed by the algorithm; these are highlighted in Table 15.

Table 14: PWR fuel assembly properties

Parameter	Value
Core height (active)	4.2 m
Assembly layout	17×17
Pin pitch	1.2598 cm
Fuel pellet radius	0.40956 cm
Fuel pin radius	0.4751 cm
Number of fuel pins	265
Guide tube radius	0.5725 cm
Guide tube radius + cladding	0.6225 cm
Number of guide tubes	24
Gap between fuel assemblies	0.08 cm

Table 15: PWR material properties

Parameter	Value
UOX pin composition	Uranium dioxide
Uranium vector (wt%)	U234 – 0.04% U235 – 5% U238 – 94.96% (algorithm controlled)
Plutonium vector (wt%)	Pu238 – 4% Pu239 – 50% Pu240 – 23% Pu241 – 12% Pu242 – 9.5% Am241 – 1.5%
MOX pin composition	Uranium / plutonium dioxide (algorithm controlled)
Maximum wt% Pu per MOX pin	20 %
MOX pin U235 enrichment (wt%)	0.2 %
UOX-gadolinium pin composition	Gadolinium oxide / uranium dioxide (algorithm controlled)
Gadolinium vector (wt%)	Gd152 – 0.2% Gd154 – 2.18% Gd155 – 14.8% Gd156 – 20.47% Gd157 – 15.65% Gd158 – 24.84% Gd160 – 21.86%
Maximum gadolinium oxide per Gd-UOX pin (wt%)	10%
Gadolinium oxide pin U235 enrichment (wt%)	2.6%
Cladding material	Zircaloy-4[10]
Coolant material	Borated water (700 ppm, based on EPR Cycle 1 nominal power with xenon equilibrium (EDF, 2012))

[10] The UK EPR uses Zircaloy M5, but this is approximated to Zircaloy-4 as correlations for thermal conductivity are more easily accessible. Since the main differences between the two are concerned with fuel performance and not neutronics or thermal hydraulics, this was judged as an acceptable simplification.

Table 16: EPR coolant properties

Parameter	Value
Coolant inlet temperature	295.6 ˚C
Coolant velocity	500 cm / s
Core inlet pressure	155 bar

Both the MOX and UOX assemblies were assumed to have $1/8^{th}$ symmetry, giving 40 unique pin positions for each assembly. When generating the initial population, a maximum of five pins per $1/8^{th}$ of each assembly can be gadolinium pins (based on the original design documentation). However, during the optimization process, there is no upper limit on how many pins can be gadolinium, as this is naturally counterbalanced by the objective of maximizing the amount of plutonium contained within the MOX assembly. Three types of MOX pin are allowed with plutonium oxide concentrations up to 20 wt% per pin. The U235 enrichment for MOX pins is kept fixed at 0.2 wt%, but for UOX pins it can vary up to 5 wt%. MOX pins are confined to the MOX assembly and UOX pins are confined to the UOX assembly to preserve heterogeneity – only gadolinium pins can be placed in both assemblies. The value of each design variable for each assembly is determined by the MOJADE algorithm in its function to generate solutions which best satisfy the objectives.

4.2.4. *Moderator temperature coefficient constraint*

All solutions generated by the algorithm were constrained to have a negative Moderator Temperature Coefficient (MTC) of reactivity, which is typical for LWRs under nominal conditions. This constraint is imposed before the solution is evaluated against the objectives in order to reduce computational running time. Solutions which fail to satisfy the MTC constraint are rejected outright and new solutions which do satisfy the constraint are generated to replace them. The MTC was not selected as an objective to optimize, as requiring it to be minimized could have resulted in unrealistic assembly designs: a negative MTC is desirable but a large negative value of MTC places unacceptable demands on the reactivity control system, particularly for certain cool-down accident scenarios such as a mainline steam break. The MTC is primarily affected by the moderator to fuel ratio and increases with the amount of fuel in the reactor (e.g. increasing the wt% Pu in the MOX pins). Therefore, due to the objectives of the study, the MTC value was not expected to be excessively negative. In the UK EPR, the MTC ranges between -20 and ~-80 pcm/°C.

4.2.5. *Baseline comparison*

In order to provide some indication as to the effectiveness of the optimization algorithm, a comparison solution was generated based on data from the publicly available literature on the EPR design in (EDF, 2012). Some assumptions were necessary as not all the data is in the public domain. These include:

- No gadolinium oxide pins were included in the baseline design. In the available literature, the EPR is described as being capable of handling up to 50% MOX assemblies, although core layout pictures only depict up to a 30% loading, with the MOX assemblies surrounded by UOX assemblies with varying numbers of gadolinium oxide pins. The majority of assemblies surrounding MOX assemblies do not have gadolinium oxide pins in the layouts provided.
- Region averages of plutonium content were assumed for each of the three MOX pin types. In the baseline design a maximum limit of 7.44 wt% Pu per fuel rod is applied to comply with fabrication limits and also to limit the impact on the void coefficient[11], according to (EDF, 2012). For designs generated by the algorithm, this limit was changed to 20 wt% (consistent with other studies e.g. (Lattarulo, et al., 2014)) in order to see the effect of pins with higher wt% Pu. Given this study is a demonstration of the capabilities of the algorithm and the resulting trade-offs between objectives, and is not intended to provide new assembly designs that would be suitable for a final design, this was deemed to be an acceptable constraint relaxation. The supercell baseline design layout is shown in Figure 27, which shows the values of wt% Pu within the MOX pins that are normally controlled by the optimization algorithm.

[11] Increasing Pu content in MOX assemblies increases the void coefficient due to the peak in thermal capture of Pu239 at ~0.3eV, which encourages hardening of the spectrum.

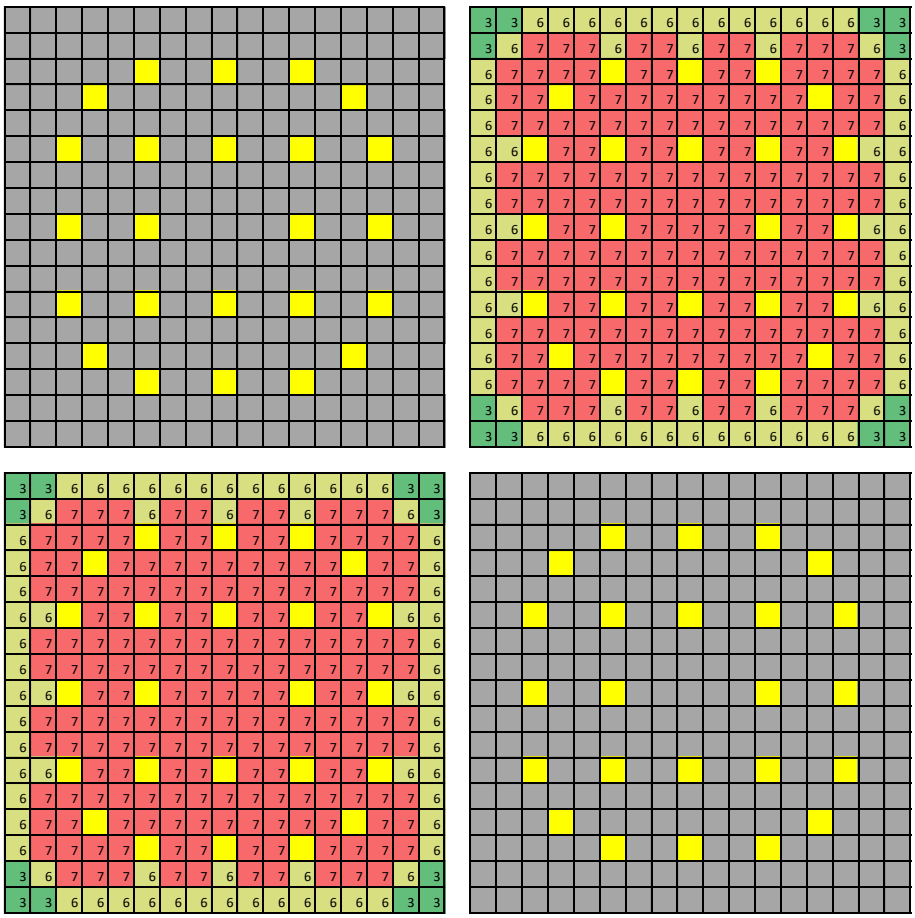

Figure 27: Baseline EPR supercell. 3.44 wt% Pu in MOX type 1 (dark green), 6.44 wt% Pu in MOX type 2 (light green), 7.44 wt% Pu in MOX type 3 (red)

This model was evaluated using the same WIMS sequence as algorithm-generated solutions, and its objective values were used to provide a baseline comparison.

4.3. ABWR test problem

4.3.1. *The ABWR*

The ABWR is the latest design of generation III+ reactor in operation by GE Hitachi Nuclear Energy. It has a rated full power of 1350 MWe (Hitachi, 2014). Currently in operation at three sites in Japan, there have been numerous plans to construct additional reactors in Japan, Taiwan, the United States and in the UK. Unfortunately, all of these projects have either been suspended or cancelled for financial reasons, with the UK project being the latest to face cancellation (BBC, 2019). However, the design remains a possible future reactor choice. As BWRs differ substantially in operation to PWRs with more complicated thermal hydraulics (the primary coolant undergoing a phase change inside the core), they

offer unique problems on which to test the performance of our design optimization framework, utilizing multi-physics software. Two of these features, which were modelled in the problem, are detailed below.

Firstly, due to the primary coolant phase change, the axial fuel composition of BWR fuel pins is generally more heterogeneous than PWR fuel pins. BWRs can utilize partial-length rods to decrease the amount of fuel in the upper regions of the core, which offsets the increased neutron mean free path in steam and reduces the likelihood of U238 in the fuel absorbing a neutron and creating Pu239. The pressure drop is also reduced, potentially allowing for more fuel rods or a larger fuel rod diameter.

Secondly, water rods placed in the centre of the bundle increase the moderation effect, decrease the maximum local power factor and reduce the magnitude of the void coefficient of reactivity (the reactivity response of the reactor as the voidage increases) by increasing the fuel-to-moderator ratio (Bozzola, 1982).

4.3.2. *Test problem*

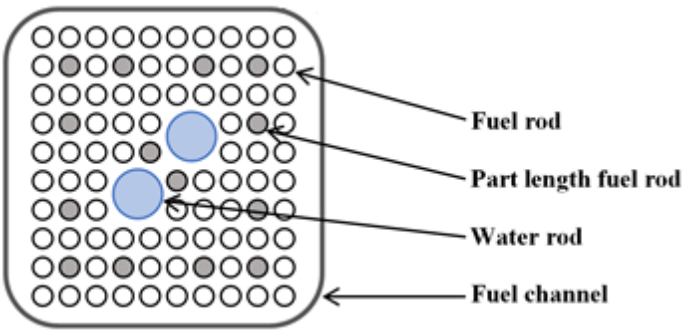

Figure 28: One quadrant (lower right) of an ABWR cell, featuring one fuel bundle, adapted from (Hitachi-GE, 2017)

As before, the same development version of the lattice reactor physics code WIMS is used to determine the flux profile and individual pin powers, along with the integrated thermal hydraulics solver. This test problem concerns a single BWR fuel assembly (Figure 28, above), modelled as three 10×10 grids of fuel pins and two water rods, with reflective boundary conditions, to represent three axial layers of a 3D fuel bundle inside the reactor core (Figure 29, below). Three layers were chosen as a compromise between accuracy and computational speed.

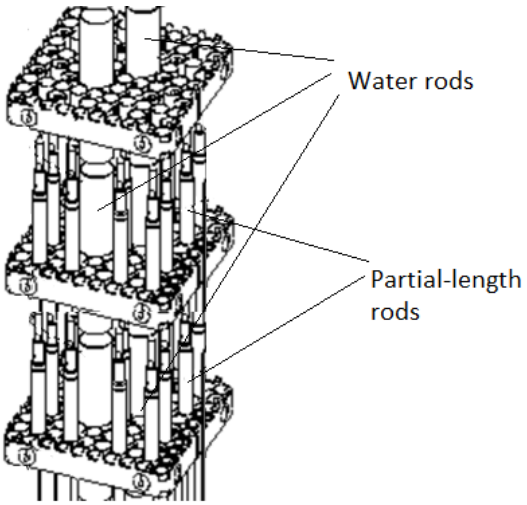

Figure 29: Three axial layers comprising the 3D representation of ABWR assembly used in this study, showing water rods and partial-length fuel rods (full-length fuel rods not shown here), adapted from (Hitachi-GE, 2017)

Each axial layer is first solved for the neutron flux using the MoC. These layers are then merged to form a 3D model which is solved for the neutron flux in 3D using the simplified spherical harmonics method (Gelbard, et al., 1959), with reflective boundaries along the radial edges and vacuum boundaries at the top and bottom. The 3D flux solution is used to determine the power distribution for the thermal-hydraulic feedback, which then updates the material properties (density and temperature) for the axial slices, and the process continues until convergence on k-effective is achieved. This model allows simulation of both full- and partial-length fuel rods within the assembly, something that would not be possible in a less sophisticated 2D model.

Tie-rods, tie-plates, end plugs and springs, the assembly shroud, grid spacers, the control blade and axial reflectors are not modelled here. This problem is intended to showcase the concept of linking optimization methods to complex multi-physics problems, but not to undertake the detailed analysis that would be required in perfecting the design. Therefore, these omissions are deemed acceptable for the current scope, as they would only serve to increase the accuracy of the solution, and not the ability of the algorithm to optimize.

Convergence between thermal hydraulics and neutronics is once again performed for every test assembly within the multi-physics software. Unlike the looser coupling used in the previous PWR problem, the software continues to run until the difference between k-effective of the neutronics from one iteration is at least within 100 pcm of the previous iteration. It should be emphasized that this level of convergence is not suitable for detailed design work, although may be appropriate for ranging studies performed at the concept design stage.

The test problem concerns optimization of the design of heterogeneous BWR fuel within the assembly, with the following objectives:

1. Minimize the gadolinium concentration within the assembly
2. Maximize the amount of plutonium in the assembly
3. Minimize the PPF in the assembly
4. Maximize the minimum Critical Heat Flux Ratio (CHFR) in the assembly

For BWRs, a priority safety criterion for thermal hydraulics is to prevent dryout from occurring within the coolant channels and uses the Critical Power Ratio (CPR). Dryout happens when the CHF is exceeded and the annular flow regime within the channel dissipates to expose the fuel pin to vapour coolant only. This leads to highly reduced heat transfer and potential breaching of thermal limits. The standard method in safety analysis involves determining the correlation between the boiling length (the distance between the dryout point and the point at which the local quality (the ratio of the mass of the steam to the mass of the mixture) is zero, i.e. sub-cooled boiling is no longer possible) and the critical quality (Hench & Gillis, 1981). This is in contrast to PWR thermal hydraulics where local conditions, such as heat flux, dominate the process. In ARTHUR, the CHF correlation is selected by the user, and the option chosen for this study was the EPRI correlation, which was designed with both PWR and BWR applications in mind (Reddy & Fighetti, 1983). This correlation has demonstrated good agreement with experimental results (Chen, et al., 1984), and is considered to be sufficient for steady-state BWR analysis (Ferroni, et al., 2009). It is used here to calculate a CHFR, which will be a performance objective to maximize and is not intended to represent the CPR.

According to the literature, the ABWR is capable of handling a 100% MOX core (Ihara, et al., 2009) (Hitachi-GE, 2017). It is therefore assumed, for the purposes of this investigation, that all the fuel pins, whether full- or partial-length, are MOX pins. Three different concentrations of MOX pin are allowed, up to 20 wt% Pu each, and one type of partial-length rod MOX concentration is allowed. The optimization algorithm can vary the distribution and number of each type of full-length MOX pin and partial-length pin across the assembly (although the position and number of water rods is kept constant). All fuel pins (full-length and partial-length) have one radius, which is allowed to vary from 0.3 to 0.55 cm and has a fixed clad radius of 0.066 cm. Each of the two water rods is modelled in the lattice code simply as four separate water rods in a 2×2 configuration, with a radius of 0.5325 cm each, to conserve mass.[12] The control blade is not modelled. The layout is shown in Figure 28. The assemblies are

[12] The thermal hydraulics module in the development version of WIMS used in this study did not feature cross-channel mixing (i.e. the coolant in a channel surrounding one fuel pin does not mix with neighbouring channels). Therefore modelling a single water rod as four separate rods does not have the same thermal-hydraulic implications here as it would in real life.

evaluated as before using the multi-physics software in order to determine their performance against the objectives, which determines which designs will be chosen for the next generation. This process repeats until a generation limit of 50 is reached.

In the same manner as for the PWR problem, physical (Table 17), material (Table 18) and coolant properties (Table 19) were sourced from the ABWR Pre-Construction Safety Report, specifically Chapter 11 – Reactor Core (Hitachi-GE, 2017) as well as (IAEA, 2011) and (Peakman, et al., 2019). Some material property data was sourced from (IAEA, 2006). Some properties will be changed by the optimization algorithm; these are highlighted in Table 18.

Table 17: BWR fuel assembly properties

Parameter	Value
Core height (active)	3.810 m
Partial-rod length	2.540 m (due to three axial layers modelled)
Assembly layout	10×10
Pin pitch	1.295 cm
Fuel pin radius	0.3 – 0.55 cm (algorithm controlled)
Fuel cladding thickness	0.066 cm
Number of fuel pins	92 (49 with ½ assembly symmetry)
Water pin radius (Each modelled as 4 smaller pins in a 2×2 configuration)	1.161 cm, modelled as 4 pins with radius of 0.5325 cm each

Table 18: BWR material properties

Parameter	Value
Plutonium vector (wt%)	Pu238 – 4% Pu239 – 50% Pu240 – 23% Pu241 – 12% Pu242 – 9.5% Am241 – 1.5%
MOX pin composition	Uranium / plutonium dioxide (algorithm controlled)
Maximum wt% Pu per MOX pin	20%
MOX pin U235 enrichment (wt%)	0.07 – 5% (algorithm controlled)
Cladding material	Zircaloy-2
Coolant material	Non-borated water

Table 19: BWR coolant properties

Parameter	Value
Coolant inlet temperature	278 ˚C
Coolant mass flow rate per assembly	16,628.00 kg/s
Core pressure	71.7 bar

Assemblies were assumed to have ½ symmetry, giving 49 unique pin positions per assembly. No limit was placed on the number of partial-length pins since the total amount of plutonium in the assembly is reduced if a partial-length rod is used, which reduces the performance against objective 2.

4.3.3. *Void coefficient constraint*

All solutions generated by the algorithm were constrained to have a negative Void Coefficient (VC) of reactivity. Solutions which fail to satisfy the VC constraint are rejected outright and new solutions which do satisfy the constraint are generated to replace them.

4.3.4. *Baseline comparison*

As before, a baseline was generated using available data from the literature. However, as there was no information available for the design of MOX ABWR assemblies, the baseline comparison is for a UOX-only ABWR assembly, which features a uniform enrichment of 4.9 wt% and zero partial-length rods. The radius of the fuel pins was 0.447 cm. The radius of the equivalent water rods was kept at 0.5325 cm.

4.4. Results and discussion

4.4.1. *EPR test results*

The Pareto-front solutions from 20 independent runs of the design optimization process were recorded and an overall Pareto-front against all three objectives was identified. Figure 30 and Figure 31 show the performance of PPF *vs.* –MOXT and –DNBR *vs.* –MOXT respectively, with the baseline design included for comparison (in orange). Since all objectives are to be minimized, the lower left quadrant is the most optimal "ideal" location for each graph, although in reality this may not be possible to reach. Solutions where all MOX pins have at least 15 wt% Pu are coloured in red. Solutions where all MOX pins have less than 10 wt% Pu are blue, and solutions which have MOX pin plutonium concentrations between 10 and 15 wt% are coloured in green. For Figure 31, the horizontal line denotes where the DNBR limit is breached and solutions above this line exceed the CHF. In real-world analysis, this cutoff is usually placed lower (for example the UK EPR uses a DNBR limit of 1.21 for high pressure accidents, and a limit of 1.12 for low pressure accidents). In Figure 31 the line is purely there for reference to the CHF and is not a comment on the suitability of solutions against real-world DNBR limits.

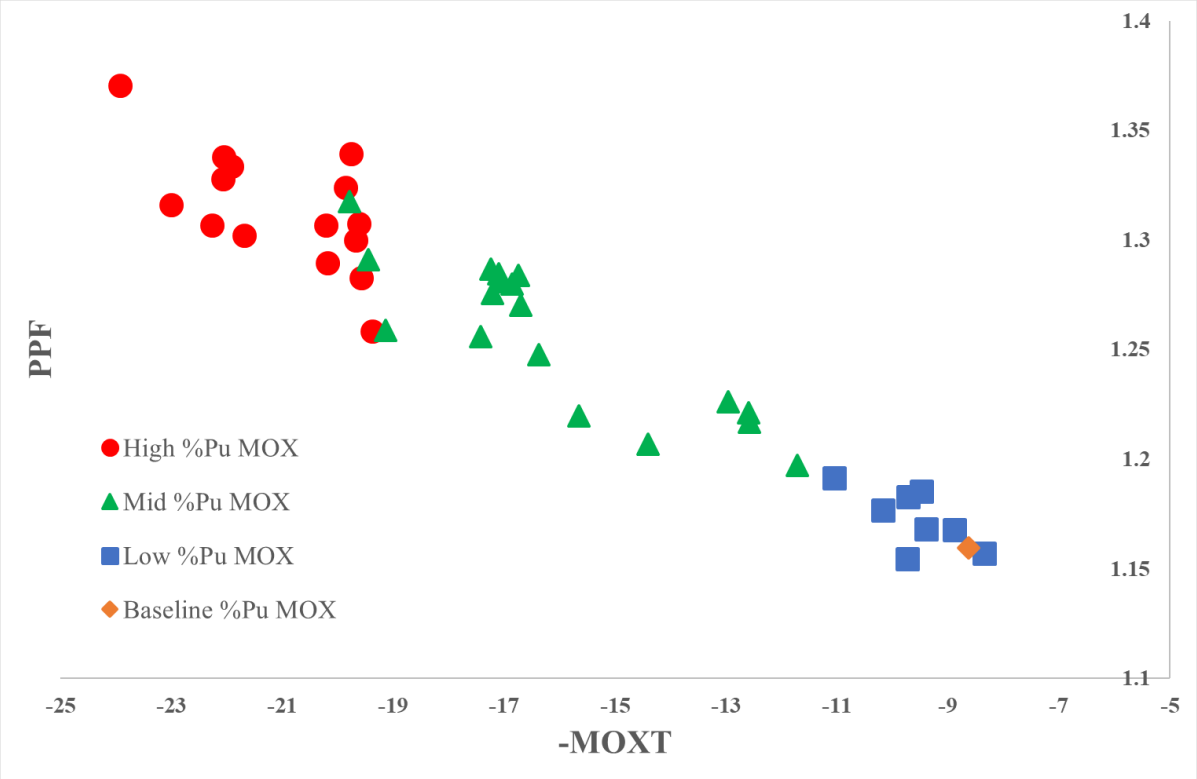

Figure 30: PPF *vs.* –MOXT plotted for Pareto-front solutions from the EPR problem

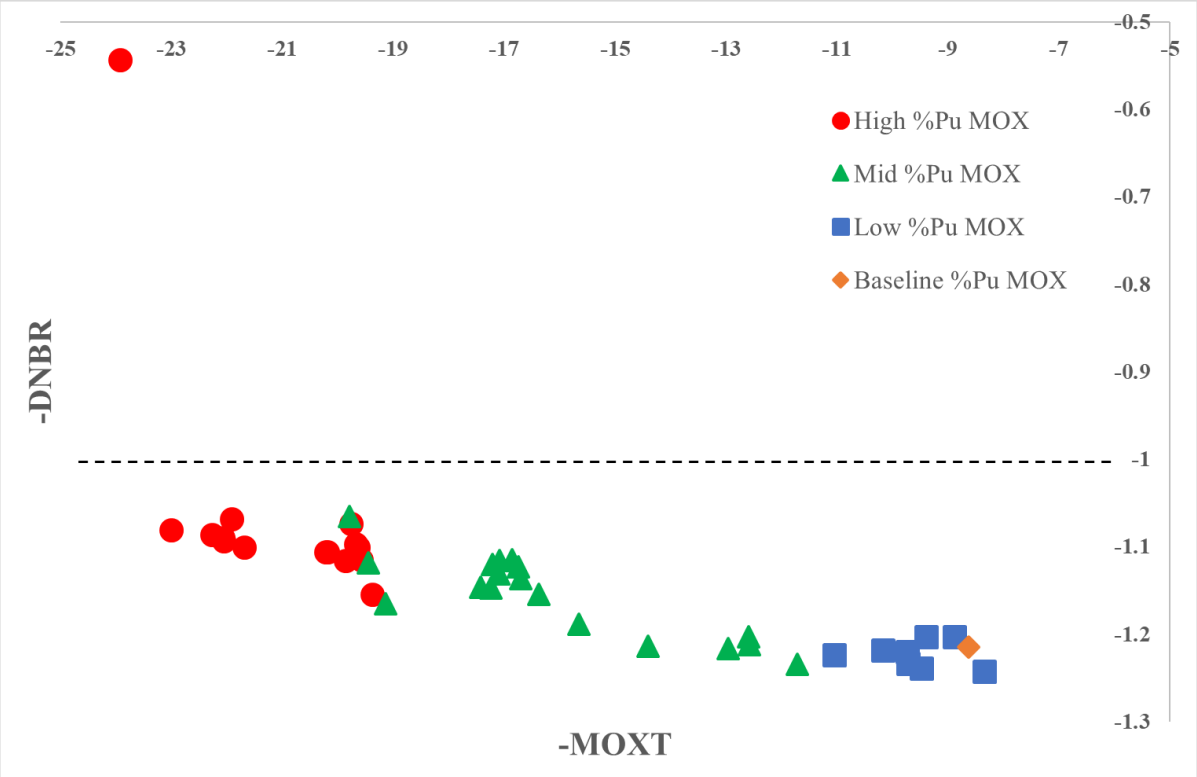

Figure 31: –DNBR *vs.* –MOXT plotted for Pareto-front solutions for the EPR problem

As Figure 30 and Figure 31 show, the optimization algorithm was able to find a variety of solutions which feature higher values of plutonium content, solutions which have lower PPF values, and solutions which have higher margins to CHF (–DNBR). The outlier solution on Figure 31 has a –DNBR value of ~-0.55, clearly unacceptable for any real-world application. It also shows that the algorithm was not able to find a Pareto-front solution with a MOXT value of greater than 23 that also had a DNBR greater than one. This suggests a limit on the maximum plutonium content permissible without performing other design changes, such as increasing the pin pitch to increase the moderator to fuel ratio and soften the spectrum, as well as improving thermal-hydraulic conditions.

These graphs suggest that the algorithm may produce solutions that dominate the reference solution, although it is hard to be conclusive just by displaying the data in these simple two-dimensional formats. This highlights an additional challenge posed by multi-objective problems: how to visualize multi-dimensional data. For problems with more than two objectives, displaying the results showing the trade-off between various objectives in a clear manner is not straightforward. One solution is to use Parallel Coordinates (PC), developed by (Inselberg, 1985). By mapping multi-variate relations into indexed subsets, this constrains the display of information to a two-dimensional space. What is then produced is a series of polylines, which represent individual Pareto-front solutions on a 2D graph with multiple y-axes separated equidistantly. Each *y*-axis represents a variable, and where the line crosses that axis denotes the value of that variable for that solution (likewise, if the *y*-axis represents the value of an objective, the intersection denotes that solution's performance against that objective). Visualizing complex multi-dimensional data in this way can reveal commonalities between solutions and trends in the plotted data, which can lead to greater understanding of the nature of trade-offs and the features of highly performing solutions.

Pins are numbered according to Figure 32. The Pareto-front solutions formed from 20 independent runs on this problem are displayed using the PC software Xdat (Xdat, 2019) in Figure 33. In this figure, the first 40 *y*-axes represent the plutonium concentrations / gadolinium content within the octant of the MOX assembly. The second set of 40 *y*-axes then show the gadolinium content in the pins for the UOX assemblies.

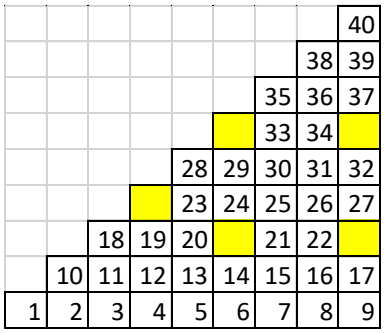

Figure 32: Numbering of pins in EPR assemblies with octant symmetry

In both cases, negative values on the y-axes indicates the gadolinium content in the pin. The objective values of –MOXT, PPF and –DNBR for each Pareto-front solution are shown on the right-hand side of Figure 33, inverted so that the 'best' solutions are at the top. The same colour scheme used for the previous graphs is used here. The highlighted black line corresponds to the one solution found that dominates (has better values of all three objectives than) the baseline design (the orange line). Figure 34 shows the dominating supercell design.

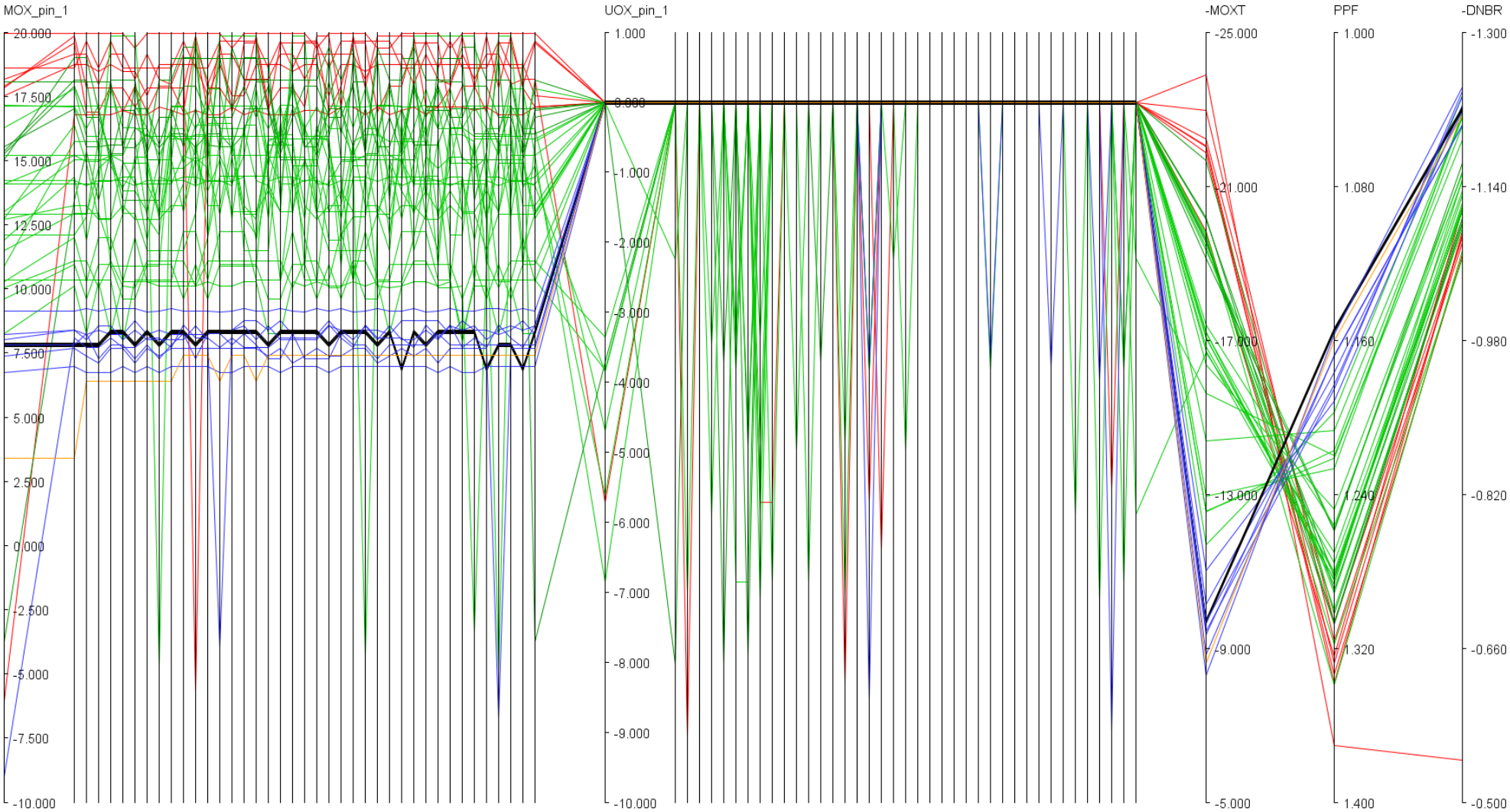

Figure 33: PC plot of each Pareto-front solution for the EPR problem and corresponding objective values, with the dominating solution highlighted in black

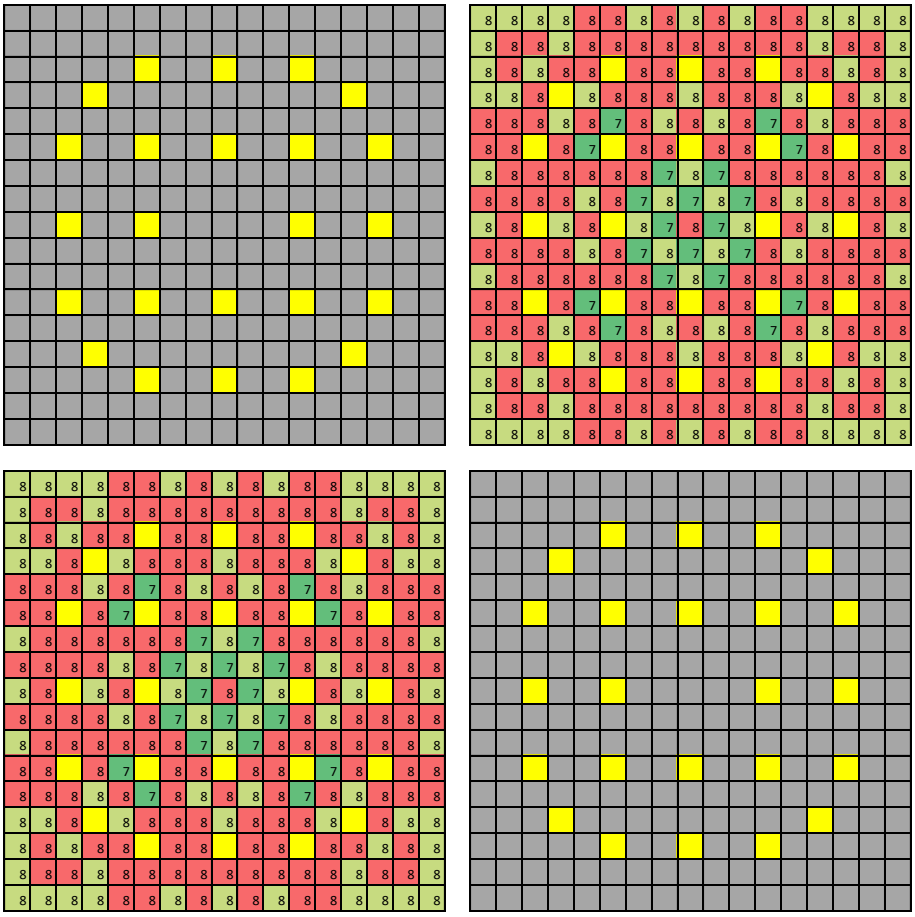

Figure 34: Supercell design of the one solution found that dominates the EPR baseline design (Figure 27). Numbers inside the assemblies denote wt% Pu rounded to nearest integer of MOX type 1 (dark green), MOX type 2 (light green) and MOX type 3 (red) pins

4.4.2. *Discussion of EPR test results*

The figures above show results which are typical of such optimization problems. MOX assemblies which contain high amounts of plutonium naturally do better at the –MOXT objective, but perform worse against PPF and –DNBR than their low –MOXT counterparts, and there appears to be a direct correlation between PPF and –DNBR as one would expect. Whilst the Pareto-front contains a wide variety of wt% Pu pin compositions, there do not appear to be large differences in the three wt% Pu MOX pin types determined for each solution (the largest difference between MOX pin types in a single solution was 6.87 wt% compared to 4 wt% for the baseline). Filtering these to focus on the one solution that dominates the baseline design and the two supercell layouts shown in Figure 27 and Figure 34, we can see the range of wt% Pu MOX pins has been further decreased to between 7 and 9 wt% Pu. The lower wt% Pu pins have been moved into the central locations to reduce the radial power peaking. No gadolinium pins have been used in the MOX or UOX assemblies, and this trend in the results is discussed further below.

The problem did not contain a specific objective for k-effective, as has been the case in other optimization studies, as setting a 'target' would introduce subjectivity into the results based on the target chosen. As a result, the employment of gadolinium in designs created by the optimization algorithm was solely to improve performance against the objectives of reducing PPF and maximizing DNBR over the life of the assembly. Since placement of gadolinium inside the MOX assemblies would negatively affect the performance against the objective of maximizing the amount of plutonium inside those assemblies, most solutions on the Pareto-front feature very few, if any, gadolinium oxide pins inside the MOX assemblies. This can be seen in Figure 33, with the average number of gadolinium oxide pins inside MOX assemblies amongst the Pareto-front solutions being just 0.02 per $1/8^{th}$ assembly due to symmetry. However, as Figure 33 shows, many Pareto-front solutions do feature gadolinium inside the UOX assemblies.

Figure 35 below shows the average amount of gadolinium per pin in the supercell *vs.* the change in k-effective over one cycle, using the same colour coded wt% Pu MOX assemblies as before. As one would expect, there is a general trend for supercells with higher average gadolinium oxide contents to have a smaller reduction in k-effective over the course of depletion, as the presence of burnable poisons suppresses reactivity at the beginning of life, enabling more fissile material to be loaded into the core in order to increase the cycle length. The design with the highest gadolinium oxide content (highlighted in the black circle on the graph) has a high estimated wt% Pu MOX value, with no gadolinium oxide pins in the MOX assembly (but 6 per $1/8^{th}$ UOX assembly) and objective values of –19.36, 1.26 and –1.16 for –MOXT, PPF and –DNBR, respectively. In comparison, other high wt% Pu MOX designs feature larger reactivity swings, and, in some cases, worse PPF, –DNBR, or –MOXT values. This highlights the benefit in careful selection of objectives and variables: optimization can yield additional information about the search space without requiring separate sensitivity studies for each variable, potentially reducing time and cost on the project. In this case, designs using gadolinium are produced which reduce reactivity swings, PPF and DNBR without requiring a specific objective to include gadolinium or an objective to reach a target k-effective.

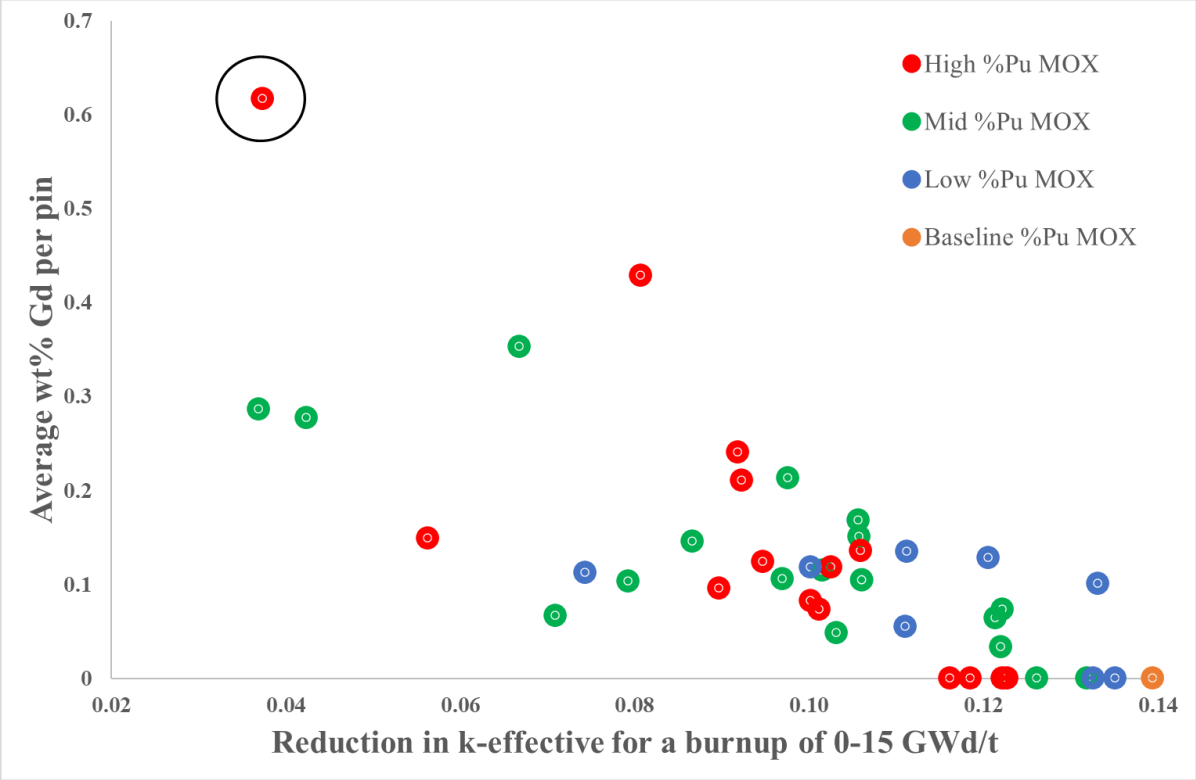

Figure 35: Average wt% Gd per pin inside the MOX assemblies for the EPR problem Pareto-front solutions *vs.* their corresponding reduction in k-effective for a burnup of 0-15 GWd/t

It should be noted that, whilst the baseline comparison did not feature gadolinium oxide poison, UK-EPR reactor fuel assemblies obviously do in real life, with designs featuring 8, 12 or 16 gadolinium oxide rods per UOX assembly. In a potential future study designed to optimize EPR fuel assemblies, gadolinium oxide would need to be included in the baseline comparison case in order to properly evaluate any objective relating to k-effective.

4.4.3. *EPR test conclusions*

As well as demonstrating the continued applicability of multi-objective optimization to multi-physics nuclear engineering problems, this study serves to reinforce the following benefits of non-dominated multi-objective optimization:

1. MO optimization can reveal additional information about the search space, even outside of the pre-set objectives, and can assist engineers in managing trade-offs through identifying important variables such as gadolinium distribution
2. The MO optimization algorithm MOJADE is capable of generating designs of four PWR assemblies arranged in a 2×2 supercell, with 40 MOX pin locations and compositions and 40 UOX pin locations and compositions that result in Pareto-equivalent objective performance to the established baseline design or perform better across all objectives throughout the depletion of the assembly

4.4.4. *ABWR test results*

With four objectives, projection onto 2D graphs would reveal little about the nature of the Pareto-front. However, PC can again be used to visualise and analyze the results. Figure 36 below shows a PC plot of the four objectives using data from a single optimization run. The blue lines are the starting population, created randomly using the CPU clock at initialization as the random seed. The red lines are the resultant Pareto-front solutions after 50 generations of the MOJADE algorithm. The green line is the baseline solution provided for comparison.

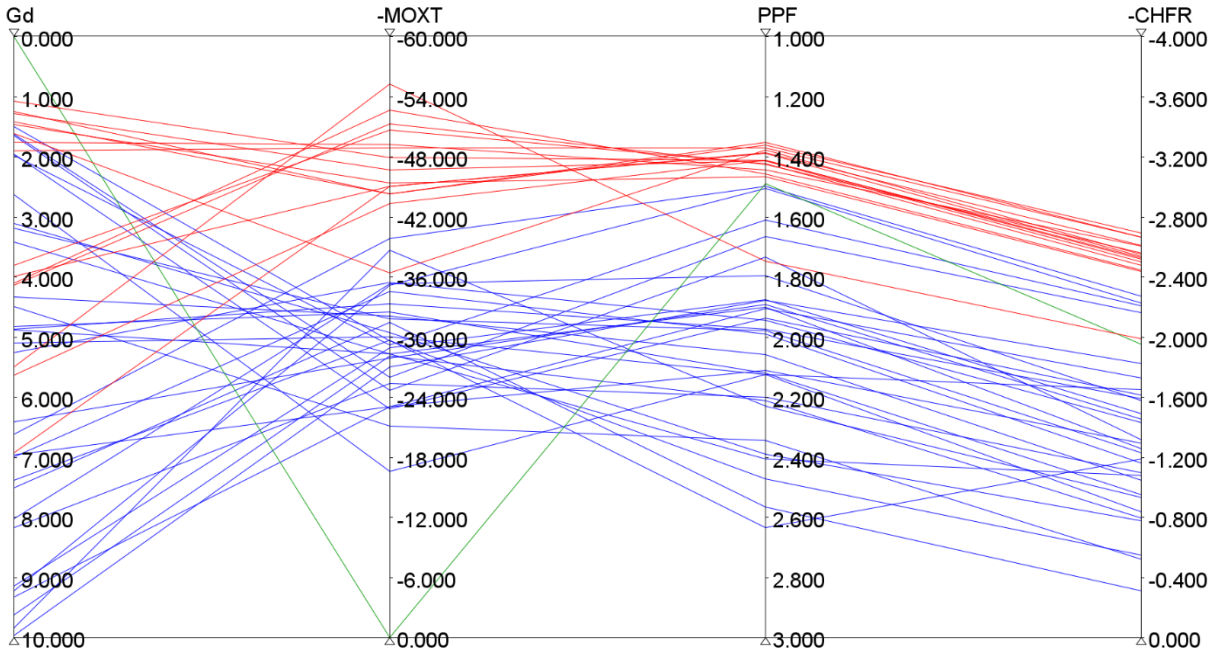

Figure 36: PC plot of the objective performance of Pareto-front solutions from one run on the ABWR problem

It is shown in the figure above that the algorithm has been able to improve on the starting population and find a Pareto-front. It can also be seen that the found Pareto-front solutions improve on the two safety related objectives – PPF and CHFR, whilst increasing the MOX content and minimizing (relative to other solutions) the gadolinium content.

Visualizing the full Pareto-front of 20 independent optimization runs becomes impractical even when using PC, due to the number of Pareto-front solutions[13]. Other features of the Pareto-front include a smaller pin radius of ~0.34 cm on average with a standard deviation of 0.02 cm, compared to the baseline of 0.447 cm. This indicates the algorithm favoured increasing the moderator-to-fuel ratio at the

[13] As the number of competing objectives increases, the number of trade-offs increase and the likelihood that one solution is non-dominated decreases. With four objectives it is more likely that solutions are Pareto-equivalent rather than dominating/being dominated.

cost of smaller fuel elements and hence less overall plutonium in the assembly (although this was not explicitly reflected in the –MOXT objective since it was based on a wt%). This clearly contributed to the improved performance against PPF and particularly –CHFR, where every solution was able to improve on the baseline. Figure 37 shows the frequency in % of each pin in an assembly (numbered 1 to 49, as shown in Figure 37) either being a partial-length rod or a gadolinium rod.

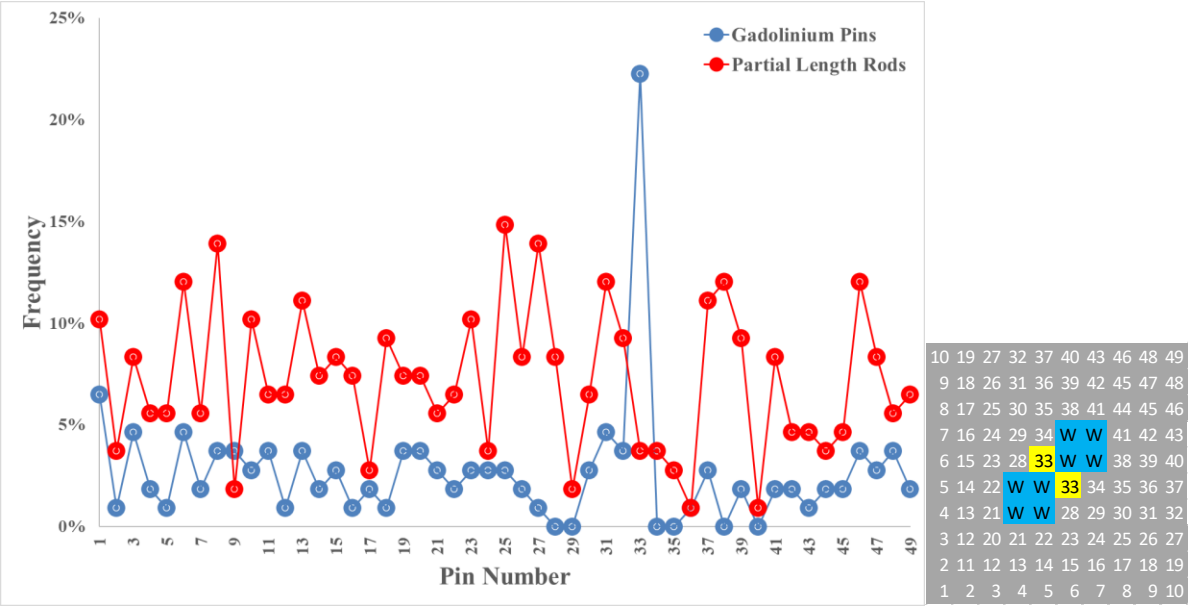

Figure 37: Frequency of a gadolinium rod (blue) or a partial-length rod (red) featured (left) for each of the possible 49 unique pin positions in the ABWR test assembly (right) in the Pareto-front solutions found in 20 independent optimization runs. Pin position 33 is highlighted in yellow.

Figure 37 shows that in the Pareto-front solutions, the algorithm made use of partial-length rods up to 15% of the time for each pin, and no location was particularly favourable to having a partial-length rod. As for gadolinium rods, the central pin (pin 33) location was most commonly (22% of the time) found to be gadolinium. In the real world, the central pin is often a partial-length fuel rod, and gadolinium is dispersed in the assemblies with axial heterogeneity (Bozzola, 1982) as a means of reducing excess reactivity at the beginning of life, rather than a means of reducing the PPF. Nevertheless, MOJADE clearly used both partial-length rods and gadolinium rods in an attempt to improve the objectives relating to power peaking and thermal hydraulics, and evidently found that placing a gadolinium or a partial-length rod in the central pin reduces power peaking.

4.4.5. *ABWR test conclusions*

The algorithm MOJADE was able to tackle a fully 3D optimization problem featuring 10 different types of rods and 49 different rod locations and generated a set of designs, which when considering the overall Pareto-front from 20 independent runs, improved on the PPF and CHFR of the baseline solution in 87% of cases. Analysis showed that MOJADE used the optional gadolinium and partial-length rods to reduce power peaking in the central assembly regions as it attempted to optimize the thermal-hydraulic objectives.

4.5. Conclusions

This study serves to show that multi-objective algorithms can be applied successfully to nuclear engineering design optimization problems with more realistic levels of complexity, utilising multi-physics analysis methods to identify solutions which have the potential to outperform reference designs. It has been demonstrated that when combined with some of the latest coupled multi-physics codes, MOJADE is still capable of converging on optimized designs and operates in a multi-objective manner by exploring the trade-offs involved using optional non-fuel elements. For the EPR problem, MOJADE optimized both UOX and MOX assemblies simultaneously considering thermal hydraulics, depletion and burnable poison non-fuel elements. A solution that dominates the reference design was found, and analysis also showed that the results gave insight into using gadolinium to reduce reactivity changes over the cycle. For the ABWR problem, a single BWR fuel assembly was optimized using a tight coupling of neutronics and thermal hydraulics and considering both gadolinium and partial-length rods as non-fuel elements. In both cases, a Pareto-front and dominating solutions compared to baseline solutions based on the available literature were found.

This study is not intended to provide superior designs to either the EPR or ABWR designs or to point out deficiencies in the existing designs, but rather to show how multi-objective optimization can work with complex 3D multi-physics problems and provide insight on the search space which can inform the design process. Further work could look at establishing the convergence criteria necessary for the algorithm to have optimal performance, as well as further testing on real-world problems for which complete data about existing fuel assembly designs is publicly available.

5. Conclusions and future work recommendations

5.1. Conclusions

The purpose of this project was to develop a multi-objective optimization system with the capability of optimizing heterogeneous LWR fuel assemblies utilizing both multi-dimensional and multi-physics analysis methods, thereby presenting a step forward in the state of the art of applying optimization methods to nuclear fuel assemblies.

A review of the literature (Section 1.3) showed that optimization is rarely done on a MO basis utilizing the concept of Pareto-dominance, which makes it quite difficult to draw general conclusions on the performance of the algorithms used as they are tuned to particular problems with subjective weighting. Fuel design optimization is also typically less frequently studied than core reloading pattern optimization, which has fewer continuous variables. Studies that feature multi-physics analysis (e.g. featuring both neutronics and thermal hydraulics) within the optimization are not coupled to minimize computational cost, and as a consequence these studies are generally treated by the optimization algorithm as separate problems, which limits the ability of the algorithm to optimize the design. Finally, the most popular type of algorithms used are Genetic Algorithms, which feature a high number of algorithm control parameters that require setting by the user. However, this popularity is not necessarily because they exhibit superior performance than other algorithms, as algorithm performance comparisons demonstrating superiority over others are few and far between. Differential Evolution offers a potential solution for problems with a mix of discrete and continuous variables, as well as requiring fewer control parameters to be set by the user.

Given the above information, DE was selected as a suitable algorithm to test the concept of multi-objective optimization on different fuel assembly design problems. In Chapter 2, two new algorithms were developed, based on the JADE algorithm by (Zhang & Sanderson, 2009). Featuring archives for Pareto-equivalent and dominated solutions, as well as using the concept of Pareto-dominance to perform the selection step in multi-objective space, these algorithms were ready to be used on MO problems, something which had not yet been attempted in the literature, fulfilling Requirement 1 of Section 1.4.1. Initial testing of the algorithms confirmed their ability to optimize in a MO environment on simple academic problems.

The design problems featured in this thesis were created from those used previously (Lattarulo, et al., 2014) or adapted from related studies found from the literature (Yilmaz, et al., 2006) in Chapter 3, or modelled specifically for this project in Chapter 4. The first problem tested the ability of the algorithms to place plutonium MOX fuel pins inside a CORAIL-based PWR assembly, where the presence of both

uranium and plutonium can result in an uneven neutron flux across the assembly. Statistical analysis of the results showed MOμJADE and MOJADE outperformed the existing EA method. The smaller population of MOμJADE caused more variability in the quality of results and suggested that MOJADE was more suitable for studies where the initial population is drawn randomly, whilst MOμJADE may be able to converge quicker and therefore might be more effective in problems where evaluating solutions has a very high computational cost. This confirmed the suitability of DE to fuel assembly design optimization problems. The second problem included burnable poisons, adding a new level of complexity over which to optimize. This study further demonstrated that MOJADE outperformed MOμJADE, and sensitivity analyzes showed that MOJADE was robust to changes in its control parameters and does not require extensive tuning, which supports Requirement 2 of Section 1.4.1.

The next two problems investigated were optimization of a UK-EPR-like MOX-UOX 2×2 Supercell featuring 3D modelling, depletion and loosely-coupled neutronics / thermal hydraulics, and 3D optimization of an ABWR fuel assembly with tightly-coupled neutronics and thermal hydraulics. These tests cover Requirements 3 and 4 in Section 1.4.1, showing that MOJADE was able to identify Pareto-fronts and dominating solutions in both cases, and analysis revealed the algorithm was able to provide additional information about the system (*i.e.* the effect of gadolinium concentration on reactivity changes over the cycle, despite this not being a pre-selected objective).

Requirement 5, as listed in Section 1.4.1, concerns the ability of the system to produce results given a reasonable computational budget. This is often the bane of optimization research, particularly when using stochastic methods such as DE that use a random seed to generate an initial population and/or utilize multi-physics software requiring internal convergence before a solution is found, or for studies incorporating depletion where the fuel inventory must be tracked through the life of the assembly. Populations should be large enough to generate enough points on the Pareto-front, and multiple runs should be performed in order to give reliability to the results. Computational cost can grow exponentially, and, during the course of this research, some concept problems would have taken longer to generate results than running a real reactor loaded with a test fuel assembly for its entire cycle length! Hence careful design of the optimization problem must be undertaken. Collection of data for the problems covered in this thesis could take up to a month each in some cases, running on the hardware described in Table 6 and Table 8. This is acceptable given that at no time was the hardware running on more than 20% cluster capacity (the cluster is a shared computational resource), and any small-to-medium-sized company in this industry would be using more powerful hardware). It should also be noted that 99% of the computational time was spent evaluating solutions with WIMS (as one would hope!).

In conclusion, this work has achieved its requirements and offers a novel and effective tool for performing optimization on nuclear fuel assembly design problems, with the ability to handle complex

analysis methods as chosen by the user. It provides strong evidence that there is a clear benefit to using formal optimization methods at the fuel assembly design level and constitutes a basis for future work which may seek to extend the application to clusters or quarter-core level analysis. It has advanced the state of the art in both multi-objective optimization and its application to the design of nuclear fuel assemblies, and presents an opportunity to improve the nuclear design process by utilizing computational resources to achieve performance gains on existing designs or to perform exploratory studies to guide the conceptual design stage. This technology does not require experts to tune algorithms to individual problems, nor does it need high-end computer hardware in order to generate results. By exploiting mathematical optimization, this project has shown that the performance of fuel assembly designs can be improved at practically zero additional cost and time for the designer. In the current climate where civil nuclear power programmes face huge cost and time overruns, the research presented in this thesis offers a means to reduce some of that cost, some of that time, and hopefully improve the attractiveness of a technology that is vital to a lower-carbon future.

5.2. Future work recommendations

There are a number of possible improvements to the system as proposed in this work which could be applied in future work. Firstly, the algorithms themselves could benefit from parallelization, allowing for multiple solutions (i.e. each member within the population) to be evaluated simultaneously during one generation. Although this increases the computational requirement in terms of number of simultaneously running processes, there is a trend in computing power for more cores per CPU, and in some cases more threads per core (hyper-threading). Therefore, future computing technology is likely to permit more parallelization. MOJADE already features inherent parallelization in that the evaluation of one member of the population does not affect another member within the same generation, therefore all solutions of a given generation can be evaluated simultaneously. MOμJADE, on the other hand, utilizes the evaluation of one solution in creating the next test solution. This makes MOμJADE potentially greedier, and this trade-off in approaches could be investigated further. A possible improvement would be to allow for greedier searches at the beginning of an optimization study to 'accelerate' the process and find the area of the Pareto-front more quickly, before switching to a more sequential operation to prevent biasing the population within a generation. Other acceleration techniques could include utilizing surrogate / reduced-order models in place of the fully detailed model used to analyze candidate designs, which could drastically reduce the run time of the analysis software (or in some cases negate the evaluation step by providing an interpolated evaluation from a look-up table of previously generated solutions). Once again, this could allow the algorithm to quickly converge on the general area of the Pareto-front and spend the majority of the computational time optimizing over the Pareto-front itself. Another way would be to eliminate economically unsound solutions by

coupling to some form of cost analysis, although this does increase the risk of introducing subjective bias.

Another application of optimization studies could be in the area of automated testing that occurs in some design companies. The design process is often split up between different teams, each with their own area of focus and responsibility (e.g. one team might analyze core thermal performance in steady state, another might focus on potential unintended transient scenarios, and another might focus on the refuelling process). Any potential changes to the design must be circulated to all teams, and in doing so will require re-running of a set of test scenarios to see how the changes perform. This set of test scenarios is often automated to be run during periods of low activity (e.g. nights and weekends) where computational load is lower than during the working day. This period could also be used to perform optimization studies of the current design, using previous versions of the design as an initial seed population. This could be carried out by any company with sufficient resources to perform automated testing.

It is also possible to apply stochastic optimization techniques to stochastic analysis methods such as Monte-Carlo simulations in an effort to derive a more accurate solution. However, assessing the performance of the optimization algorithm in these cases is even more difficult as one must determine if variability in the results is due to the analysis method or the optimization algorithm itself. DE has already shown itself to be a robust choice for optimization on fuel assembly designs and so may still remain a reliable optimization tool for stochastic analysis. Further work to evaluate integration with a Monte-Carlo solver would be merited.

Finally, another use of this system could be for supporting safety case work and demonstrating that the ALARP principle, one of the foundations of the British nuclear regulatory body, the Office for Nuclear Regulation (ONR), has been met. In this methodology, a design is deemed to be safe not only when it fulfils certain pre-set criteria (e.g. the maximum tolerable failure rates of components per year or ‘no additional’ risk beyond the site boundary during normal operation) but also demonstrates that the design outperforms these criteria as much as could reasonably be expected. This is a classic trade-off problem and requires the designer to demonstrate the design has been optimized for safety first and foremost. If the system as described in this work was applied to safety case studies, it could provide additional validation of the design by showing how variations in design parameters affect performance of safety criteria, giving confidence to the designer and demonstrating to the regulator that the ALARP principle has been followed. When combined with some of the performance improvements that are outlined above, the time and money required by the designer to get their design through the GDA process required by the ONR could be reduced, which would decrease the lead time before construction and hence speed up completion of nuclear projects in the UK.

6. References

Ackley, D. H., 1987. *A connectionist machine for genetic hillclimbing,* Boston: Kluwer Academic Publishers.

Ahmad, A. & Ahmad, S., 2018. Optimization of fuel loading pattern for a material test reactor using swarm intelligence. *Progress in Nuclear Energy,* 103(1), pp. 45-50.

Ando, S. & Suzuki, E., 2006. *Distributed Multi-objective GA for Generating Comprehensive Pareto Front in Deceptive Optimization Problems.* Vancouver, Canada, 2006 IEEE International Conference on Evolutionary Computation.

ANSWERS, 2017. *Developments to the SP3 and SUBCHANNEL models in WIMS (presentation).* Poole, ANSWERS.

ANSWERS, 2018. *WIMS: A Modular Scheme for Neutronics Calculations: User Guide for Version 10,* Dorchester: The ANSWERS Software Service.

Armand, A. A., 1959. *The Resistance During the Movement of a Two-phase System in Horizontal Pipes.* 1st ed. Harwell: Atomic Energy Research Establishment.

Babazadeh, D., Boroushaki, M. & Lucas, C., 2009. Optimization of fuel core loading pattern design in a VVER nuclear power reactors using Particle Swarm Optimization (PSO). *Annals of Nuclear Energy,* 36(7), pp. 923-930.

BBC, 2019. *Nuclear plant in Anglesey suspended by Hitachi.* [Online]
Available at: www.bbc.co.uk/news/business-46900918
[Accessed May 2019].

Bell, G. I. & Glasstone, S., 1970. *Nuclear Reactor Theory.* 1st ed. Washington D.C.: US AEC.

Bergh, F. V. D., 2002. *An Analysis of Particle Swarm Optimizers,* PhD Thesis: University of Pretoria.

Bezerra, L., Lopez-Ibanez, M. & Stutzle, T., 2015. Automatic Component-Wise Design of Multiobjective Evolutionary Algorithms. *IEEE Transactions on Evolutionary Computation,* 20(3), pp. 403-417.

Blasius, H., 1913. Das Aehnlichkeitsgesetz bei Reibungsvorgängen in Flüssigkeiten [German]. *Mitteilungen über Forschungsarbeiten auf dem Gebiete des Ingenieurwesens,* 131(1), pp. 1-41.

Boltzmann, L., 1872. Weitere Studien über das Wärmegleichgewicht unter Gas-molekülen. *Sitzungs Berichte Keiserl Akad der Wissenschaften,* 66(2), pp. 275-370.

Bozzola, S., 1982. *Fundamentals of Boiling Water Reactor (BWR).,* Vienna, Austria: IAEA INIS RN: 15025513, International Atomic Energy Agency.

Bremermann, H. J., 1962. *Self-Organizing Systems.* Washington, D.C.: Spartan Books.

Brown, C., Jin, Y., Leach, M. & Hodgson, M., 2015. muJADE: adaptive differential evolution with a small population. *Soft Computing,* 2013(1), pp. 1-10.

Cantu-Paz, E., 2000. *Efficient and Accurate Parallel Genetic Algorithms.* New York: Kluwer Academic.

Castillo, A. et al., 2014. Comparison of heuristic optimization techniques for the enrichment and gadolinia distribution in BWR fuel lattices and decision analysis. *Annals of Nuclear Energy,* 63(1), pp. 556-564.

Castillo, A., Ortiz-Servin, J. J., Perusquia, R. & Silvestre, Y. C., 2011. Fuel lattice design with Path Relinking in BWRs. *Progress in Nuclear Energy,* 53(4), pp. 368-374.

Cerny, V., 1985. Thermodynamical approach to the traveling salesman problem: An efficient simulation algorithm. *Journal of Optimization Theory and Applications,* 45(1), pp. 41-51.

Charles, A., 2015. *A Comparison of Optimization Methods for Heterogeneous Fuel Assembly Design,* MSc Thesis: Imperial College London.

Charles, A. J. & Parks, G. T., 2017. *Mixed Oxide LWR Assembly Design Optimization Using Differential Evolution Algorithms.* Shanghai, PRC, Proceedings of ICONE25.

Charles, A. J. & Parks, G. T., 2019. Application of Differential Evolution algorithms to multi-objective optimization problems in mixed-oxide fuel assembly design. *Annals of Nuclear Energy,* 127(1), pp. 165-177.

Charles, A. J. & Parks, G. T., 2020. Multi-objective, multi-physics optimization of 3D mixed-oxide LWR fuel assembly designs using the MOJADE algorithm. *Annals of Nuclear Energy,* 145(1), pp. 1-14.

Chen, B. C. J., Chien, T. H., Sha, W. T. & Kim, J. H., 1984. *Assessment of Biasi and Columbia University CHF correlations with GE 3x3 rod bundle experiment..* Washington, D.C., In proceedings of the Joint Meeting of the American Nuclear Society and the Atomic Industrial Forum.

Chen, L., Yan, C. & Wang, J., 2013. Multi-objective optimal design of vertical natural circulation steam generator. *Progress in Nuclear Energy,* 68(1), pp. 79-88.

Clerc, M. & Kennedy, J., 2002. The particle swarm - explosion, stability, and convergence in a multidimensional complex space. *IEEE Transactions on Evolutionary Computation,* 6(1), pp. 58-73.

Coello-Coello, C. A., Lamont, G. B. & van Veldhuizen, D. A., 2007. *Evolutionary Algorithms for Solving Multi-Objective Problems.* 2nd ed. New York: Springer.

Dall'Osso, A., 2016. Application of the inverse generalized perturbation theory to the optimization of fuel assembly design. *Annals of Nuclear Energy,* 90(1), pp. 417-421.

Das, S. & Suganthan, P. N., 2010. Differential Evolution: A Survey of the State-of-the-Art. *IEEE Transactions on Evolutionary Computation,* 15(1), pp. 4-31.

Deb, K., Pratap, A., Agarwal, S. & Meyarivan, T., 2002. A fast and elitist multiobjective genetic algorithm: NSGA-II. *IEEE Transactions on Evolutionary Computation,* 6(2), pp. 182-197.

DeChaine, M. D. & Feltus, M. A., 1996. Fuel Management Optimization Using Genetic Algorithms and Expert Knowledge. *Nuclear Science and Engineering,* 124(1), pp. 188-196.

del Campo, C. M., Francois, J. L., Barragan, A. M. & Palomera, M. A., 2007. Boiling Water Reactor Fuel Lattice Enrichment Distribution Optimization Using Tabu Search and Fuzzy Logic. *Nuclear Technology,* 157(3), pp. 251-260.

del Campo, C. M., Francois, J. L., Carmona, R. & Oropeza, I. P., 2007. Optimization of BWR fuel lattice enrichment and gadolinia distribution using genetic algorithms and knowledge. *Annals of Nuclear Energy,* 34(4), pp. 248-253.

del Campo, C. M., Francois, J. L. & Morales, L. B., 2002. Boiling Water Reactor Fuel Assembly Axial Design Optimization Using Tabu Search. *Nuclear Science and Engineering,* 142(1), pp. 107-115.

del Campo, C. M., Francois, J. & Lopez, H., 2001. AXIAL: a system for boiling water reactor fuel assembly axial optimization using genetic algorithms. *Annals of Nuclear Energy,* 28(16), pp. 1667-1682.

Dittus, F. W. & Boelter, L. M. K., 1985. Heat transfer in automobile radiators of the tubular type. *International Communications in Heat and Mass Transfer,* 12(1), pp. 3-22.

Dorigo, M., 1992. *Optimization, Learning and Natural Algorithms (Italian),* PhD Thesis: Politechnico di Milano.

Dorigo, M., Maniezzo, V. & Colorni, A., 1996. Ant system: optimization by a colony of cooperating agents. *IEEE Transactions on Systems, Man, and Cybernetics, Part B: Cybernetics,* 26(1), pp. 29-41.

Eberhart, R. & Kennedy, J., 1995. *A new optimizer using particle swarm theory.* New York, IEEE, pp. 39-43.

EDF, 2012. *Pre-Construction Safety Report - Sub-chapter 4.3 - Nuclear Design. UKEPR-0002-043 Issue 05,* s.l.: EDF.

Engrand, P., 1997. *Multi-objective optimization approach based on simulated annealing and its application to nuclear fuel management.* Clamart, Electricité de France.

Evers, G. & Ben Ghalia, M., 2009. *Regrouping particle swarm optimization: A new global optimization algorithm with improved performance consistency across benchmarks.* New York, IEEE, pp. 3901-3908.

Fadilah, S. & Lewins, J., 1975. Optimal control rod programs in power reactors. *Annals of Nuclear Energy,* 2(6), pp. 443-450.

Ferroni, P., Handwerk, C. & Todreas, N., 2009. Steady state thermal-hydraulic analysis of hydride-fueled grid-supported BWRs. *Nuclear Engineering and Design,* 239(8), pp. 1544-1559.

Francois, J., del Campo, C. M., Francois, R. & Morales, L., 2003. A practical optimization procedure for radial BWR fuel lattice design using tabu search with a multiobjective function. *Annals of Nuclear Energy,* 30(12), pp. 1213-1229.

Francois, J.-L.et al., 2013. Comparison of metaheuristic optimization techniques for BWR fuel reloads pattern design. *Annals of Nuclear Energy,* 51(1), pp. 189-195.

Fukuda, K. et al., 2000. *MOX fuel use as a back-end option: trends, main issues, and impacts of fuel cycle management,* Vienna: IAEA.

Geem, Z. W., 2009. *Music-Inspired Harmony Search Algorithm: Theory and Applications.* Berlin Heidelberg: Springer-Verlag.

Geem, Z. W., Kim, J. H. & Loganathan, G., 2001. A New Heuristic Optimization Algorithm: Harmony Search. *SIMULATION,* 76(2), pp. 60-68.

Gelbard, E., Davis, J. & Pearson, J., 1959. Iterative Solutions to the P1 and Double-P1 Equations. *Nuclear Science and Engineering,* 13(5), pp. 36-44.

Glover, F., 1986. Future Paths for Integer Programming and Links to Artificial Intelligence. *Computers and Operations Research - Special issue: Applications of integer programming,* 13(5), pp. 533-549.

Glover, F., 1998. A template for scatter search and path relinking. In: J. Hao, et al. eds. *Artificial Evolution.* Berlin Heidelberg: Springer-Verlag, pp. 1-51.

Goldberg, D. E., 1989. *Genetic Algorithms in Search, Optimization and Machine Learning.* 1st ed. Boston: Addison-Wesley Longman.

Goldberg, D. E. & Richardson, J., 1987. *Genetic Algorithms with Sharing for Multimodal Function Optimization.* Hillsdale, L. Erlbaum Associates, pp. 41-49.

Gong, W., Cai, Z. & Wang, Y., 2014. Repairing the crossover rate in adaptive differential evolution. *Applied Soft Computing,* 15(1), pp. 149-168.

Groeneveld, D. C. et al., 2017. Lookup Tables for Predicting CHF and Film-Boiling Heat Transfer: Past, Present, and Future. *Nuclear Technology,* 152(1), pp. 87-104.

Hayase, T. & Motoda, H., 1980. Boiling Water Reactor Control Rod Programming Using Heuristic and Mathematical Methods. *Nuclear Technology,* 48(2), pp. 91-100.

Hench, J. E. & Gillis, J. C., 1981. *Correlation of critical heat flux data for application to boiling water reactor conditions. Final report,* Palo Alto, California: EPRI.

Hewitt, G. F., Shires, G. L. & Bott, T. R., 1994. *Process Heat Transfer.* 1st ed. Ann Arbor: CRC Press.

Hill, N. J. & Parks, G. T., 2015. Pressurized water reactor in-core nuclear fuel management by tabu search. *Annals of Nuclear Energy,* 75(1), pp. 64-71.

Hirano, Y., Hida, K., Sakurada, K. & Yamamoto, M., 1997. Optimization of Fuel Rod Enrichment Distribution to Minimize Rod Power Peaking throughout Life with BWR Fuel Assembly. *Journal of Nuclear Science and Technology,* 34(1), pp. 5-12.

Hitachi, 2014. *Introduction to the UK Advanced Boiling Water Reactor*. [Online]
Available at: http://www.hitachi-hgne-uk-abwr.co.uk/reactor.html
[Accessed March 2020].

Hitachi-GE, 2017. *UK ABWR Generic Design Assessment, Generic PCSR Chapter 11: Reactor Core, Hitachi-GE UE-GD-0182,* s.l.: Hitachi-GE.

Holland, J. H., 1992. *Adaptation in Natural and Artificial Systems.* Cambridge: MIT Press.

Hu, Z., Xiong, S., Su, Q. & Zhang, X., 2013. Sufficient Conditions for Global Convergence of Differential Evolution Algorithm. *Journal of Applied Mathematics,* Article ID 193196, 14 pages.

IAEA, 2006. *Thermopyhysical properties database of materials for light water reactors and heavy water reactors,* Vienna, Austria: IAEA-TECDOC-1496, International Atomic Energy Agency.

IAEA, 2011. *Status report 97 - Advanced Boiling Water Reactor (ABWR),* Vienna, Austria: International Atomic Energy Agency.

Ihara, T., Sasagawa, M. & Iwata, Y., 2009. *Ohma Full MOX-ABWR.* Tokyo, Japan, Proceedings of ICAPP 2009.

Inselberg, A., 1985. The plane with parallel coordinates. *The Visual Computer,* 1(2), pp. 69-91.

International Energy Agency, 2018. *World Energy Outlook,* s.l.: International Energy Agency.

Jagawa, S., Yoshii, T. & Fukao, A., 2001. Boiling Water Reactor Loading Pattern Optimization Using Simple Linear Perturbation and Modified Tabu Search Methods. *Nuclear Science and Engineering,* 138(1), pp. 67-77.

Janin, D. et al., 2016. *HCSMR Fuel Assembly Optimization with APOLLO2, TRIPOLI-4 and URANIE codes.* s.l., Proceedings of PHYSOR 2016.

Jayalal, M. L., Murty, S. A. V. S. & Baba, M. S., 2015a. A Survey of Genetic Algorithm Applications in Nuclear Fuel Management. *Journal of Nuclear Engineering & Technology,* 4(1), pp. 45-62.

Jayalal, M. et al., 2015b. Application of Genetic Algorithm methodologies in fuel bundle burnup optimization of Pressurized Heavy Water Reactor. *Nuclear Engineering and Design,* 281(1), pp. 58-71.

Jessee, M. A. & Kropaczek, D. J., 2007. Coupled Bundle-Core Design Using Fuel Rod Optimization for Boiling Water Reactors. *Nuclear Science and Engineering,* 155(3), pp. 378-385.

Karahroudi, M. R., Shirazi, S. M. & Sepanloo, K., 2013. Optimization of designing the core fuel loading pattern in a VVER-1000 nuclear power reactor using the genetic algorithm. *Annals of Nuclear Energy,* 57(1), pp. 142-150.

Kawai, T., Motoda, H., Kiguchi, T. & Ozawa, M., 1976. A Method for Generating a Control Rod Program for Boiling Water Reactors. *Nuclear Technology,* 28(1), pp. 108-118.

Khoshahval, F. & Fadaei, A., 2012. Application of a hybrid method based on the combination of genetic algorithm and Hopfield neural network for burnable poison placement. *Annals of Nuclear Energy,* 47(1), pp. 62-68.

Khoshahval, F., Minuchehr, H. & Zolfaghari, A., 2011. Performance evaluation of PSO and GA in a PWR core loading pattern optimization. *Nuclear Engineering and Design,* 241(3), pp. 799-808.

Khoshahval, F., Zolfaghari, A. & Minuchehr, H., 2014a. A new method for multi-objective in core fuel management optimization using biogeography based algorithm. *Annals of Nuclear Energy,* 73(1), pp. 294-303.

Khoshahval, F., Zolfaghari, A., Minuchehr, H. & Abbasi, M., 2014b. A new hybrid method for multi-objective fuel management optimization using parallel PSO-SA. *Progress in Nuclear Energy,* 76(1), pp. 112-121.

Kim, J. H., Park, S. H. & Na, M. G., 2014. Design of a model predictive load-following controller by discrete optimization of control rod speed for PWRs. *Annals of Nuclear Energy,* 71(1), pp. 343-351.

Kirkpatrick, S., Gelatt, C. D. & Vecchi, M. P., 1983. Optimization by Simulated Annealing. *Science,* 220(4598), pp. 671-680.

Knowles, J., Thiele, L. & Zitzler, E., 2006. *A Tutorial on the Performance Assessment of Stochastic Multiobjective Optimizers,* Zurich, Switzerland: TIK Report 241, Swiss Federal Institute of Technology.

Kropaczek, D. J. & Turinsky, P. J., 1991. In-core nuclear fuel management optimization for Pressurized Water Reactors utilizing Simulated Annealing. *Nuclear Technology,* 95(1), pp. 9-32.

Kruskal, W. H. & Wallis, W. A., 1952. Use of ranks in one-criterion variance analysis. *Journal of American Statistics Association,* 47(260), pp. 583-621.

Lampinen, J. & Zelinka, I., 1999. *Mixed Integer-Discrete-Continuous Optimization by Differential Evolution - Part 2: A Practical Example.* Proceedings of the Fifth International Mendel Conference on Soft Computing, Brno, Brno University of Technology, pp. 45-55.

Lattarulo, V., Lindley, B. & Parks, G., 2014. *Application of the MOAA for the optimization of CORAIL assemblies for nuclear reactors.* Proceedings of the IEEE Congress on Evolutionary Computation, New York, IEEE, pp. 1413-1420.

Lattarulo, V. & Parks, G., 2012. *A preliminary study of a new multi-objective optimization algorithm.* Proceedings of the IEEE Congress on Evolutionary Computation, New York, IEEE, pp. 1-8.

Lee, S. W. et al., 2011. Design of a Load Following Control for APR+ Nuclear Plants. *Nuclear Engineering and Technology,* 44(4), pp. 369-378.

Lellouche, G. S. & Zolotar, B. A., 1982. *Mechanistic model for predicting two-phase void fraction for water in vertical tubes, channels, and rod bundles,* Palo Alto, California: EPRI.

Li, G. et al., 2018. Optimization of Th-U fuel breeding based on a single-fluid double-zone thorium molten salt reactor. *Progress in Nuclear Energy,* 108(1), pp. 144-151.

Lin, C., 1990. An Automatic Control Rod Programming Method for a Boiling Water Reactor. *Nuclear Technology,* 92(1), pp. 118-126.

Lin, C. & Lin, T.-H., 2012. Automatic fuel lattice design in a boiling water reactor using a particle swarm optimization algorithm and local search. *Annals of Nuclear Energy,* 47(1), pp. 98-103.

Lindley, B. et al., 2015. Release of WIMS10: A Versatile Reactor Physics Code for Thermal and Fast Systems. *Proceedings of ICAPP*.

Lin, L. S. & Lin, C., 1991. A Rule-Based Expert System for Automatic Control Rod Pattern Generation for Boiling Water Reactors. *Nuclear Technology,* 95(1), pp. 1-8.

Liu, C., Peng, J.-F., Zhao, F.-Y. & Li, C., 2009. Design and optimization of fuzzy-PID controller for the nuclear reactor power control. *Nuclear Engineering and Design,* 239(11), pp. 2311-2316.

Liu, S. & Cai, J., 2014. Design & optimization of two breeding thorium-uranium mixed SCWR fuel assemblies. *Progress in Nuclear Energy,* 70(1), pp. 6-19.

Lo, A. Y. & Chow, A. T., 2015. The relationship between climate change concern and national wealth. *Climate Change,* 131(1), pp. 335-348.

Maldonado, G. I., 2005. Optimizing LWR Cost of Margin One Fuel Pin at a Time. *IEEE Transactions on Nuclear Science,* 52(4), pp. 996-1003.

Marler, R. T. & Arora, J. S., 2004. Survey of multi-objective optimization methods for engineering. *Structural and Multidisciplinary Optimization,* 26(1), pp. 369-395.

Metropolis, N. et al., 1953. Equation of State Calculations by Fast Computing Machines. *The Journal of Chemical Physics,* 21(6), pp. 1087-1092.

Montes, J., Francois, J. & del Campo, C. M., 2007. *LPPF prediction in a BWR fuel lattice using artificial neutral networks.* Monterey, California, ANS.

Montes, J. L. et al., 2011. Fuel lattice design in a boiling water reactor using an ant-colony-based system. *Annals of Nuclear Energy,* 38(6), pp. 1327-1338.

Montes-Tadeo, J.-L.et al., 2015. Searching for enrichment and gadolinia distributions in BWR fuel lattices through a Heuristic-Knowledge Method. *Progress in Nuclear Energy,* 85(1), pp. 213-227.

Na, M. G. & Hwang, I. J., 2006. Design of a PWR power controller using model predictive control optimized by a genetic algorithm. *Nuclear Engineering and Technology,* 38(1), pp. 81-93.

Nissan, E., 2019. An Overview of AI Methods for in-Core Fuel Management: Tools for the Automatic Design of Nuclear Reactor Core Configurations for Fuel Reload, (Re)arranging New and Partly Spent Fuel. *Designs,* 3(3), pp. 1-45.

Odeh, F. & Yang, W., 2016. Core design optimization and analysis of the Purdue Novel Modular Reactor (NMR-50). *Annals of Nuclear Energy,* 94(1), pp. 288-299.

OECD/NEA, 1992. *JEFF 2.2 Data Library.* [Online]
Available at: https://www.oecd-nea.org/dbforms/data/eva/evatapes/jef_22/
[Accessed May 2020].

OECD/NEA, 2012. *OECD/NRC Benchmark Based on NUPEC PWR Sub-channeland Bundle Test (PSBT),* Paris: NEA.

OECD, 2019. *JANIS - JAva-based Nuclear Information Service.* [Online]
Available at: www.oecd-nea.org/janis/
[Accessed July 2019].

ONR, 2016. *United Kingdom's stocks of civil plutonium and uranium.* [Online]
Available at: www.onr.org.uk/safeguards/civilplut16.htm
[Accessed December].

Orano & EDF, 2007. *UK EPR GDA.* [Online]
Available at: http://www.epr-reactor.co.uk/
[Accessed March 2020].

Ortiz, J. J., Castillo, A., Montes, J. L. & Perusquia, R., 2007. A New System to Fuel Loading and Control Rod Pattern Optimization in Boiling Water Reactor. *Nuclear Science and Engineering,* 157(2), pp. 236-244.

Ortiz, J. J. et al., 2009. Nuclear Fuel Lattice Optimization Using Neural Networks and a Fuzzy Logic System. *Nuclear Science and Engineering,* 162(2), pp. 148-157.

Pacific Northwest Laboratory, 1983. *COBRA/TRAC - A Thermal-Hydraulics Code for Transient Analysis of Nuclear Reactor Vessels and Primary Coolant Systems,* Richland: NRC.

Pan, I., Das, S. & Gupta, A., 2011. Tuning of an optimal fuzzy PIR controller with stochastic algorithms for networked control systems with random time delay. *ISA Transactions,* 50(1), pp. 28-36.

Parks, G. T., 1990. An Intelligent Stochastic Optimization Routine for Nuclear Fuel Cycle Design. *Nuclear Technology,* 89(2), pp. 233-246.

Parks, G. T., 1996. Multiobjective Pressurized Water Reactor Reload Core Design by Nondominated Genetic Algorithm Search. *Nuclear Science and Engineering,* 124(1), pp. 178-187.

Peakman, A., Grove, C., Fitzgerald, K. & Gregg, R., 2019. Development of an equilibrium loading pattern and whole-core fuel performance assessment in the Advanced Boiling Water Reactor (ABWR) with UO2 and U3Si2 fuels. *Progress in Nuclear Energy,* 117(1), pp. 1-13.

Pereira, C. M., 2004. Evolutionary multicriteria optimization in core designs: basic investigations and case study. *Annals of Nuclear Energy,* 31(11), pp. 1251-1264.

Pereira, C. M. & Lapa, C. M., 2003. Coarse-grained parallel genetic algorithm applied to a nuclear reactor core design optimization problem. *Annals of Nuclear Energy,* 30(5), pp. 555-565.

Pereira, C. M. & Sacco, W. F., 2008. A parallel genetic algorithm with niching technique applied to a nuclear reactor core design optimization problem. *Progress in Nuclear Energy,* 50(7), pp. 740-746.

Pereira, C. M., Schirru, R. & Martinez, A. S., 1999. Basic investigations related to genetic algorithms in core designs. *Annals of Nuclear Energy,* 26(3), pp. 173-193.

Qvist, S., 2015. Optimization method for the design of hexagonal fuel assemblies. *Annals of Nuclear Energy,* 75(1), pp. 498-506.

Raza, W. & Kim, K.-Y., 2008. Multiobjective Optimization of a Wire-Wrapped LMR Fuel Assembly. *Nuclear Technology,* 162(1), pp. 45-52.

Reddy, D. G. & Fighetti, C. F., 1983. *Parametric study of CHF data. Volume 2. A generalized subchannel CHF correlation for PWR and BWR fuel assemblies. Final report,* Palo Alto, California: Technical Report EPRI-NP-2609-Vol2, Electric Power Research Institute.

Reddy, D. G., Sreepada, S. R. & Nahavandi, A. N., 1982. *Two-phase Friction Multiplier Correlation for High-pressure Steam-water Flow,* New York: Columbia University.

Reuters, 2017. *Areva's Finland reactor to start in 2019 after another delay.* [Online]
Available at: uk.reuters.com/article/uk-finland-nuclear-olkiluoto/arevas-finland-reactor-to-start-in-2019-after-another-delay-idUKKBN1CE1NR
[Accessed May 2019].

Reyes-Sierra, M. & Coello, C. A. C., 2006. Multi-objective particle swarm optimizers: A survey of the state-of-the-art. *International Journal of Computational Intelligence Research,* 2(3), pp. 287-308.

Rogers, T., Ragusa, J., Schultz, S. & Clair, R. S., 2009. Optimization of PWR fuel assembly radial enrichment and burnable poison location based on adaptive simulated annealing. *Nuclear Engineering and Design,* 239(6), pp. 1019-1029.

Ronen, Y., 1979. Inverse Perturbation Theory. *Nuclear Science and Engineering,* 72(1), pp. 110-113.

Sacco, W. F., Machado, M. D., Pereira, C. M. & Schirru, R., 2004. The fuzzy clearing approach for a niching genetic algorithm applied to a nuclear reactor core design optimization problem. *Annals of Nuclear Energy,* 31(1), pp. 55-69.

Sacco, W. et al., 2009. Differential evolution algorithms applied to nuclear reactor core design. *Annals of Nuclear Energy,* 36(8), pp. 1093-1099.

Sawaragi, Y., Nakayama, H. & Tanino, T., 1985. Theory of Multiobjective Optimization. *Elsevier Science,* 176(1), pp. 2-5.

Sekimizu, K., 1975. Optimization of In-Core Fuel Management and Control Rod Strategy in Equilibrium Fuel Cycle. *Journal of Nuclear Science and Technology,* 12(5), pp. 287-296.

Shirvan, K. & Kazimi, M., 2017. BWR-HD: An Optimized Boiling Water Reactor with High Power Density. *Nuclear Technology,* 184(3), pp. 261-273.

Smith, K. I. et al., 2008. Dominance-Based Multi-Objective Simulated Annealing. *IEEE Trans. on Evol. Comp.,* 12(3), pp. 323-342.

Sorensen, K., 2015. Metaheuristics: the metaphor exposed. *International Transactions in Operational Research,* 22(1), pp. 3-18.

Storn, R. & Price, K., 1997. Differential Evolution - A Simple and Efficient Heuristic for Global Optimization over Continuous Spaces. *Journal of Global Optimization,* 11(4), pp. 341-359.

Stout, R. B. & Robinson, A. H., 1973. Determination of Optimum Fuel Loadings in Pressurized Water Reactors. *Nuclear Technology,* 20(2), pp. 86-102.

Suzuki, A. & Kiyose, R., 1971. Application of Linear Programming to Refueling Optimization for Light Water Moderated Power Reactors. *Nuclear Science and Engineering,* 46(1), pp. 112-130.

Tabak, D., 1968. Optimization of Nuclear Reactor Fuel Recycle via Linear and Quadratic Programming. *IEEE Transactions on Nuclear Science,* 15(1), pp. 60-64.

Taner, M. S., Levine, S. H. & Hsiao, M.-Y., 1992. A Two-Step Method for Developing a Control Rod Program for Boiling Water Reactors. *Nuclear Technology,* 97(1), pp. 27-38.

Tang, J. & Zhao, X., 2010. A Hybrid Particle Swarm Optimization with Adaptive Local Search. *Journal of Networks,* 5(4), pp. 411-418.

Thom, J. R. S., Walker, W. M., Fallon, T. A. & Reising, G. F. S., 1965. *Boiling in sub-cooled water during flow up heated tubes or annuli.* London, Institution of Mechanical Engineers.

Tokumasu, S., Ozawa, M., Hiranuma, H. & Yokomi, M., 1985. A Mathematical Method for Boiling Water Reactor Control Rod Programming. *Nuclear Technology,* 71(3), pp. 568-579.

Tollit, B. et al., 2018. *Development of a Subchannel Model within the ANSWERS Software Service WIMS Reactor Physics Code.* Cancun, Mexico, Proceedings of PHYSOR 2018.

Tong, L. & Weisman, J., 1996. *Thermal Analysis of Pressurized Water Reactors.* 3rd ed. Ann Arbor: American Nuclear Society.

Trivedi, V., Varshney, P. & Ramteke, M., 2020. A simplified mult-objective particle swarm optimisation algorithm. *Swarm Intelligence,* 14(1), pp. 83-116.

Tsouri, N., Rootenberg, J. & Lidofsky, L., 1975. Optimal Control of a Large Core Reactor in Presence of Xenon. *IEEE Transactions on Nuclear Science,* 22(1), pp. 702-710.

Tung, W.-H., Lee, T.-T., Kuo, W.-S. & Yaur, S.-J., 2015. Fuel lattice design in a boiling water reactor using a knowledge-based automation system. *Nuclear Engineering and Design,* 293(1), pp. 63-74.

Turinsky, P. J., Keller, P. M. & Abdel-Khalik, H. S., 2005. Evolution of nuclear fuel management and reactor operation aid tools. *Nuclear Engineering and Technology,* 37(1), pp. 79-90.

Tusar, T. & Filipic, B., 2007. Differential Evolution versus Genetic Algorithms in Multiobjective Optimization. In: S. Obayashi, et al. eds. *Evolutionary Multi-Criterion Optimization.* Berlin Heidelberg: Springer-Verlag, pp. 257-271.

UK Government, 2013. *Long-term Nuclear Energy Strategy,* London: HM Government.

UK Government, 2016. *Manging the UK Plutonium Stockpile.* [Online]
Available at: http://researchbriefings.files.parliament.uk/documents/POST-PN-0531/POST-PN-0531.pdf
[Accessed May 2020].

van Laarhoven, P. J. M. & Aarts, E. H. L., 1987. *Simulated Annealing: Theory and Applications.* New York: Springer.

Vivas, G. C., Parish, T. & Curry, G., 2002. Optimization of MOX enrichment distributions in typical LWR assemblies using a simplex method-based algorithm. *Annals of Nuclear Energy,* 29(17), pp. 2001-2017.

Wang, C.-D. & Lin, C., 2013. Automatic boiling water reactor control rod pattern design using particle swarm optimization algorithm and local search. *Nuclear Engineering and Design,* 255(1), pp. 273-279.

Washington, J. & King, J., 2017. Optimization of plutonium and minor actinide transmutation in an AP1000 fuel assembly via a genetic search algorithm. *Nuclear Engineering and Design,* 311(1), pp. 199-212.

Weyland, D., 2010. A Rigorous Analysis of the Harmony Search Algorithm: How the Research Community Can Be Misled by a "Novel" Methodology. *International Journal of Applied Metaheuristic Computing,* 1(2), pp. 50-60.

Weyland, D., 2015. A critical analysis of the harmony search algorithm: How not to solve sudoku. *Operations Research Perspectives,* 2(1), pp. 97-105.

World Nuclear Association, 2019. *Plans For New Reactors Worldwide.* [Online]
Available at: www.world-nuclear.org/information-library/current-and-future-generation/plans-for-new-reactors-worldwide.aspx
[Accessed 20 March 2019].

World Nuclear News, 2017. *Duke seeks to cancel plans for Lee AP1000s.* [Online]
Available at: www.world-nuclear-news.org/NN-Duke-seeks-to-cancel-plans-for-Lee-AP1000s-2908175.html
[Accessed May 2019].

World Nuclear News, 2018. *EDF revises schedule, costs of Flamanville EPR.* [Online]
Available at: www.world-nuclear-news.org/Articles/EDF-revises-schedule,-costs-of-Flamanville-EPR
[Accessed May 2019].

World Nuclear, 2019. *Nuclear Power in China.* [Online]
Available at: www.world-nuclear.org/information-library/country-profiles/countries-a-f/china-nuclear-power.aspx#ECSArticleLink7
[Accessed May 2019].

Xdat, 2019. *Xdat - A free parallel coordinates software.*. s.l.:Free Software Foundation.

Yadav, R. & Gupta, H., 2011. Optimization studies of fuel loading pattern for a typical Pressurized Water Reactor (PWR) using particle swarm method. *Annals of Nuclear Energy*, 38(9), pp. 2086-2095.

Yamate, K., Mori, M., Ushio, T. & Kawamura, M., 1997. Design of a gadolinia bearing mixed-oxide fuel assembly for Pressurized Water Reactors. *Nuclear Engineering & Design*, 170(1-3), pp. 35-51.

Yang, Z., 2013. *PWR Heterogeneous Fuel Assembly Optimization*, MPhil Thesis: University of Cambridge.

Yilmaz, O. F. & Tufekci, S., 2017. *Handbook of Research on Applied Optimization Methodologies in Manufacturing Systems.* 1st ed. s.l.:IGI Global.

Yilmaz, S., Ivanov, K., Levine, S. & Mahgerefteh, M., 2006. Application of genetic algorithms to optimize burnable poison placement in pressurized water reactors. *Annals of Nuclear Energy*, 33(5), pp. 446-456.

Yoshida, H. et al., 2000. A particle swarm optimization for reactive power and voltage control considering voltage security assessment. *IEEE Transactions on Power Systems*, 15(4), pp. 1232-1239.

Youinou, G. et al., 2001. *Heterogeneous assembly for plutonium multi recycling in PWRs: the Corail concept.* s.l., Proceedings of the Global 2001 International Conference, p. 5.

Zhang, J. & Sanderson, A. C., 2009. JADE: Adaptive Differential Evolution with Optional External Archive. *IEEE Transactions on Evolutionary Computation*, 13(5), pp. 945-958.

Zhong, W.-L. & Weisman, J., 1984. Automated Control Rod Programming in Boiling Water Reactor Cores. *Nuclear Technology*, 65(3), pp. 383-394.

Zio, E. & Viadana, G., 2011. Optimization of the inspection intervals of a safety system in a nuclear power plant by Multi-Objective Differential Evolution (MODE). *Reliability Engineering & System Safety*, 96(11), pp. 1552-1563.

Zitzler, E., Deb, K. & Thiele, L., 2000. Comparison of Multiobjective Evolutionary Algorithms: Empirical Results. *Evolutionary Computation*, 8(2), pp. 173-195.